Study of Nitrite Sensors Based on Co(III)/Rh(III)-Ligand Complexes as Selective Ionophores

by

Si Yang

A dissertation submitted in partial fulfillment
of the requirements for the degree of
Doctor of Philosophy
(Chemistry)
in The University of Michigan
2014

Doctoral Committee:
Professor Mark E. Meyerhoff, Chair
Associate Professor Nicolai Lehnert
Associate Professor Stephen Maldonado
Professor Levi T. Thompson, Jr.

To my family

Acknowledgements

First and foremost I would like to thank my advisor, Dr. Mark E. Meyerhoff, for his guidance and support throughout my five years of research, especially when I encountered difficulties. It is his enthusiasm and encouragement that motivates me during tough times in the pursuit of my Ph.D.. I sincerely appreciate his insightful suggestions and advice not only for research but also for my future career. I would also like to thank Dr. Stephen Maldondo, Dr. Nicolai Lehnert and Dr. Levi T. Thompson for serving as my committee members over the past five years as well as for their challenging questions and valuable suggestions.

I would like to express my deep thanks to my colleagues. I have been lucky working with so many lovely people. Thanks to Dr. Kebede Gemene who was my mentor and led me into the world of ionophore-based sensors when I joined Dr. Meyerhoff's lab as a rotation student; thanks to Dr. Lajos Höfler, Dr. Dipankar Koley and Dr. Gary Jensen for their help and discussion in the electrochemistry area; thanks to Dr. Kun Liu and Dr. Wenyi Cai for their help and suggestions in organic synthesis; thanks to Dr. Yu Qin for her help and discussion regarding polymeric film optodes; and thanks to Scott Hogan for his help on the rhodium(III) corrole project. Special thanks go to Dr. Bo Peng for her precious support and discussions not only research-wise but also life-wise. I also wish to thank all the current and former Meyerhoff group members: Dr. Jun Yang, Dr. Lin Wang, Dr. Laura Zimmerman, Dr. Qinyi Yan, Dr. Natalie Crist, Teng Xue, Dr. Xuewei

Wang, Dr. Gergely Lautner, Andrea Bell-Vlasov, Hang Ren, Elizabeth Brisbois, Alexander Wolf, Alexander Ketchum, Zheng Zheng, Yaqi Wo, Joanna Zajda, Kyoung Ha Cha, Dakota Suchyta, Alessandro Colletta, Anant Balijepalli, and Eunsoo Yoon. I also want to thank all my dearest friends in Ann Arbor for making my life in graduate school enjoyable and sharing the many memorable moments.

I would like to express my sincere appreciation to my mom, Fuxiu Zhao, my dad, Huilong Yang, my mother-in-law, Xiuqing Zhao, and my father-in-law, Qingmin Wang, for their unconditional love and support. Last but not least, I would like to thank my husband Chenyi Wang. The best outcome from these past five years is finding my best friend, soul-mate, and husband. It is his love, persistent support and belief that accompany me during my good and bad times.

Table of Contents

List of Figures

List of Tables

Abstract

Study of Nitrite Sensors Based on Co(III)/Rh(III)-Ligand Complexes as Selective Ionophores

by

Si Yang

Chair: Mark E. Meyerhoff

In this dissertation, fundamental and applied studies of new ionophore-based ion-selective electrodes and optodes for selective nitrite detection are reported. The new ionophore systems are shown to be useful in the fabrication of sensitive and selective nitrite sensors via both electrochemical (potentiometric) and optical measurements.

First, two metal ion ligand complexes, cobalt(III) 5,10,15-tris(4-tert-butylphenyl) corrole (Co-tBC) and rhodium(III) 5,10,15-tris(4-tert-butylphenyl) (Rh-tBC) are synthesized and characterized. The two complexes are then used, for the first time, within plasticized poly(vinyl chloride) membranes and studied as neutral carrier ionophores for developing potentiometric nitrite selective sensors. Both of the ionophores exhibit good binding affinity to nitrite, but Co-tBC has a stronger binding constant (log β = 5.57) toward nitrite than Rh-tBC (log β = 4.04). Co-tBC-based

potentiometric sensors exhibit Nernstian response and greatly enhanced selectivity to nitrite over all other common anions. The selectivity to nitrite over thiocyanate is greater than that obtained from sensors prepared with a commercially available nitrite ionophore, a Co(III) aquocyanocobyrinate species. Sensing membranes doped with Rh-tBC also show Nernstian response and good selectivity to nitrite over most common anions. However, they suffer substantial interference from thiocyanate.

The newly studied Co-tBC ionophore can also be incorporated along with an appropriate proton chromoionophore into plasticized poly(vinyl chloride) films to fabricate nitrite-selective bulk optodes via absorbance measurements. The resulting films yield sensitive, fast, and fully reversible optical nitrite response with significantly enhanced nitrite selectivity. Compared to previously studied ionophore-based optical sensors for nitrtie, the Co-tBC-based optical sensors have enhanced selectivity to nitrite over thiocyanate. The optical nitrite sensors are shown to be useful for detecting nitric oxide (NO) emission rates from NO releasing polymers containing *S*-nitroso-*N*-acetyl-penicillamine (SNAP).

Finally, the use of an electropolymerized film of rhodium(III) porphyrin on a fluorine-doped tin oxide (FTO) electrode for developing an amperometric sensor for nitrite is examined. Results suggest that at an applied potential of +0.6 V vs. Ag/AgCl, the modified electrode has rapid amperometric response to nitrite, with a linear range of 0.01 mM to 0.1 mM, a lower detection limit of 4.7 μM.

Chapter 1

Introduction

1.1. Nitrite Detection

1.1.1. Importance of Nitrite Detection

There is a growing interest in devising simple sensors to detect nitrite, since nitrite plays an important role in many fields and such sensors would have a wide range of potential applications. In the past, physiologically and biologically nitrite was predominantly known as an undesired residue of the food chain with potentially carcinogenic effects. It was also considered as an oxidative end product of endogenous nitric oxide (NO) metabolism. However, it is now recognized that physiologically, the presence of nitrite can be viewed as a storage pool for NO since nitrite can be reduced in blood and tissues to form NO, a diverse and potent biological messenger, via several enzymatic and nonenzymatic pathways [1-3]. Further, the catalytic reduction of nitrite to NO can be greatly enhanced during hypoxia and ischaemic stress, which may enable nitrite to exhibit a therapeutic value [4]. Indeed, nitrite shows strong cytoprotective properties and protects against ischaemia-reperfusion

injury in connection with organ transplant surgery [5-6]. Nitrite also has vasodilatory and hence blood-pressure lowering effects [7-8].

In the food industry, nitrite has been used as a food preservative, especially in cured meat and bacon for many years. Nitrite is employed mainly to inhibit the growth of pathogens, most notably *Clotridium botulinum*, and these antibacterial effects have been attributed to NO formation [9]. Nitrite can also react with secondary amines to produce nitrosamines, carcinogenic substances [10]. The amount of nitrosamine present is determined by the amount of nitrite added and the amount of secondary amines originally in the meat. As established by the U.S. Department of Agriculture (USDA) in their Meat Inspection Regulations, the use of nitrites, nitrates, or the combinations of them cannot result in more than 200 ppm within meats, calculated as sodium nitrite, in the finished meat product.

Ground waters, including well water, river water, etc., contain inorganic nitrite which may get into our daily drinking water. This has led the Environmental Protection Agency (EPA) to set a maximum contaminant level (MCL) of 10 ppm for nitrite in public water supplies. Users of private water supplies should have their water tested annually, especially in areas where fertilizers are commonly used.

1.1.2. Common Methods for Nitrite Detection

Many methods have been developed to quantitate nitrite concentrations [11], including chromatographic [12-15], spectroscopic [16-19] and electrochemical [20-22]. In chromatographic detection, especially gas chromatography, complicated sample

pretreatment/derivatization is usually necessary (e.g., oxidation of nitrite to nitrate followed by conversion of nitrate to electrophilic nitronium ion (NO_2^+) and then nitration of an activated aromatic species [23]). Sometimes it is possible to realize direct sample introduction with HPLC type ion chromatography systems. Ion chromatography coupled with conductometric or UV detection provides low detection limits (e.g., 4.4 nM [24]). However, the equipment is expensive and not suitable for portable device development that would enable field use.

Electrochemical detection of nitrite can be accomplished using amperometric or potentiometric methods. In amperometry, the working electrode is usually modified with a mediator due to the slow kinetics of charge transfer for nitrite oxidation or reduction, which complicates the detection process [25]. In potentiometric detection of nitrite, an ion-selective membrane electrode is most commonly used. The partition of ions between solution and organic membrane creates a potential (EMF) difference which can be monitored. A plasticized poly(vinyl chloride) (PVC) membrane containing an appropriate ionophore, an ion-exchanger and a plasticizer is widely used and can be readily miniaturized to yield a simple, inexpensive and portable nitrite sensing device. However, the key to achieving low detection limits in real samples relates to the inherent selectivity of the ionophore used in preparing the polymeric membrane of the sensor (see below). Detection can be directly performed without the requirement of sample pretreatment.

Various spectroscopic methods for nitrite determination have been developed,

including UV-Vis [14, 26-34] and fluorimetric [18-19, 35-39] detection. Spectroscopic detection methods are the ones most widely used so far, with the most common approach being the Griess assay. The Griess method involves using a suitable aromatic amine (an azo dye agent, e.g., *N*-(1-naphthyl)ethylenediamine)) that is able to undergo a diazotization reaction with the diazonium salt formed from acidified nitrite and sulphonamide, and yields a highly colored azo product [26]. Direct UV-Vis determination is usually employed to measure the absorbance at 500-600 nm of the chromophoric azo derivative that is formed in an amount proportional to the nitrite concentration in the original sample (see Fig 1.1). This technique is not reversible and samples cannot be recovered, which is a drawback in certain situations. An alternative way to detect nitrite is to employ ionophore-based optical sensors which are reusable and provide direct measurements. Similar to ISEs, it is possible to make miniaturized nitrite sensing devices using this type of optical sensor principle (see below).

Comparing all the methods discussed above, the ionophore-based potentiometric and optical sensors can provide simple, inexpensive and portable devices for nitrite sensing that can be employed for many practical analytical applications [40-43].

1.2. Ionophore-Based Electrochemical and Optical Sensors

1.2.1. Ion-Selective Electrodes

The field of ion-selective electrodes (ISEs) has developed rapidly since the 1960s [44-46]. Such devices are attractive because they are readily miniaturized, highly portable, relatively simple to operate and can provide accurate measurements of ion concentrations with low cost and low energy consumption instrumentation. ISEs are widely used in clinical, environmental and industrial analysis [40-43].

There are three major types of ISEs depending on the ion-selective membrane material employed to fabricate the device. The earliest such electrodes were made with glass membranes, including silicates and chalcogenides, and exhibit potentiometric response to single charged cations. The most famous glass membrane electrodes are pH electrodes [47] and sodium electrodes [48]. The second type of ISEs are based on crystalline membrane materials which have good selectivity towards ions that can be introduced into the crystal lattice of the membrane, such as fluoride-selective electrodes prepared with a LaF_3 crystal [49] and Ag_2S-based membrane electrodes that selectively detect silver or sulfide ions [50]. The third type is based on organic polymer membranes containing a lipophilic ion-exchanger species and/or an iononophore (ion-carrier) with specific binding affinity to the target ion. This last type has become the most widely used class of ISEs, ever since the development of the potassium-selective electrode that utilized valinomycin as the recognition ionophore in the oganic membrane [51]. Indeed, polymeric membrane ISEs for sodium, calcium, ammonium, chloride, magnesium and protons (pH) are widely used in commercial instruments. Since nitrite is an anion, this chapter will mainly focus on anion detection with such polymer membrane-based sensors,

including the fundamental response mechanisms, examples of membrane formulations and the factors that influence the observed ion selectivity.

The introduction of ISEs based on ion-binding chemistry (with ionophores or ion carriers) within organic polymeric phases transformed the field of ISEs. Fig. 1.2 shows the general measurement setup of an ISE cell with a polymer membrane-based electrode as the working electrode and a conventional reference electrode (e.g., Ag/AgCl) both in contact with the sample solution. In the working electrode, there is an internal reference electrode immersed within the inner filling solution inside the electrode body and a plasticized polymeric membrane at the distal end that separates the inner solution from the outer sample solution. During the measurement, a cell potential difference will be created between the two electrodes, which is referred to as electromotive force (EMF), and measured under zero-current conditions.

The EMF across the cell can always be written as:

$$EMF=E_W-E_{ref}+E_j \qquad \text{(Eq. 1.1)}$$

where E_W is the working electrode potential, E_{ref} is the reference electrode potential and E_j is the liquid junction potential. The junction potential arises from the charge separation at the interface between the sample liquid and the solution that fills the external reference electrodes. This potential is usually minimized as much as possible and kept relatively constant by using a high concentration of equitransferent electrolyte as the reference electrolyte solution. Ideally, the reference electrode potential should be stable throughout the measurement process. The true potential change upon the change

of ion activity is from the working ion-selective electrode potential change, which is the sum of membrane potential E_M and internal reference electrode potential $E_{inner, ref.}$ The latter is constant for a given inner solution composition:

$$E_W = E_M + E_{inner, ref} \quad \text{(Eq. 1.2)}$$

Since the membrane is a separate phase with two discrete sides, the membrane potential is actually contributed from the phase boundary potentials at each of the two interfaces and a diffusion potential within the membrane:

$$E_M = E_{PB, mem/int. sol} - E_{PB, sam/mem} + E_{diff} \quad \text{(Eq. 1.3)}$$

where $E_{PB, sam/mem}$ is the phase boundary potential at the sample/membrane interface and $E_{PB,mem/int.sol}$ is the phase boundary potential that develops at the membrane/inner filling solution interface. Usually, it is assumed that the phase boundary potential at the membrane/inner filling solution interface is sample independent and governed by the activity of the target ion that is added at a given concentration/activity to the inner solution of the ISE. Also, the diffusion potential E_{diff} within the membrane can be neglected in most cases, especially for those measurements made with well-conditioned membranes [52]. Thus, the membrane potential can be expressed as:

$$E_M = E_{PB, sam/mem} + E_{const} \quad \text{(Eq. 1.4)}$$

While the phase boundary potential at the sample/membrane interface is related to ion activity and determined by the difference of electrical potentials of the two phases, it can be derived from the basic thermodynamic considerations of electrochemical potentials

(μ). For the aqueous phase:

$$\mu(aq)=\mu(aq)+z_X F\phi(aq)=\mu^0(aq)+RT\ln a_X(aq)+z_X F\phi(aq) \quad \text{(Eq. 1.5)}$$

For the contacting organic membrane phase:

$$\mu(org)=\mu(org)+z_X F\phi(org)=\mu^0(org)+RT\ln a_X(org)+z_X F\phi(org) \quad \text{(Eq. 1.6)}$$

where μ is the chemical potential, μ^0 is the standard chemical potential, a_X is the activity of the free analyte ion, z_X is the ion valency, ϕ is the electrical potential and R, T, F have their well-established meanings. Assume that the ion transfer across the interface and complexation reaction between the target ion and the ionophore within the membrane are very fast, the electrochemical potential should be the same in both phases at equilibrium.

$$\mu(aq)=\mu(org) \quad \text{(Eq. 1.7)}$$

Combining equations 1.4 to 1.6, the phase boundary potential which is the difference of two electrical potentials of two phases can be given by:

$$E_{PB}=\phi(org)-\phi(aq)=-\frac{\mu^0(org)-\mu^0(aq)}{z_x F}+\frac{RT}{z_x F}\ln\frac{a_X(aq)}{a_X(org)} \quad \text{(Eq. 1.8)}$$

Thus, equation 1.1 can be rewritten as:

$$E_{cell}=E_{const}-\frac{\mu^0(org)-\mu^0(aq)}{z_x F}+\frac{RT}{z_x F}\ln\frac{a_X(aq)}{a_X(org)} \quad \text{(Eq. 1.9)}$$

The second term on the right of the above equation is sample-independent and holds constant for a given ion transfer process. It is the function of the relative free energies of solvation in the ion within the sample and membrane phases. If the activity of the free ion in the membrane phase ($a_X(org)$) stays unaltered, equation 1.9 reduces to the well-known Nernst equation for ISEs:

$$E_{cell}=E_{const}+\frac{RT}{z_x F}\ln a_X(aq) \quad \text{(Eq. 1.10)}$$

The measured potential is directly proportional to the logarithmic activity of the analyte ion in the aqueous sample phase and the theoretical slope of Nernstian response is expected to be $59.2/z_x$ mV per decade at 298 K. For the case of nitrite, a Nernstian response slope should be close to -59.2 mV/dec at room temperature.

In the presence of lipophilic ion-exchanger within the membrane phase, permselectivity of one type of ion can be guaranteed. For general anion detection, a lipophilic anion-exchanger is required within the polymeric membrane (i.e., tridodecylmethylammonium chloride (TDMACl), see Fig. 1.3a). Since there is no specific interaction between the ions and such cationic sites, the degree of EMF response toward different anions will depend solely on how well the ion of interest is solvated in the organic phase and how well it is de-solvated from the aqueous phase. The tendency of ions to partition from the aqueous phase to the organic phase follows the trend in hydration energy of the anions, which is also termed the "Hofmeister selectivity pattern" and follow the Nicolsky-Eisenman equation [53]:

$$ClO_4^- > SCN^- \sim I^- > Sal^- > Br^- > NO_2^- \sim Cl^- > HCO_3^- > H_2PO_4^- \sim F^-$$

$$E_{cell} = E_{const} + \frac{RT}{z_X F}\ln(a_X + \sum k_{X,Y}^{pot} a_Y^{z_X/z_Y}) \quad \text{(Eq. 1.11)}$$

where the observed cell potential is determined by both the target ion activity (a_X) and interfering ion activity (a_Y) as well as the corresponding selectivity coefficient ($k_{X,Y}^{pot}$)

and charges of the above ions (z_X and z_Y). With only an anion-exchanger in the membrane phase, the selectivity coefficient is governed by the single ion partition coefficient of the ions based on their lipophilicity, which is given by:

$$\ln K_{X,Y}^{pot} = \ln \frac{k_Y}{k_X} \qquad \text{(Eq. 1.12)}$$

where k_X and k_Y are the partition coefficients of the primary anion (X) and the interfering ion (Y), respectively. The lower the $K_{X,Y}^{pot}$ value is, the better selectivity that can be achieved. In the Hofmeister series, nitrite is not the most preferred anion since more lipophilic anions (e.g., perchlorate, thiocyanate and nitrate, etc.) have larger partition coefficients into the organic membrane phase that is primarily derived from their lower aqueous phase solvation energies (more positive ΔG^{o}_{hyd} values). Therefore, with anion-exchanger-based ISEs, selective nitrite detection is not possible if interfering ions coexist in the sample solution.

If an anion ionophore is added into the membrane, the potentiometric selectivity pattern will be quite different than the classical Hoffmeister pattern. Ionophores are ion recognition units which have a special affinity for the target ions and selectively complex with the ions of interest in the membrane phase. An anionic ionophore can act as a neutral carrier (electrically neutral when not complexed and negatively charged when complexed with the target anion) or a charged carrier (electrically positively charged when not complexed and neutral when complexed to the target anion). In the neutral carrier mechanism, an anion-exchanger, like tridodecylmethylammonium chloride

(TDMACl), is required in the polymeric membrane phase (see Fig. 1.4b). After the target anion enters the membrane, it will bind with the ionophore. The neutral ionophore will become negatively charged and the lipophilic anion-exchanger is the counter-ion for this ion/ionophore complex. The amount of anion-exchanger determines the concentration of anion/ionophore complex in the bulk of the organic membane phase which also determines the concentration of free and exchangeable anion in the organic membrane phase. Therefore, the EMF response at the membrane/sample interface is only related to the activity of the target anion in the sample solution. However, in the case of the charged carrier mechanism, a negatively charged cation-exchanger (i.e., potassium salt of tetrakis[3,5-bis(trifluoromethyl)]phenylborate (KTFPB), see Fig. 1.3b) must be added to the membrane phase (see Fig. 1.4c). Before the anion enters the membrane, the negatively charged lipophilic cation-exchanger is the counter-ion of the positively charged ionophore. Therefore, the amount of ion-exchanger still can dictate the concentration of the ion/ionophore complex which also determines the concentration/activity of free and exchangeable anion within the membrane. The EMF response is only related to the activity of the target anion in the sample solution, just as in the neutral carrier mechanism.

In the presence of ionophores that possess a strong yet reversible interaction with the target ion, selectivity is not only determined by partition coefficients of the ions but also the binding affinity between ions and ionophores. Thus, equation 1.13 can be rewritten as:

$$\ln K_{X,Y}^{pot} = \ln \frac{k_Y}{k_X} + \ln \frac{\beta_Y}{\beta_X} \qquad \text{(Eq. 1.14)}$$

where β_X is the binding constant of between the ionophore and the primary ion (X), while β_Y is the binding constant of between the ionophore and the interfering ion (Y). It is obvious in the equation that a much larger binding constant of the primary ion (β_X) can compensate for the smaller single partition coefficient (k_X) to realize selective detection of a less lipophilic anion (more hydrophilic) over a more lipophilic anion and yield a selectivity pattern which is completely different than the Hofmeister series.

Therefore, knowledge of the binding strength between the target ion and the ionophore is essential for understanding the selectivity observed with carrier/ionophore-based ISEs. A simple potentiometric method to determine the ion/ionophore complex formation constants in polymeric membranes has proven to be a useful technique to access these binding affinity constants [53-57]. This method was originally reported by Russian researchers in Russian journals [58-59] and then Bakker reintroduced this method to the larger scientific community [60].

As described previously, the membrane potential is the potential difference between the two phase boundaries, the sample/membrane interface and the membrane/inner filling solution interface (assuming the membrane is well conditioned without ion concentration gradient in the membrane), which can be written as follows:

$$E_M = E_{PB,\ mem/int.\ sol} - E_{PB,\ sam/mem} = \frac{RT}{z_X F} \ln \frac{a_X(aq)' a_X(org)''}{a_X(org)' a_X(aq)''} \qquad \text{(Eq. 1.15)}$$

where a prime (') indicates the ion activity at the sample/membrane interface and a double

prime (") at the inner filling solution/membrane interface. The corresponding phases are noted in parentheses as (aq) indicating aqueous phase and (org) indicating organic membrane phase. Since no concentration gradient occurs in the membrane, $a_X(org)' = a_X(org)''$. If the sample solution and inner filling solution are the same, then $a_X(aq)' = a_X(aq)''$. As a result, the membrane potential is 0 for individual membranes regardless of their membrane formulations (see Fig. 1.5a and 1.5b). To determine the binding strength, a two-layer sandwich membrane is employed. The compositions of both segments are almost identical with the only difference being that one side contains an ionophore and the other doesn't (see Fig. 1.5c). If the two-layer segmented sandwich membrane contacts two aqueous solutions of exactly the same ionic composition without interference species present, equation 1.15 can be reduced to:

$$E_M = \frac{RT}{z_X F} \ln \frac{a_X(org)''}{a_X(org)'} \qquad \text{(Eq. 1.16)}$$

where $a_X(org)'$ is not equal to $a_X(org)''$. Owing to the strong complexation between extracted ion and the ionophore, the free and uncomplexed ion activity in the membrane with ionophore is dramatically decreased, leading to a much smaller value of $a_X(org)'$ than $a_X(org)''$. Thus, a membrane potential is induced, unlike the case of individual membranes where the membrane potential would be zero. The membrane potential of a segmented sandwich membrane can be obtained from experiments and then the complex formation constant of the ion with the ionopohore can be determined by the following equation (without considering ion-pairing) [60]:

$$\beta_{XI_n} = (I_T - \frac{nR_T}{z_X})^{-n} \exp(\frac{E_M z_X F}{RT}) \quad \text{(Eq. 1.17)}$$

where x is the tested ion, and I is the ionophore. The symbol I_T is the total concentration of ionophore in the membrane and R_T is the total concentration of ion additives in the membrane phase. The value of n is the complex stoichiometry and z is the charge of the ion which is -1 for nitrite. The above equation provides a powerful tool and allows for the convenient determination of ion-ionophore complex formation constants within the exact membrane of interest. It should be noted that the segmented sandwich membrane is required to be made fresh and assembled just prior to measurement, because the membrane components (ionophore, ion-exchangers, etc.) can diffuse from one membrane segment to another thus eventually making the two membranes identical to each other and thus yielding a membrane potential that is zero.

1.2.2. Ion-Selective Optodes

In this dissertation work, ion-selective optodes for nitrite are also examined. These type of optical sensors are based on the mass transfer of the target ions into a polymeric film via a coexaction of both the analyte ions and protons (for anion detection) from the sample phase into the bulk of the sensing film to yield an optical signal change [61-62]. Like ISEs, optodes can also provide a simple, inexpensive fully reversible and highly portable ion sensing device. A plasticized polymer film, containing an appropriate lipophilic ionophore, a chromoionophore (e.g., lipophilic pH indicator that stays in the

polymeric film (see below)) and, if necessary, an ion-exchanger is widely used to create such ion-selective optical sensors. Many of the ionophores that are used to fabricate polymer membrane-based ISEs have been adopted for preparing ion-selective optodes [63-64].

To obtain sufficient optical changes of the polymer films, in addition to the ionophore, a reference ionophore, which interacts specifically to a reference ion in the sample phase (e.g., protons) and transfers the binding of the target ion with the ionophore to yield an optical response signal, must be introduced into the film [61]. This reference ionophore is also known as a chromoionophore or fluoroionophore, and is typically a lipophilic pH indicator. Depending on their electrical charge, there are two types of chromoionophores, neutral and charged chromoionophores [65]. The neutral chromoionophores are electrically neutral when deprotonated and positively charged when protonated, while the charged chromoionophores are negatively charged when deprotonated and electrically neutral when protonated. Different combinations of ionophores and chromoionophores (see Fig. 1.6 for examples of commonly used chromoionophores and their pKa values in *o*-nitrophenyl octyl ether (*o*-NPOE) plasticized PVC films) in sensing films can provide different sensing mechanisms. The most important principle is the conservation of charge neutrality within the film, which is guaranteed if the extraction of the primary target ion into the polymer film is accompanied by the extraction of oppositely charged ions with a corresponding amount of total charge.

Fig. 1.7 illustrates the response mechanism for detection of anions with polymeric films containing a neutral ionophore and a neutral chromoionophore (see Fig. 1.7a) or a charged chromoionophore in the presence of appropriate lipophilic ionic site additives (see Fig. 1.7b). In the presence of a neutral chromoionophore and neutral carrier, the binding of the analyte ion and the ionophore is accompanied by a concomitant protonation of the chromoionophore to maintain charge neutrality within the film. In contrast, if a charged chromoionophore is incorporated into the polymeric membrane, an appropriate amount of lipophilic ionic sites should also be introduced to act as the initial counterion to the chromoionophore. As the binding of the analyte ion and the ionophore occurs, the ion-ionophore complex becomes charged and this must be accompanied by coextraction of protons into the sensing film to protonate the chromoionophore to a neutral state. Because of the presence of the lipophilic ionic additive (e.g., R^+ sites in Fig. 1.7(b)), the electroneutrality of the sensing film is still ensured.

This chapter will focus on the theory of ion-extraction systems for polymeric films that contain a neutral ionophore I (interacting with the analyte anion X^{z-} to form $XI_n^{\ z-}$ complex) and a neutral chromoionophore C (forming CH^+ when binds with H^+). Other systems can often be described by complete analogy [61, 65-66]. The coextraction process can be summarized as a simple net ionic equation:

$$zH^+(aq)+X^{z-}(aq)+nI(org)+zC(org) \rightleftharpoons XI_n^{z-}(org)+zCH^+(org) \qquad \text{(Eq. 1.18)}$$

with the corresponding coextraction constant, that depends on both ion-ionophore complex formation constant (β_{XIn}) and the acidity constant (K_a) of the chromoionophore:

$$K^{X}_{coex}=\left(\frac{[CH^{+}]}{a_{H^{+}}[C]}\right)^{z}\frac{[XI^{z-}_{n}]}{a_{X^{z-}}[I]^{n}} \qquad \text{(Eq. 1.19)}$$

In order to relate the actual optical spectrum change to the analyte ion activities, the normalized absorbance α, is introduced. The value of α is the fraction of deprotonated chromoionophore ($[C]/[C_T]$), where C_T is the total amount of chromoionophore, The value of 1-α is the degree of protonation of the chromoionophore ($[CH^+]/[C_T]$), which can be given by:

$$1-\alpha=\frac{A-A_{deprot}}{A_{prot}-A_{deprot}} \qquad \text{(Eq. 1.20)}$$

where A is the absorbance of the chromoionophore for a given equilibrium condition, and A_{prot} and A_{deprot} are the absorbance values at fully protonated and deprotonated forms respectively. It should be noted that to obtain optimal sensitivity, the absorbance values should be measured at the λ_{max} for the protonated and deprotonated chromoionophore species.

Assuming mass balance conditions, ($I_T=[I]+n[XI^{z-}_n]$ and $C_T=[C]+[CH^+]$, where I_T is the total amount of the ionophore) and the neutrality conditions for the film ($[CH^+]=z[XI^{z-}_n]$), equation 1.18 can be rewritten in an analytically more useful form to relate proton (a_{H^+}) and ion activities ($a_{X^{z-}}$) to optical responses and membrane parameters as the following [61]:

$$a_{H^{+}}\cdot a_{X^{-}}=\frac{1}{K^{X}_{coex}}\cdot\frac{(1-\alpha)^{z+1}}{\alpha^{z}}\cdot\frac{1}{\left(\frac{[I_T]}{[C_T]}-\frac{n}{z}(1-\alpha)\right)^{n}\cdot z\cdot[C_T]^{n-1}} \qquad \text{(Eq. 1.21)}$$

It can be seen that the measured response is relative to the activity of both the analyte

anion and protons in the sample. However, in a buffered sample system, 1-α is only dependent on the analyte anion activity since the proton activity is constant. For the case of nitrite detection with the chelating stoichiometry between nitrite and the ionophore of 1:1, the above equation can be reduced to:

$$a_{X^-} = \frac{1}{K^X_{coex}} \cdot \frac{(1-\alpha)^2}{\alpha} \cdot \frac{1}{(\frac{[I_T]}{[C_T]} - (1-\alpha))} \qquad \text{(Eq. 1.22)}$$

For the interfering monovalent anion Y^-, the single ion response can be given by:

$$a_{Y^-} = \frac{1}{K^Y_{coex}} \cdot \frac{(1-\alpha)^2}{\alpha} \cdot \frac{1}{(\frac{[I_T]}{[C_T]} - (1-\alpha))} \qquad \text{(Eq. 1.23)}$$

In the case of a one to one stoichiometry of the two ion-ionophore complexes (IX^- and IY^-) in response to a monovalent target anion (e.g., nitrite) and the interfering monovalent anion (Y^-), respectively, the selectivity coefficient is given by:

$$K^{opt}_{X^-,Y^-} = \frac{K^Y_{coex}}{K^X_{coex}} \qquad \text{(Eq. 1.24)}$$

So,

$$\log K^{opt}_{X^-,Y^-} = \log K^Y_{coex} - \log K^X_{coex} \qquad \text{(Eq. 1.25)}$$

The logarithmic selectivity coefficient is graphically accessible by plotting the single ion response calibration curve ((1-α) vs. log ion activity) according to equations 1.22 and 1.23 for all anions of interest. For the buffered sample solutions, the selectivity coefficient of optical sensors can be estimated from the horizontal distance of two optical response calibration curves at a given degree of protonation 1-α (e.g., 0.5) of the

chromoionophore.

Compared with potentiometric sensors, polymeric film optical sensors sometimes have advantages such as lower detection limits, tunable response range, higher sensitivity, more flexible sensor design and application for high-throughput automated measurements (e.g., using optical films as detectors at the bottom of microtiter plate wells [67]). However, unlike ion-selective electrodes where a potential change occurs at the phase boundary, ion-selective optodes measure the ion activity change in the bulk sensing film which leads to much longer response times, usually several minutes. In addition, usually, the sensing films are quite thin (e.g., a few μm thick), limiting the lifetime of use due to faster extraction of the ionophore and chromophore from the polymer film. In addition, since ion-selective optodes rely on an optical signal change for detection, turbid sample solutions cannot be tested directly and proper pretreatment procedures for such samples are required.

1.3. Nitrite-Selective Ionophores

As discussed previously, for anion detection, in order to achieve selectivity for the target anion and avoid response based on ion lipophilicity (selectivity based on free energy of hydration of the anions), ionophores with specific binding affinity to the primary target anion through axial ligation reactions are often incorporated into the

polymeric membrane/film. Among many of the anion-selective ionophores examined to date, hydrophobic metal ion-ligand complexes are often the most useful, including metallocorrins, metalloporphyrins, and metallosalophens. It has been reported that both the metal ion center and the specific surrounding ligand structure can influence anion selectivity [68-70]. Obviously, a strong yet reversible axial ligation reaction between the metal ion center of the ionophore and target anion to form a host-guest complex helps to achieve sensitive and selective response. The degree of binding between ionophore and target anion can, however, also be altered by the specific ligand structure employed to form the complex.

In the mid-1980s the first metal ion-ligand complex studied as a nitrite selective ionophore was a cobalt(III) complex with a vitamin B_{12} derivative as the ligand [71-72], which showed greatly enhanced selectivity for nitrite over perchlorate and comparable response to thiocyanate ($\log K^{pot}_{NO_2^-,X}$ (SSM): SCN^-, +0.2; ClO_4^-, -2.2; NO_3^-, -3.5; Br^-, -3.3; Cl^-, -3.7; membrane composed of PVC, *o*-NPOE, KTFPB and Co(III)-VB_{12} derivative) [73]. Ever since then, many other cobalt(III) complexes have also been examined as nitrite ionophores in polymeric membranes to fabricate ISEs, including cobalt(III) tetraphenylporphyrins [74]. Besides cobalt(III), other metal ion-ligand complexes were studied for nitrite sensor development as well, including Pd(II) benzylbis(triphenylphosphine) [75], UO_2-salophen [76], Rh(III) porphyrins and Rh(III) salophens [77]. Fig. 1.8 illustrates the structures of nitrite-selective ionophores mentioned above.

Among all the metal-ion ligand complexes studied to date, Rh (III)-porphyrins have recently been discovered to exhibit the best performance, in terms of selectivity for nitrite over other anions ($\log K^{pot}_{NO_2^-,X}$ (SSM): SCN^-, -0.4; ClO_4^-, -1.7; NO_3^-, -2.8; Br^-, -3.2; Cl^-, -3.8; membrane composed of PVC, *o*-NPOE, TDMACl, and Rh(III)-5,10,15,20-tetra(*p-tert*-butylphenyl)porphyrin chloride). However, membranes containing Rh(III) porphyrins that were doped with either TDMACl or KTFPB as lipophilic ion additives exhibit excellent selectivity to nitrite, indicating that Rh(III)-porphyrins can function as either/both a charged carrier and neutral carrier type ionophore within the membrane phase and this complicates the sensing chemistry. In the neutral carrier mode, two nitrites must bind as axial ligands to the Rh(III) center to create a negatively charged complex; for the charged carrier mechanism to be operable, only one nitrite binds as an axial ligand, yielding a neutral species (see Fig. 1.9). The same response behavior has also been observed with cobalt(III) porphyrins doped within polymer membranes to create nitrite selective ISEs [74].

1.4. Statement of Research

The primary purpose of this dissertation work is the development, fundamental study, and application of polymeric membrane/film based ion-selective electrodes and optodes with novel ionophores for sensitive and selective nitrite detection. Monitoring of nitrite

levels is important, yet very challenging. Examining the number of publications relating to ionophore-based ISEs and optical sensors over the last 30+ years, the number of ionophores for anion detection is far less than that for cation detection. This thesis provides fundamental and applied studies of new ionophores that may be useful in the development of novel electrochemical and optical polymeric membrane/film type nitrite-selective sensors.

Chapter 2 describes the employment of a cobalt(III) corrole species as a neutral carrier for nitrite detection in polymeric membranes to fabricate potentiometric sensors. This cobalt(III) complex has relatively high binding affinity to nitrite, and the resulting membrane electrode yields reversible and Nernstian response toward nitrite. Enhanced nitrite selectivity is observed over other anions, including lipophilic anions such as thiocyanate and perchlorate when an appropriate amount of lipophilic cationic sites are added to the membrane phase. Interestingly, it is also shown in this work that using tributylphosphate as the plasticizer with the cobalt(III) corrole species yields electrodes with enhanced nitrate selectivity. Most of this chapter was published in Electroanalysis, 25, 2579-2585 (2013).

Chapter 3 describes nitrite sensor development by incorporating a rhodium(III) corrole species as the ionophore into plasticized polymeric membranes to determine nitrite concentration using potentiometry. Unlike rhodium(III) porphyrins examined previously, the rhodium(III) corrole ionophore functions only as a neutral carrier. Different polymer membrane compositions have been studied to optimize sensor

response. Results show enhanced nitrite sensitivity and selectivity over most common anions.

Chapter 4 describes the fabrication of nitrite-selective bulk optodes by using cobalt(III) 5,10,15-tris(4-tert-butylphenyl) corrole with a triphenylphosphine axial ligand and rhodium(III) 5,10,15,20-tetra(*p-tert*-butylphenyl)porphyrin as ionophores in polymeric films to detect nitrite via an absorbance mode. The selectivity patterns are consistent with selectivity obtained with potentiometric sensors based on the same ionophores. The optical nitrite sensors are shown to be useful for detecting rates of emission of nitric oxide (NO) from NO releasing polymers containing *S*-nitroso-*N*-acetyl-penicillamine. The content of this chapter was submitted for publication to Analytica Chimica Acta.

Chapter 5 describes the use of rhodium (III) metalloporphyrins electropolymerized on a solid electrode to fabricate an amperometric nitrite sensor. The properties of the electropolymerized porphyrin film were studied, including conductivity, UV-Vis absorption and electrochemical behavior. Such a sensor was studied to detect nitrite amperometrically at a lower applied potential than typically reported for electrochemical oxidation of nitrite.

Chapter 6 summarizes this dissertation work and suggests future research directions.

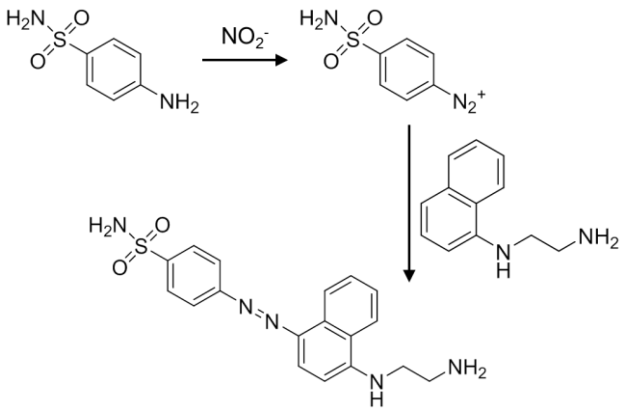

Fig. 1.1. Griess assay reaction with sulphonamide and N-(1-naphthyl)ethylenediamine.

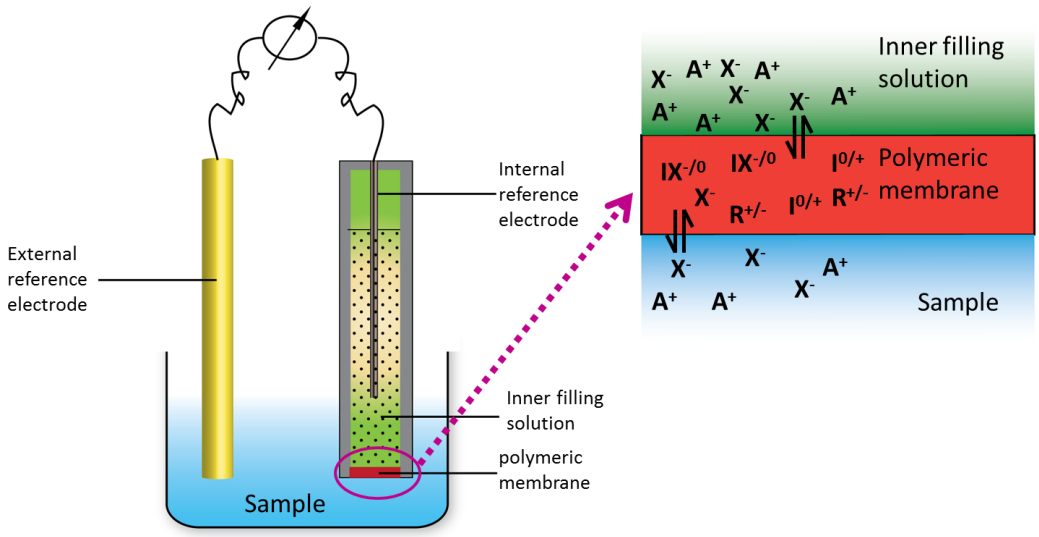

Fig. 1.2. Schematic diagram of a polymeric membrane electrode measuring circuit. Note: X^- = analytes; $R^{+/-}$ = ion additive; $I^{0/+}$ = ionophore; A^+ = counterion.

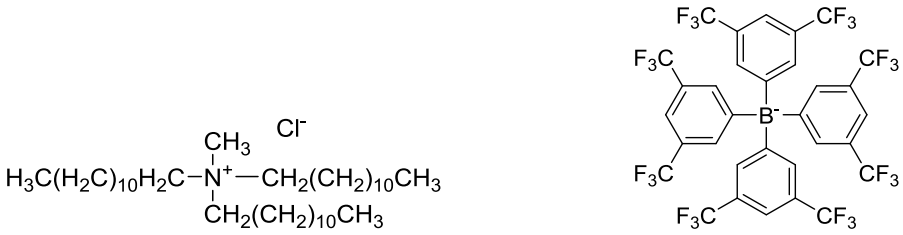

(a) (b)

Fig. 1.3. Structure of ion-exchanger type salts often used to prepare polymer membrane cation and anion selective electrodes; (a) tridodecylmethylammonium chloride (TDMACl) for anion sensors, and (b) potassium tetrakis[3,5-bis(trifluoromethyl)]phenylborate (KTFPB) for cation sensors.

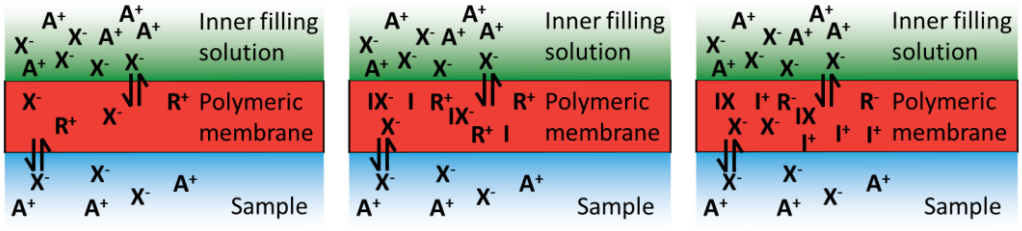

(a) (b) (c)

Fig. 1.4. Schematic to presentation of (a) ionophore-free (only anion exchanger in membrane), (b) neutral carrier and (c) charged carrier response mechanisms for ISE. Note: X^-= primary ion; R^+= ion-exchanger; I= ionophore.

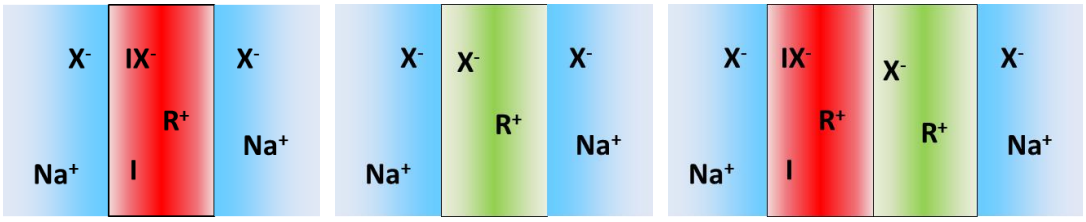

(a) (b) (c)

Fig. 1.5. Illustration of individual membranes with the same plasticized polymer membrane doped with (a) and without (b) ionophore and segmented sandwich membrane (c) by fusing the two individual membranes (a) and (b) together. Note: X^-= primary ion; R^+= ion-exchanger; I= ionophore.

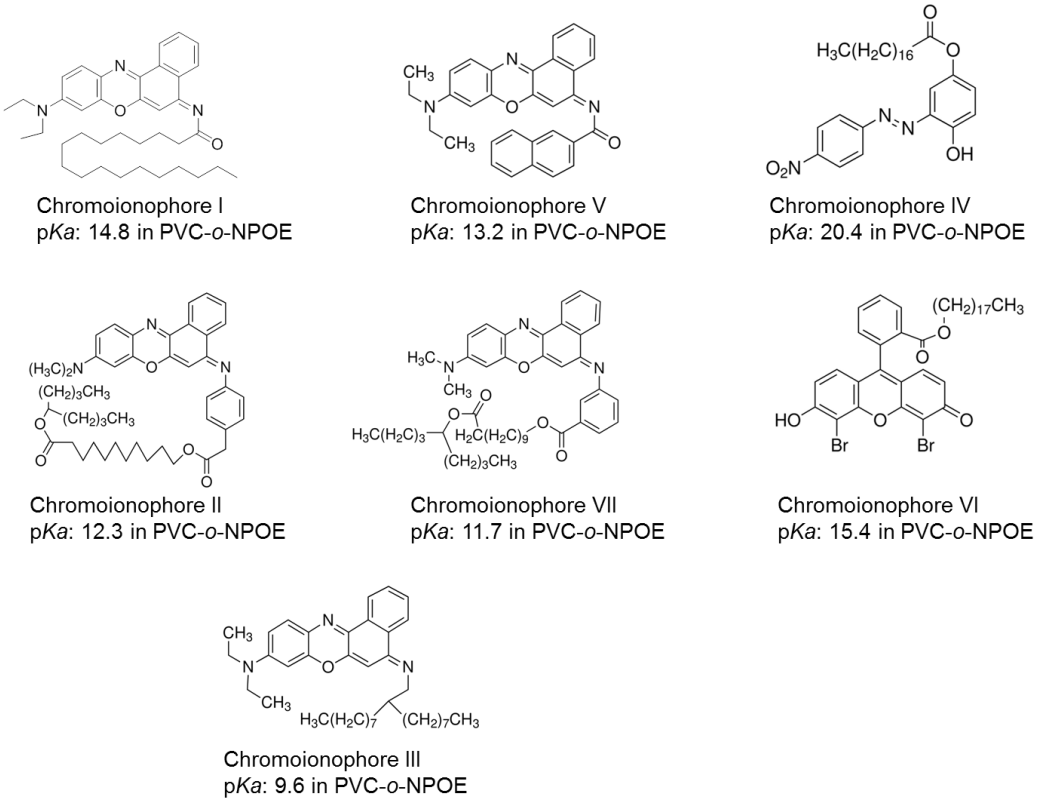

Fig. 1.6. Structures and p*Ka* values of seven commonly used hydrogen-selective chromoiono-phores in PVC/*o*-nitrophenyl octyl ether (*o*-NPOE) films.

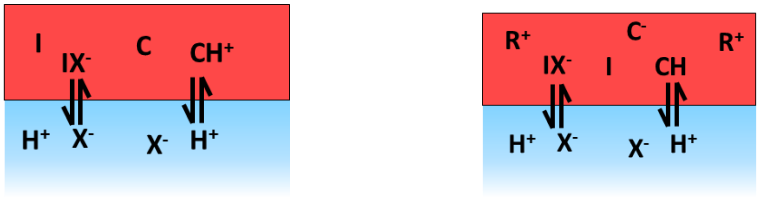

(a) (b)

Fig. 1.7. Optical sensing schemes for anions using a neutral carrier type ionophore coupled with (a) a neutral chromoionophore, and (b) a charged chromoionophore and lipophilic cationic sites. Note: C=chromoionophore, I = ionophore, X^- = anion, R^+ = lipophilic cationic site additive.

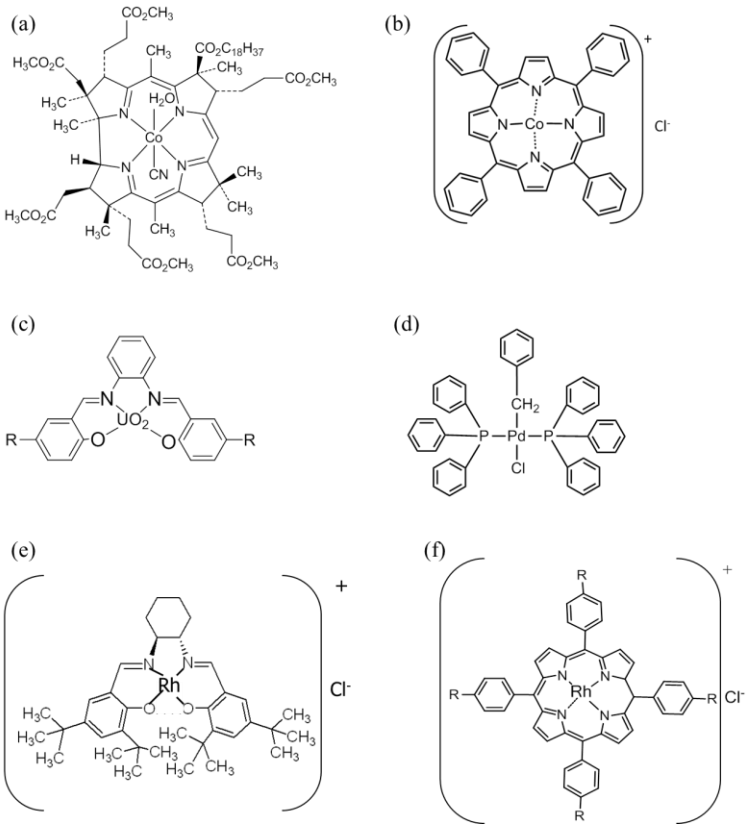

Fig. 1.8. Structures of previously reported nitrite ionophores. (a) aquocyano-Co(III)-a,b,d,e,f,g-hexamethyl c-octadecyl cobyrinate; (b) cobalt(III) 5,10,15,20-tetraphenylporphyrin; (c) uranyl salophen derivatives; (d) benzylbis(triphenylphosphine) palladium(II) chloride; (e) rhodium(III) (*S*,*S*)-(+)-*N*,*N*′-bis(3,5-di-*tert*-butylsalicylidene)-1,2-cyclohexanediamine; (f) rhodium(III) 5,10,15,20-tetraphenylporphyrin chloride when R=H, or rhodium(III) 5,10,15,20-tetra(*p*-*tert*-butylphenyl)porphyrin chloride when R=*tert*-butyl.

1.5. References

[1] N. Benjamin, F. Odriscoll, H. Dougall, C. Duncan, L. Smith, M. Golden, H. McKenzie, "Stomach NO synthesis", *Nature*, **1994**, *368*, 502-502.

[2] J. O. N. Lundberg, E. Weitzberg, J. M. Lundberg, K. Alving, "Intragastric nitric oxide production in humans-measurements in expelled air", *Gut*, **1994**, *35*, 1543-1546.

[3] J. L. Zweier, P. H. Wang, A. Samouilov, P. Kuppusamy, "Enzyme-independent formation of nitric oxide in biological tissues", *Nat. Med.*, **1995**, *1*, 804-809.

[4] J. O. Lundberg, E. Weitzberg, M. T. Gladwin, "The nitrate-nitrite-nitric oxide pathway in physiology and therapeutics", *Nat. Rev. Drug Discov.*, **2008**, *7*, 156-167.

[5] A. Webb, R. Bond, P. McLean, R. Uppal, N. Benjamin, A. Ahluwalia, "Reduction of nitrite to nitric oxide during ischemia protects against myocardial ischemia-reperfusion damage", *Proc. Natl. Acad. Sci. USA*, **2004**, *101*, 13683-13688.

[6] M. R. Duranski, J. J. M. Greer, A. Dejam, S. Jaganmohan, N. Hogg, W. Langston, R. P. Patel, S. F. Yet, X. D. Wang, C. G. Kevil, M. T. Gladwin, D. J. Lefer, "Cytoprotective effects of nitrite during in vivo ischemia-reperfusion of the heart and liver", *J. Clin. Investig.*, **2005**, *115*, 1232-1240.

[7] C. J. Hunter, A. Dejam, A. B. Blood, H. Shields, D. Kim-Shapiro, R. F. Machado, S. Tarekegn, N. Mulla, A. O. Hopper, A. N. Schechter, G. G. Power, M. T. Gladwin, "Inhaled nebulized nitrite is a hypoxia-sensitive NO-dependent selective pulmonary vasodilator", *Nat. Med.*, **2004**, *10*, 1122-1127.

[8] K. Tsuchiya, Y. Takiguchi, M. Okamoto, Y. Izawa, Y. Kanematsu, M. Yoshizumi, T. Tamaki, "Malfunction of vascular control in lifestyle-related diseases: Formation of systemic hemoglobin-nitric oxide complex (HbNO) from dietary nitrite", *J. Pharmacol. Sci.*, **2004**, *96*, 395-400.

[9] D. Reddy, J. R. Lancaster, D. P. Cornforth, "Nitrite inhibition of clostridium-botulinum-electron-spin resonance detection of iron nitric oxide complexes", *Science*, **1983**, *221*, 769-770.

[10] W. Fiddler, J. W. Pensabene, E. G. Piotrowski, J. G. Phillips, J. Keating, W. J. Mergens, H. L. Newmark, "Inhibition of formation of volatile nitrosamines in fried bacon by tuse of cured-solubilized alpha-tocopherol", *J. Agric. Food. Chem.*, **1978**, *26*, 653-656.

[11] M. J. Moorcroft, J. Davis, R. G. Compton, "Detection and determination of nitrate and nitrite: a review", *Talanta*, **2001**, *54*, 785-803.

[12] H. Kodamatani, S. Yamazaki, K. Saito, T. Tomiyasu, Y. Komatsu, "Selective determination method for measurement of nitrite and nitrate in water samples using high-performance liquid chromatography with post-column photochemical reaction and chemiluminescence detection", *J. Chromatogr. A*, **2009**, *1216*, 3163-3167.

[13] A. K. Malik, W. Faubel, "Capillary electrophoretic determination of tetramethylthiuram disulphide (Thiram)", *Anal. Lett.*, **2000**, *33*, 2055 - 2064.

[14] G. M. Greenway, S. J. Haswell, P. H. Petsul, "Characterisation of a micro-total analytical system for the determination of nitrite with spectrophotometric detection", *Anal. Chim. Acta,* **1999**, *387*, 1-10.

[15] Z. Liu, X. Xi, S. Dong, E. Wang, "Liquid chromatography-amperometric detection of nitrite using a polypyrrole modified glassy carbon electrode doped with tungstodiphosphate anion", *Anal. Chim. Acta,* **1997**, *345*, 147-153.

[16] S. Senra-Ferreiro, F. Pena-Pereira, I. Lavilla, C. Bendicho, "Griess micro-assay for the determination of nitrite by combining fibre optics-based cuvetteless UV-Vis micro-spectrophotometry with liquid-phase microextraction", *Anal. Chim. Acta,* **2010**, *668*, 195-200.

[17] M. J. Martínez-Tomé, R. Esquembre, R. Mallavia, C. R. Mateo, "Development of a dual-analyte fluorescent sensor for the determination of bioactive nitrite and selenite in water samples", *J. Pharm. Biomed. Anal.*, **2010**, *51*, 484-489.

[18] M. I. H. Helaleh, T. Korenaga, "Fluorometric determination of nitrite with acetaminophen", *Microchem. J.*, **2000**, *64*, 241-246.

[19] A. Lapat, L. Székelyhidi, I. Hornyák, "Spectrofluorimetric determination of 1,3,5-trinitro-1,3,5-triazacyclohexane (Hexogen, RDX) as a nitramine type explosive", *Biomed. Chromatogr.*, **1997**, *11*, 102-104.

[20] S. M. Shariar, T. Hinoue, "Simultaneous voltammetric determination of nitrate and nitrite ions using a copper electrode pretreated by dissolution/redeposition", *Anal. Sci.*, **2010**, *26*, 1173-1179.

[21] M. Muchindu, T. Waryo, O. Arotiba, E. Kazimierska, A. Morrin, A. J. Killard, M. R. Smyth, N. Jahed, B. Kgarebe, P. G. L. Baker, E. I. Iwuoha, "Electrochemical nitrite nanosensor developed with amine- and sulphate-functionalised polystyrene latex beads self-assembled on polyaniline", *Electrochim. Acta,* **2010**, *55*, 4274-4280.

[22] A. P. Doherty, M. A. Stanley, D. Leech, J. G. Vos, "Oxidative detection of nitrite at an electrocatalytic [$Ru(bipy)_2$poly-(4-vinylpyridine)$_{10}$Cl]Cl electrochemical sensor applied for the flow injection determination of nitrate using a Cu/Cd reductor column", *Anal. Chim. Acta*, **1996**, *319*, 111-120.

[23] D. Tsikas, F.-M. Gutzki, J. Frölich, "Analysis of nitrite and nitrate as 1-nitro-2,4,6-trimethoxybenzene derivatives by reversed-phase HPLC with UV-detection", *Fresenius J. Anal. Chem.*, **1992**, *342*, 95-97.

[24] V. Rizzo, L. Montalbetti, A. L. Rozza, W. Bolzani, C. Porta, G. Balduzzi, E. Scoglio, R. Moratti, "Nitrite/nitrate balance during photoinduced cerebral ischemia in the rat determined by high-performance liquid chromatography with UV and electrochemical detection", *J. Chromatogr. A,* **1998**, *798*, 103-108.

[25] Z. F. Zhao, X. H. Cai, "Determination of trace nitrite by catalytic polarography in ferrous iron thiocyanate medium", *J. Electroanal. Chem.*, **1988**, *252*, 361-370.

[26] A. Daniel, D. Birot, M. Lehaitre, J. Poncin, "Characterization and reduction of interferences in flow-injection analysis for the in situ determination of nitrate and nitrite in sea water", *Anal. Chim. Acta*, **1995**, *308*, 413-424.

[27] A. A. Ensafi, A. Kazemzadeh, "Simultaneous determination of nitrite and nitrate in various samples using flow injection with spectrophotometric detection", *Anal. Chim. Acta*, **1999**, *382*, 15-21.

[28] R. S. Braman, S. A. Hendrix, "Nanogram nitrite and nitrate determination in environmental and biological materials by vanadium(III) reduction with chemiluminescence detection", *Anal. Chem.*, **1989**, *61*, 2715-2718.

[29] J. Hilton, E. Rigg, "Determination of nitrate in lake water by the adaptation of the hydrazine-copper reduction method for use on a discrete analyser: performance statistics and an instrument-induced difference from segmented flow conditions", *Analyst*, **1983**, *108*, 1026-1028.

[30] K. Horita, M. Satake, "Column preconcentrationanalysis-spectrophotometric determination of nitrate and nitrite by a diazotization-coupling reaction", *Analyst*, **1997**, *122*, 1569-1574.

[31] M. Miro, A. Cladera, J. M. Estela, V. Cerda, "Sequential injection spectrophotometric analysis of nitrite in natural waters using an on-line solid-phase extraction and preconcentration method", *Analyst*, **2000**, *125*, 943-948.

[32] H. Chen, Y. Fang, T. An, K. Zhu, J. Lu, "Simultaneous spectrophotometric determination of nitrite and nitrate in water samples by flow-injection analysis", *Int. J. Environ. Anal. Chem.*, **2000**, *76*, 89-98.

[33] P. F. Pratt, K. Nithipatikom, W. B. Campbell, "Simultaneous determination of nitrate and nitrite in biological samples by multichannel flow injection analysis", *Anal. Biochem.*, **1995**, *231*, 383-386.

[34] L. C. Green, D. A. Wagner, J. Glogowski, P. L. Skipper, J. S. Wishnok, S. R. Tannenbaum, "Analysis of nitrate, nitrite, and [15N]nitrate in biological fluids", *Anal. Biochem.*, **1982**, *126*, 131-138.

[35] S. H. Lee, L. R. Field, "Postcolumn fluorescence detection of nitrite, nitrate, thiosulfate, and iodide anions in high-performance liquid chromatography", *Anal. Chem.*, **1984**, *56*, 2647-2653.

[36] A. Büldt, U. Karst, "Determination of nitrite in waters by microplate fluorescence spectroscopy and HPLC with fluorescence detection", *Anal. Chem.*, **1999**, *71*, 3003-3007.

[37] H. Wang, W. Yang, S. C. Liang, Z. M. Zhang, H.-S. Zhang, "Spectrofluorimetric determination of nitrite with 5,6-diamino-1,3-naphthalene disulfonic acid", *Anal. Chim. Acta*, **2000**, *419*, 169-173.

[38] N. Jie, D. Yang, Q. Jiang, Q. Zhang, L. Wei, "A fluorescence quenching method for the determination of nitrite with indole", *Microchem. J.*, **1999**, *62*, 371-376.

[39] H. Li, C. J. Meininger, G. Wu, "Rapid determination of nitrite by reversed-phase high-performance liquid chromatography with fluorescence detection", *J. Chromatogr. B*, **2000**, *746*, 199-207.

[40] S. C. Ma, V. C. Yang, M. E. Meyerhoff, "Heparin-responsive electrochemical sensor: a preliminary study", *Anal. Chem.*, **1992**, *64*, 694-697.

[41] P. W. Dierkes, S. Neumann, G. Klees, W.-R. Schlue, "Multi-barrelled ion-selective

microelectrodes as tools for the investigation of volume regulation mechanisms in invertebrate nerve cells under hyperosmotic conditions", *Electrochim. Acta,* **2003**, *48*, 3373-3380.

[42] A. Knowles, S. Shabala, "Overcoming the problem of non-Ideal liquid ion exchanger selectivity in microelectrode ion flux measurements", *J. Membr. Biol.*, **2004**, *202*, 51-59.

[43] N. Tinkilic, O. Cubuk, I. Isildak, "Glucose and urea biosensors based on all solid-state PVC–NH_2 membrane electrodes", *Anal. Chim. Acta*, **2002**, *452*, 29-34.

[44] J. Bobacka, A. Ivaska, A. Lewenstam, "Potentiometric ion sensors", *Chem. Rev.*, **2008**, *108*, 329-351.

[45] E. Bakker, M. Telting-Diaz, "Electrochemical sensors", *Anal. Chem.*, **2002**, *74*, 2781-2800.

[46] E. Bakker, Y. Qin, "Electrochemical sensors", *Anal. Chem.*, **2006**, *78*, 3965-3984.

[47] W. S. Hughes, "The potential difference between glass and electrolytes in contact with the glass", *J. Am. Chem. Soc.*, **1922**, *44*, 2860-2867.

[48] G. Eisenman, D. O. Rudin, J. U. Casby, "Glass electrode for measuring sodium ion", *Science*, **1957**, *126*, 831-834.

[49] M. S. Frant, J. W. Ross, "Electrode for sensing fluoride ion activity in solution", *Science*, **1966**, *154*, 1553-1555.

[50] T. M. Hseu, G. A. Rechnitz, "Analytical study of a sulfide ion-selective membrane electrode in alkaline solution", *Anal. Chem.*, **1968**, *40*, 1054-1060.

[51] D. Safiulina, V. Veksler, A. Zharkovsky, A. Kaasik, "Loss of mitochondrial membrane potential is associated with increase in mitochondrial volume: Physiological role in neurones", *J. Cell. Physiol.*, **2006**, *206*, 347-353.

[52] E. Bakker, M. Nägele, U. Schaller, E. Pretsch, "Applicability of the phase boundary potential model to the mechanistic understanding of solvent polymeric membrane-based ion-selective electrodes", *Electroanalysis*, **1995**, *7*, 817-822.

[53] D. G. Hall, "Ion-Selective Membrane Electrodes: A General Limiting Treatment of Interference Effects", *J.Phys. Chem.*, **1996**, *100*, 7230-7236.

[54] Y. Qin, E. Bakker, "Evaluation of the separate equilibrium processes that dictate the upper detection limit of neutral ionophore-based potentiometric sensors", *Anal. Chem.*, **2002**, *74*, 3134-3141.

[55] Y. Qin, E. Bakker, "Quantification of the concentration of ionic impurities in polymeric sensing membranes with the segmented sandwich technique", *Anal. Chem.*, **2001**, *73*, 4262-4267.

[56] E. Bakker, P. Bühlmann, E. Pretsch, "The phase-boundary potential model", *Talanta*, **2004**, *63*, 3-20.

[57] M. M. Shultz, O. K. Stefanova, S. B. Mokrov, K. N. Mikhelson, "Potentiometric estimation of the stability constants of ion−ionophore complexes in ion-selective membranes by the sandwich membrane method: theory, advantages, and limitations", *Anal. Chem.*, **2001**, *74*, 510-517.

[58] S. B. Mokrov, O. K. Stefanova, "Manifestations of the coupling of the fluxes of ions and

neutral chelating agent in the membrane potential on the background of an ion exchanger in the membrane", *Elektrokhimiya,* **1985**, 540-543.

[59] S. B. Mokrov, O. K. Stefanova, E. A. Materova, E. E. Ivanova, "Nonequilibrium distribution of neutral complexon specifically interacting with anions in the membrane-potential", *Vestn. Leningr. Univ.,* **1984**, *16*, 41-45.

[60] Y. Mi, E. Bakker, "Determination of complex formation constants of lipophilic neutral ionophores in solvent polymeric membranes with segmented sandwich membranes", *Anal. Chem.*, **1999**, *71*, 5279-5287.

[61] K. Seiler, W. Simon, "Theoretical aspects of bulk optode membranes", *Anal. Chim. Acta,* **1992**, *266*, 73-87.

[62] K. Seiler, W. Simon, "Principles and mechanisms of ion-selective optodes", *Sens. Actuators, B*, **1992**, *6*, 295-298.

[63] W. E. Morf, K. Seiler, B. Lehmann, C. Behringer, K. Hartman, W. Simon, "Carriers for chemical sensors: design features of optical sensors (optodes) based on selective chromoionophores", *Pure Appl. Chem*, **1989**, *61*, 1613-1618.

[64] E. Bakker, P. Bühlmann, E. Pretsch, "Carrier-based ion-selective electrodes and bulk optodes. 1. general characteristics", *Chem. Rev.*, **1997**, *97*, 3083-3132.

[65] E. Bakker, W. Simon, "Selectivity of ion-sensitive bulk optodes", *Anal. Chem.*, **1992**, *64*, 1805-1812.

[66] I. H. A. Badr, "Nitrite-selective optical sensors based on organopalladium ionophores", *Anal. Lett.*, **2001**, *34*, 2019-2034.

[67] S. Dai, Q. Ye, E. Wang, M. E. Meyerhoff, "Optical detection of polycations via polymer film-modified microtiter pates: response mechanism and bioanalytical applications", *Anal. Chem.*, **2000**, *72*, 3142-3149.

[68] E. Bakker, E. Malinowska, R. D. Schiller, M. E. Meyerhoff, "Anion-selective membrane electrodes based on metalloporphyrins: The influence of lipophilic anionic and cationic sites on potentiometric selectivity", *Talanta*, **1994**, *41*, 881-890.

[69] D. Ammann, M. Huser, B. Kräutler, B. Rusterholz, P. Schulthess, B. Lindemann, E. Halder, W. Simon, "Anion selectivity of metalloporphyrins in membranes", *Helv. Chim. Acta*, **1986**, *69*, 849-854.

[70] N. A. Chaniotakis, A. M. Chasser, M. E. Meyerhoff, J. T. Groves, "Influence of porphyrin structure on anion selectivities of manganese(III) porphyrin based membrane electrodes", *Anal. Chem.*, **1988**, *60*, 185-188.

[71] P. Schulthess, D. Ammann, B. Krautler, C. Caderas, R. Stepanek, W. Simon, "Nitrite-selective liquid membrane-electrode", *Anal. Chem.*, **1985**, *57*, 1397-1401.

[72] R. Stepanek, B. Krautler, P. Schulthess, B. Lindemann, D. Ammann, W. Simon, "Aquocyanocobalt(III)-hepta(2-phenylethyl)-cobyrinate as a cationic carrier for nitrite-selective liquid-membrane electrodes", *Anal. Chim. Acta*, **1986**, *182*, 83-90.

[73] U. Schaller, E. Bakker, U. E. Spichiger, E. Pretsch, "Ionoic additives for ion-selective electrodes based on electrically charged carriers", *Anal. Chem.*, **1994**, *66*, 391-398.

[74] E. Malinowska, M. E. Meyerhoff, "Role of axial ligation on potentiometric response of

Co(III) tetraphenylporphyrin-doped polymeric membranes to nitrite ions", *Anal. Chim. Acta*, **1995**, *300*, 33-43.

[75] I. H. A. Badr, M. E. Meyerhoff, S. S. M. Hassan, "Potentiometric anion selectivity of polymer membranes doped with palladium organophosphine complex", *Anal. Chem.*, **1995**, *67*, 2613-2618.

[76] W. Wróblewski, Z. Brzózka, D. M. Rudkevich, D. N. Reinhoudt, "Nitrite-selective ISE based on uranyl salophen derivatives", *Sens. Actuators, B*, **1996**, *37*, 151-155.

[77] M. Pietrzak, M. E. Meyerhoff, "Polymeric membrane electrodes with high nitrite selectivity based on rhodium(III) porphyrins and salophens as ionophores", *Anal. Chem.*, **2009**, *81*, 3637-3644.

Chapter 2

Study of Cobalt(III) Corrole as Neutral Ionophore for Nitrite and Nitrate Detection via Polymeric Membrane Electrodes

2.1. Introduction

There remains great interest in devising new ion-selective polymeric membrane electrodes (ISEs) [1-3] because they are simple, inexpensive and portable devices that can be employed for many practical analytical applications [4-7]. For the detection of anions and cations with such ISEs, plasticized polymeric membranes containing an appropriate ionophore, a lipophilic ion-exchange additive and a plasticizer are typically utilized. To achieve selectivity for the target ion over more lipophilic ionic species in the sample phase, ionophores (ion carriers) with specific binding affinity to the target ion are required within the organic membrane phase. To date, considerable research on developing new ionophores to improve selectivity has been conducted. Among all the anion-selective ionophores examined, hydrophobic metal ion-ligand complexes are

among the most useful, including metallocorrins, metalloporphyrins, and metallosalophens. It is reported that both the metal ion center and the specific ligand structure can influence selectivity [8-10]. Indeed, a strong and selective axial ligation reaction between the ionophore and target anion to form a host-guest complex is required to yield non-Hofmeister selectivity patterns (i.e., selectivity based on free energy of hydration of the anions). The degree of binding between ionophore and target anion can, however, also be altered by the specific ligand structure.

Corroles, like porphyrins, possess a tetrapyrrolic macrocycle structure with an aromatic 18π electron system. Unlike porphyrins, there is a direct linkage between two adjacent pyrrole rings so that the skeletons of corroles are contracted by one carbon [11]. Owing to the above, corroles are trianionic tetradentate ligands when chelated with metal ions, providing interesting properties. Corroles are known to form complexes with various transition and main group metal ions, including Cr(III), Mn(III), Fe(II)/Fe(III), Ru(II)/(III)/(IV), Co(III), Rh(III), Zn(II), Ge(IV), and Sn(IV) [12]. However, relatively few metallocorroles have been reported as anion ionophores for ISEs. Indeed, only 5, 10, 15-triphenylcorrole metallated with Mn(III), Cu(II) and Fe(III) have been studied as receptors in polymeric membrane electrodes for anion detection [13]. Selectivity toward Cl^- was enhanced when Mn(III) was used as the metal ion center for a corrole ligand, while enhanced selectivity toward CO_3^{2-} and HPO_4^{2-} were observed with Cu(II) and Fe(III) as the metal centers, respectively. These findings suggest that corroles complexed with other metal ion centers are worthy of investigation as new ionophore systems for ISEs.

Early research efforts exploited lipophilic vitamin B_{12} derivative complexes with cobalt (III) as the metal center to serve as a charged carrier type ionophore to detect nitrite with high selectivity over chloride [14]. However, this ISE exhibited nearly equivalent potentiometric response to thiocyanate. The core portion of the Co(III)-B_{12} derivative is a corrin ring which resembles the corrole ring, differing in their aromaticity. Since the metal ion center plays a vital role in the anion selectivity patterns observed, a Co(III) corrole should serve as a nitrite-selective ionophore as well. In fact, there have been several other Co(III) complexes studied for preparation of nitrite ISEs, including Co(III) tetraphenylporphyrins [15] and Co(III) phthalocyanine [16].

Herein, we report on the first nitrite-selective polymeric membrane electrodes prepared using a Co(III) corrole complex (cobalt(III) 5,10,15-tris(4-tert-butylphenyl) corrole (Co-tBC); see Fig. 2.1). Unlike diprotonic porphyrins and monoprotonic corrins, corroles are -3 charged ligands when complexed to metal(III) ions. This forces the resulting ionophore to function via only a neutral carrier type response mechanism (i.e., binding of anion as axial ligand to the Co(III) center results in negatively charged complex). It will be shown that membrane electrodes prepared with this metal complex exhibit a Nernstian response to nitrite and display a selectivity pattern that differs significantly from the Hofmeister series when lipophilic cationic sites are added to the membrane phase. As also reported here, the optimal membrane composition for nitrite determination is achieved by varying the amount of lipophilic cationic sites and employing certain plasticizers (ortho-nitrophenyl octyl ether and dioctyl sebacate).

2.2. Experimental

2.2.1. Materials and Reagents

5,10,15-Tris(4-tert-butylphenyl) corrole was purchased from Frontier Scientific (Logan, UT, U.S.A.). Cobalt(II) acetate tetrahydrate ($Co(OAc)_2 \cdot 4H_2O$), sodium acetate anhydrous (NaOAc) and ethanol (EtOH) were products of Sigma Aldrich (Milwaukee, WI, U.S.A.). Triphenylphosphine (PPh_3) was obtained from TCI America (Portland, OR, U.S.A.).

For membrane preparation, poly(vinyl chloride) (PVC), *o*-nitrophenyloctyl ether (*o*-NPOE), dioctyl sebacate (DOS), tributylphosphate (TBP), tridodecylmethylammonium chloride (TDMACl), tetradodecylammonium tetrakis(4-chlorophenyl)borate (ETH 500) and anhydrous tetrahydrofuran (THF) were purchased from Fluka and used without further purification. All anion salts prepared in aqueous solutions for testing selectivity were obtained from Fluka.

2.2.2. Ionophore Preparation

The final ionophore Co(III) 5,10,15-tris(4-tert-butylphenyl) corrole was synthesized via a standard metalation reaction [17]. To prepare the ionophore, 0.104 g (0.15 mmol) of the free base corrole and 180 mg (21.96 mmol) NaOAc were dissolved in EtOH and stirred for 5 min. Then, 180 mg (7.20 mmol) $Co(OAc)_2 \cdot 4H_2O$ and 300 mg (11.46 mmol) PPh_3 were added to the solution. The reaction solution was stirred for 1.5 h at room temperature. The solvent was then evaporated, and the residue was purified by column chromoatography with silica gel and CH_2Cl_2/hexane as the eluent. The obtained product was confirmed by NMR, UV-Vis spectroscopy and ESI-MS spectrometry.

2.2.3. ISE Membrane Preparation and Potentiometric Measurements

One wt% ionophore, 33 wt% PVC, 66 wt% plasticizer (*o*-NPOE or DOS) and different amounts of TDMACl (molar ratio relative to the ionophore) were dissolved in 2 mL THF and the mixture was cast in a glass ring (i.d. 24 mm) placed on a glass slide as described elsewhere[18]. A membrane was formed after solvent evaporation. To assemble the working electrode, a disk of diameter 8 mm was cut from the parent membrane and mounted into an electrode body (Oesch Sensor Technology, Sargans, Switzerland). The inner filling solution was a phosphate buffer solution (pH 4.5, 50 mM) with 10^{-2} M NaCl and 10^{-3} $NaNO_2$ or with 10^{-2} M NaCl and 10^{-3} $NaNO_3$ for nitrite sensors and nitrate sensors, respectively. Before any testing, the assembled ISEs were conditioned in solutions with same composition of the inner filling solution for 24 h. All potentiometric measurements were at ambient temperature and recorded using an EMF16 high impedance interface with EMF Suite 1.03 software (Lawson Labs, Malvern, PA). Potentiometric selectivity coefficients were determined by the separate solutions method [19].

2.2.4. Binding Constant Measurements

The binding constant of nitrite and nitrate with the new ionophore was measured by the segmented sandwich potentiometric method reported previously [20-21]. Briefly, for measurement of the nitrite binding constant, two individual membranes were prepared. One contained 1.0 wt% ionophore, 33 wt% PVC, 66 wt% *o*-NPOE and 10 mol% TDMACl. The other membrane was formulated to contain essentially the same

composition but without any ionophore. A series of 8-mm-diameter disks were cut from the two parent membranes and conditioned in the solution of 0.1 M $NaNO_2$ and 10^{-6} M NaCl overnight. For the following measurements, both the sample and inner filling solutions were the same as the conditioning solution. Each disk was incorporated in an electrode body for an individual test before making the segmented sandwich membrane. If the cell with the membrane with ionophore and the one without ionophore had a potential value that deviated < 5 mV, those two membranes were selected. To avoid developing an aqueous phase in between the membranes, the two individual membranes were dried thoroughly with Kimwipes before making the segmented sandwich membrane ISE device. The sandwich membrane was prepared by pressing the two individual membranes disks tightly together. The sandwich membrane was immediately mounted into an electrode body after drying. During the EMF measurement, the segment containing ionophore was at the sample/membrane interface, while the segment without ionophore was at the membrane/inner filling solution interface. To calculate the membrane potential for a two-membrane system, the cell potential of an individual membrane without ionophore was subtracted from that of the cell potential measured for the sandwich membrane configuration to correct for the constant potentials coming from the inner and outer reference electrodes. The reported binding constant value was averaged for three repeated tests. For the nitrate binding constant measurement, the same procedure was followed except that one membrane was prepared with 1 wt% ionophore, 50 mol% TDMACl, 33 wt% PVC and 66 wt% TBP while the other membrane had the same formulation but without any ionophore. The conditioning solution, inner filling solution and sample solution were all 0.1 M $NaNO_3$ and 10^{-6} M NaCl.

2.3. Results and Discussion

The insertion of cobalt(III) into the corrole ring is quite facile with a rapid color change from dark green (free base corrole) to deep red (Co-tBC) within 10 min upon the addition of cobalt acetate. According to the literature [22-26], most well isolated and fully characterized Co(III) corroles are five- or six-coordinate complexes (with an axial ligand of triphenylphosphine or two axial ligands of pyridine). It was shown that in the absence of axial ligands, cobalt corroles are not stable. Indeed, they oxidize and dimerize, linking two corrole rings by forming a direct C_β-C_β bond [27]. To assure a stable Co(III) complex to serve as the ionophore, triphenylphosphine was employed as an axial ligand to help stabilize the corrole ring.

2.3.1. Potentiometric Response toward Nitrite

It is reported that membranes doped with metal ion-ligand complexes as ionophores have response to pH via the interaction between hydroxide and the central metal ion of the complex [28]. In the previous study [18], pH 4.5 was selected as the background electrolyte solutions for potentiometric nitrite detection. Fig. 2.2 shows that electrodes prepared with plasticized PVC membranes doped with Co-tBC exhibit Nernstian or near Nernstian responses (with slopes of -59.6, -58.7 and -60.3 mV decade^{-1}, respectively) to nitrite over a wide range of concentrations, with a detection limit of ca. 5 μM. The membrane electrodes have relatively short response times (< 30s) for nitrite concentrations of 30 μM and above. When switching the nitrite activity between 0.1

mM to 0.3 mM, the Co-tBC-based membrane electrodes have fast response and rapid recovery times, showing good reversibility (see Fig. 2.3). Like other cobalt(III) complexes, the Co(III) corrole can bind with nitrite effectively and reversibly as an axial ligand to provide an ISE with Nernstian response, achieving equilibrium EMF values within a short period of time.

Dielectric constants of plasticizers used to formulate the polymeric membrane can influence the ion-selective electrode performance for detection of nitrite. Plasticizers with higher dielectric constants require a lower concentration of lipophilic ionic additives in the membrane phase to provide a Nernstian response toward nitrite. Indeed, when using *o*-NPOE ($\varepsilon = 23.9$) as the plasticizer, with the addition of 10 mol% TDMACl, the response slope toward nitrite is -59.6 mV/decade, while 50 mol% TDMACl is required to yield Nernstian response if DOS ($\varepsilon = 3.9$) is employed. However, by introducing more lipophilic ionic sites via the addition of 3 wt% ETH 500 (without changing the neutrality of the entire membrane), and with the presence of 10 mol% TDMACl, a Nernstian response toward nitrite is also observed with DOS plasticized PVC membrane electrodes. All the results of the response slopes and detection limits regarding different membrane compositions are summarized in Table 2.1

2.3.2. Selectivity and Binding Constant

As shown in Fig 2.4, polymeric membrane electrodes, prepared with membranes containing 1.0 wt% Co-tBC in *o*-NPOE plasticized PVC membranes and the addition of 10 mol% TDMACl, exhibit relatively high selectivity to nitrite over other anions. Compared with the classical anion-exchanger-based membrane electrodes, Co-tBC-based

electrodes have a very different selectivity pattern from the Hofmeister sequence (ClO_4^- > SCN^- > NO_3^- > Br^- > Cl^-) with enhanced nitrite response (e.g., shift of ~ 4 logarithmic units in the case of perchlorate and chloride; shift of ~ 3 logarithmic units in the case of thiocyanate, nitrate and bromide), suggesting that nitrite can preferentially interact with the Co-tBC species to form an anion/ionophore complex within the polymeric membrane [14-16]. Such selectivity differences may be the result of the corrole ligand itself as well as the presence of the strongly bound triphenylphosphine fifth ligand.

For ionophore-based ISES, it is well known that the presence of a suitable amount of lipophilic ion-exchanger within the membrane can enhance the potentiometric selectivity toward the target ion. As shown in Fig. 2.4, in the case of *o*-NPOE plasticized membranes, improvement of nitrite selectivity over other anions can be achieved by adding 10 mol% TDMACl. As the TDMACl level increases beyond this level, the selectivity pattern changes toward the classical Hofmeister sequence. For example, when there is 25 mol% of TDMACl present in the membrane, sensors have nitrite selectivity over most anions (thiocyanate, nitrate, bromide and chloride) and only exhibit significant interference from perchlorate (data not shown), the most lipophilic anion. However, when the amount of TDMACl in the polymeric membrane reaches 50 mol%, the resulting electrodes show nitrite selectivity over only bromide and chloride and experience significant interference from more lipophilic anions, indicating the selectivity pattern reverts considerably towards the Hofmeister sequence.

The impact of different membrane plasticizers on potentiometric selectivity was also examined by using two plasticizers with different dielectric constants (*o*-NPOE, $\varepsilon = 23.9$; DOS, $\varepsilon = 3.9$). Unlike polymeric membrane electrodes plasticized with *o*-NPOE,

PVC-DOS membrane electrodes require higher levels of TDMACl additive to avoid sub-Nernstian response to nitrite and to provide significant nitrite selectivity. When the TDMACl level reaches 50 mol%, the electrodes display Nernstian response to nitrite, exhibit nitrite selectivity over most other anions (including thiocyanate, nitrate, bromide and chloride), and have equivalent response to nitrite and perchlorate. Generally, membrane electrodes with *o*-NPOE as the plasticizer offer better performance than those with DOS as the plasticizer in terms of response slope and selectivity. However, if more lipophilic ionic sites are introduced into the membrane via addition of ETH 500 (i.e., increasing ionic strength within the membrane phase), the selectivity pattern is similar to that of *o*-NPOE plasticized PVC membranes (see Fig. 2.4, membrane 7). With TDMACl levels of 10 mol%, sensors have nitrite selectivity over all other anions examined. Selectivity worsens and reverts to the Hofmeister pattern when TDMACl levels are increased. Ion selectivity provided by ion-exchanger based sensor electrodes is governed by the ratio of single ion partition coefficient in polymeric membranes with different plasticizers. With the presence of ionophore, the observed potentiometric selectivity is governed by both the single anion partition coefficient and the relative anion-ionophore complexation constant.

The complex formation constant can be determined by the following equation (without considering ion pairing) [21]:

$$\beta_{xI_n} = (I_T - \frac{nR_T}{z_x})^{-n} \exp(\frac{E_M z_x F}{RT}) \qquad \text{(Eq. 2.1)}$$

where x is the tested ion, and I is the ionophore. The symbol I_T is the total concentration of ionophore in the membrane and R_T is the total concentration of ion additives in the membrane phase. The value of n is the complex stoichiometry which is

1 in this case and z is the charge of the ion which is -1. The calculated logarithmic value of the binding constant, from the above equation, between nitrite and Co-tBC is 5.57±0.13 (for n = 3 experiments, with the potential change of 211±8 mV (see Experimental section for methodology)); based on the membrane electrode formulated with 10 mmol/kg Co-tBC, 1 mmol/kg TDMACl in *o*-NPOE plasticized PVC membrane). For the ion-exchanger-based membrane electrodes, selectivity is only determined by the ratio of single ion partition coefficients of the interfering ion and primary ion [29]. When the ionophore is incorperated into the membrane, the selectivity is dependent on both the ratio of partition coefficients of the interfering ion and analyte ion and the ratio of binding constants of those two ions with the ionophore. Comparing the calculated complex formation constant and the selectivity results, the presence of the ionophore with such binding affinity to nitrite is able to discriminate perchlorate ion by ~ 4.7 orders of magnitude compared to an ionophore-free membrane. This suggests the stronger binding affinity between the Co(III) complex and nitrite overcomes the single ion partition coeffecient resulting from ion lipophilicity (poor hydration energy) in the case of perchlorate.

To date, there is no reported complex formation constant for nitrite and a neutral ionophore such as Co-tBC. To the best of our knowledge, the only reported binding constant between nitrite and a nitrite-selective ionophore is measured with Nitrite Ionophore I [30] which is a charged-carrier type structure. The formation constants determined in that work were calculated as 10.58±0.04 or 10.59±0.08 (with membranes prepared with PVC-DOS and PVC-NPOE, respectively), which is much larger than the complex formation constant between nitrite and Co-tBC found in this work. The

weaker binding is possibly due to the presence of triphenylphosphine as a fifth axial ligand. With such a structure, the cobalt(III) center is in an approximately square pyramidal coordination environment and displaced a little off the corrole plane toward the phosphorous atom [23], making nitrite binding to the metal ion center on the opposite side less favorable.

2.3.3. Lifetime of Membrane Electrodes

According to previous studies, the lifetime of carrier-based polymeric ion-selective electrodes is limited by the loss of ionophore, plasticizer, and ionic site additives from polymeric membrane to the aqueous phase. Response slopes and selectivity are often influenced by this change of membrane composition. In this work, the long-term performance of electrodes with two different membrane formulations was examined. One membrane had the formulation of 1 wt% ionophore and 10 mol% TDMACl in an *o*-NPOE plasticized PVC membrane. The other had a formulation of 1 wt% ionophore, 10 mol% TDMACl and 3 wt% ETH 500 in a DOS plasticized PVC membrane. Starting from day 3, a slight slope drop to -57.1 mV/dec and -58.9 mV/dec for both electrodes was observed. On day 7, only sub-Nernstian response slopes were observed for these two electrodes, one with -53.8 mV/dec and the other with -54.3 mV/dec. Both formulations of the membranes exhibited nitrite selectivity during this one-week period. As soaking time reached day 14, slopes of sensors with both formulations dropped to < -50 mV/dec due to significant composition changes of the membranes.

2.3.4. Enhanced Nitrate Response

Interestingly, further investigation of the influence of the specific plasticizer on the Co-tBC-based membrane electrode response toward anions suggested that incorporation of tributylphosphate as the plasticizer yields an electrode with rather different anion selectivity pattern. With 50 mol% TDMACl present in the TBP-plasticized polymeric membrane containing 1 wt% Co-tBC, the electrodes exhibit enhanced nitrate response in terms of response slope and selectivity (see Fig. 2.5). In fact, with this membrane formulation, modest selectivity for nitrate over nitrite is observed (ca. 10-fold). In the absence of ionophore and only the TDMACl species, membrane electrodes formulated with different plasticizers have significantly different selectivity patterns, which is due to variations in the ratio of single anion partition coefficients into the organic membrane phase. The selectivity pattern of sensors plasticized with TBP (column 5 in Fig. 2.5) looks "compressed", especially for the lipophilic ions (perchlorate, thiocyanate, etc.). With the ionophore in the membrane, selectivity coefficients toward nitrate with respect to perchlorate and thiocyanate were reduced ~ 2 orders of magnitude compared to when *o*-NPOE was employed as the plasticizer (column 2 in Fig. 2.5). With the membrane formulation of 1 wt% of ionophore, 50 mol% of TDMACl in TBP plasticized PVC membrane, the resulting electrode responds to nitrate equally as well as perchlorate. This modestly enhanced selectivity to nitrate indicates that some interaction between nitrate and the ionophore may occur, especially in the presence of the TBP plasticizer. The logarithmic value for the nitrate binding constant measured via the segmented sandwich method was calculated as 2.49 ± 0.06 with the potential change of 39 ± 3.6 mV. However, no reports on the binding of nitrate ion as an axial ligand to a metal ion center or other parts of cobalt(III) corrole complex have been suggested previously. At this

point, additional studies are required to assess the exact mechanism by which nitrate might be interacting weakly with the Co-tBC complex.

2.4. Summary

In summary, a Co(III) corrole species was synthesized from free 5,10,15-tris(4-tert-butylphenyl) corrole via metallization reaction with cobalt acetate and stabilized using a triphenylphosphine axial ligand. The resulting Co(III) complex was incorporated and tested as a neutral carrier within polymeric membrane electrodes, and the resulting electrodes exhibited selectivity patterns that differ significantly from the classical Hofmeister series. Sensors with proper amounts of lipophilic cationic sites showed greatly enhanced nitrite response and selectivity, indicating a strong ligation interaction between the Co(III) corrole and nitrite. Indeed, the complex formation constant (logarithm value) of nitrite and the ionophore provided by the segmented sandwich membrane method was 5.57±0.13, which helps to decrease the observed EMF response to more lipophilic ions by ~ 4 orders of magnitude (when compared to that observed with membranes formulated with quaternary ammonium anion exchanger only). The nature of the membrane plasticizer also had substantial impact on sensor's EMF response. Generally, membranes formulated with plasticizers of a higher dielectric constant required lower amounts of lipophilic cationic sites additives in the polymeric membrane to exhibit optimal Nernstian nitrite response and good nitrite selectivity. The observed selectivity over thiocyanate for the Co-tBC-based membranes with *o*-NPOE is

the best reported to date for nitrite sensors prepared with Co(III) complexes. However, moderately enhanced nitrate response was observed when sensors were plasticized with tributylphosphate (equivalent selectivity coefficient with perchlorate), indicating some weak interaction between nitrate and the ionophore. To better understand this possible interaction, more studies regarding the binding mechanism of nitrate with this ionophore are needed.

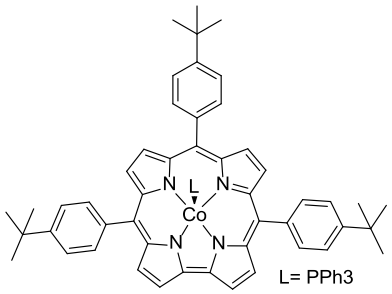

Fig. 2.1. Structure of Co(III) 5,10,15-tris(4-tert-butylphenyl) corrole with triphenylphosphine as the axial ligand.

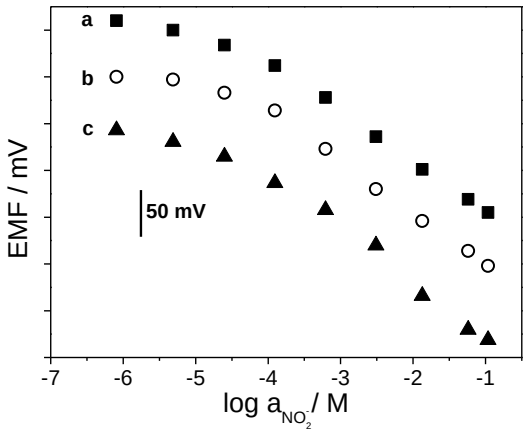

Fig. 2.2. Potentiometric nitrite responses in phosphate buffer solution (pH 4.5) for membrane electrodes with (a) 1 wt% Co-tBC and 10 mol%TDMACl in *o*-NPOE plasticized PVC; (b) 1 wt% Co-tBC and 50 mol% TDMACl in DOS plasticized PVC; and (c) 1 wt% Co-tBC, 10 mol% TDMACl and 3 wt% ETH 500 in DOS plasticized PVC.

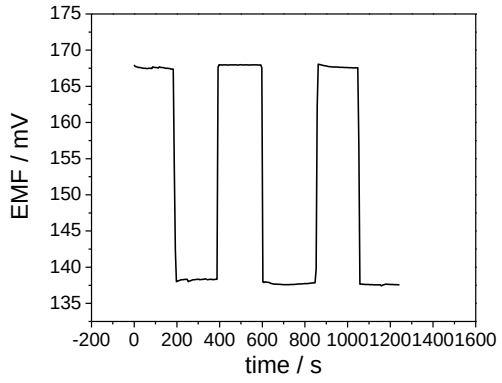

Fig. 2.3. Reversibility of nitrite potentiometric response in phosphate buffer solution (pH 4.5) for membrane electrode formulated with 1 wt% Co-tBC, 10 mol% TDMACl and 3 wt% ETH 500 in DOS plasticized PVC, when changing nitrite concentration back and forth between 0.1 mM and 0.3 mM.

Table 2.1. Potentiometric response characteristics toward nitrite for membrane electrodes formulated with different polymeric membrane compositions. All membranes are plasticized PVC membranes containing 1 wt% of the ionophore.

NO.	Membrane Composition			Slope[a] (mV/dec)	Detection Limit (M)
	TDMACl (mol %)	ETH 500 (wt %)	Plasticizer		
1	5	0	*o*-NPOE	-55.0±0.2	1.7×10^{-5}
2	10	0	*o*-NPOE	-59.6±0.5	6.9×10^{-6}
3	25	0	*o*-NPOE	-60.8±0.3	6.2×10^{-6}
4	50	0	*o*-NPOE	-61.0±0.6	3.8×10^{-6}
5	5	0	DOS	-53.6±0.5	3.1×10^{-5}
6	10	0	DOS	-56.2±0.4	4.9×10^{-5}
7	25	0	DOS	-57.3±0.3	7.9×10^{-6}
8	50	0	DOS	-58.7±0.6	5.0×10^{-6}
9	5	3	DOS	-54.0±0.6	3.7×10^{-5}
10	10	3	DOS	-60.3±0.4	6.3×10^{-6}
11	25	3	DOS	-59.8±0.4	5.1×10^{-6}
12	50	3	DOS	-61.0±0.5	5.0×10^{-6}

([a]average ± s.d. of $n = 3$ electrodes of each type.)

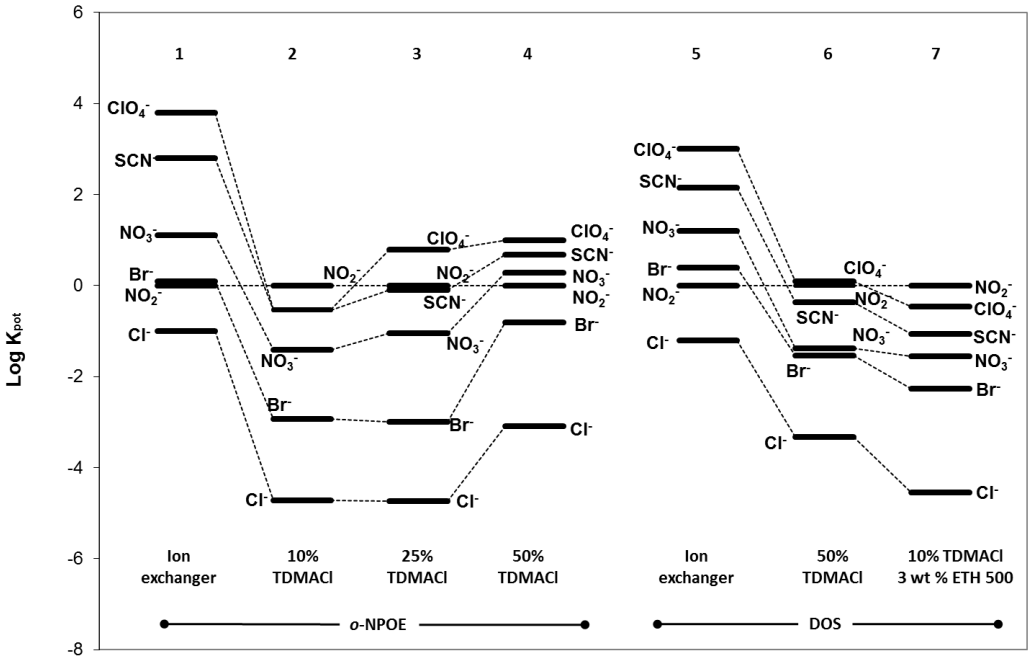

Fig. 2.4. Logarithm of potentiometric selectivity coefficients (relative to nitrite) of Co-tBC-based polymer membrane electrodes in comparison with dissociated ion-exchanger-based membrane electrodes; polymer membranes formulated with (1, 5) 0.5 wt% TDMACl; (2 - 4) 1.0 wt% Co-tBC and different mole percent of TDMACl relative to the ionophore; (6) 1.0 wt% Co-tBC and 50 mol% TDMACl; (7) 1.0 wt% Co-tBC, 10 mol% TDMACl and 3.0 wt% ETH 500. To compare the effect of membrane plasticizers, membranes 1-4 were made with *o*-NPOE, and membranes 5-7 were prepared with DOS.

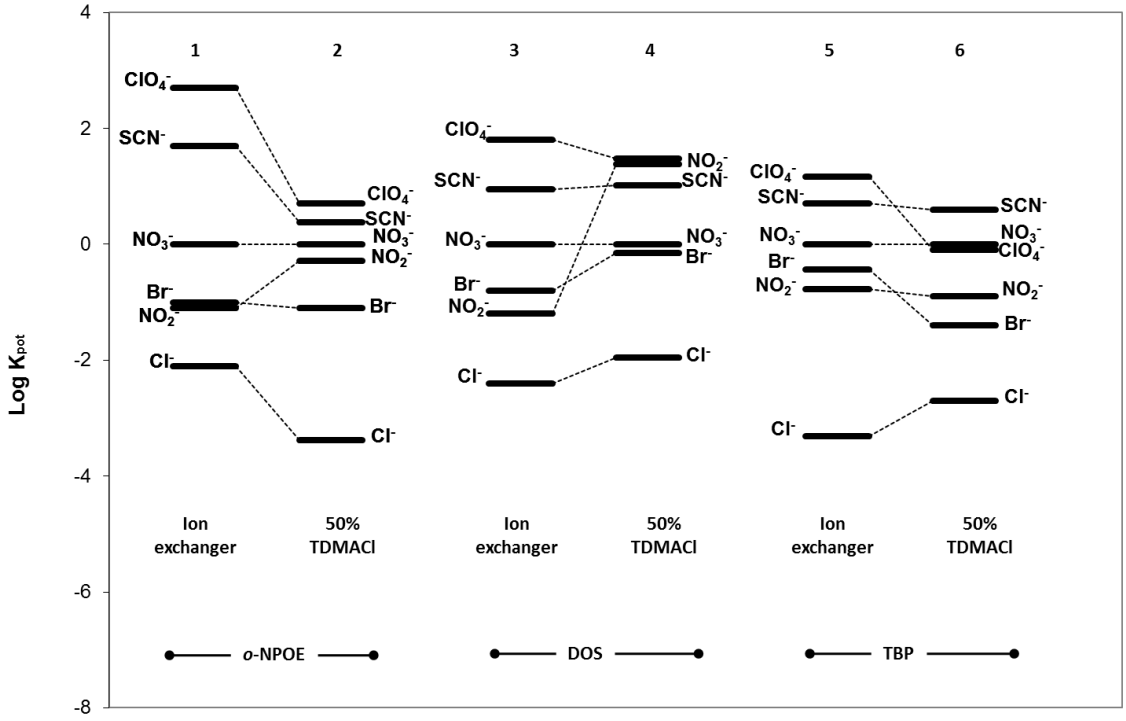

Fig. 2.5. Logarithm of potentiometric selectivity coefficients of Co-tBC-based polymer membrane electrodes (relative to nitrite) in comparison with ion-exchanger-based electrodes; Polymer membrane doped with (1, 3, 5) 0.5 wt% TDMACl; (2, 4, 6) 1.0 wt% Co-tBC and50 mol% TDMACl relative to the ionophore. To compare the effect of membrane plasticizers, membranes 1-2 were formulated with *o*-NPOE, membranes 3-4 were prepared with DOS and membranes 5-6 were cast with TBP as the plasticizer.

2.5. References

[1] J. Bobacka, A. Ivaska, A. Lewenstam, "Potentiometric ion sensors", *Chem. Rev.*, **2008**, *108*, 329-351.

[2] E. Bakker, M. Telting-Diaz, "Electrochemical sensors", *Anal. Chem.*, **2002**, *74*, 2781-2800.

[3] E. Bakker, Y. Qin, "Electrochemical sensors", *Anal. Chem.*, **2006**, *78*, 3965-3984.

[4] S. C. Ma, V. C. Yang, M. E. Meyerhoff, "Heparin-responsive electrochemical sensor: a preliminary study", *Anal. Chem.*, **1992**, *64*, 694-697.

[5] P. W. Dierkes, S. Neumann, G. Klees, W. R. Schlue, "Multi-barrelled ion-selective microelectrodes as tools for the investigation of volume regulation mechanisms in invertebrate nerve cells under hyperosmotic conditions", *Electrochim. Acta*, **2003**, *48*, 3373-3380.

[6] A. Knowles, S. Shabala, "Overcoming the problem of non-Ideal liquid ion exchanger selectivity in microelectrode ion flux measurements", *J. Membr. Biol.*, **2004**, *202*, 51-59.

[7] N. Tinkilic, O. Cubuk, I. Isildak, "Glucose and urea biosensors based on all solid-state PVC–NH_2 membrane electrodes", *Anal. Chim. Acta*, **2002**, *452*, 29-34.

[8] E. Bakker, E. Malinowska, R. D. Schiller, M. E. Meyerhoff, "Anion-selective membrane electrodes based on metalloporphyrins: The influence of lipophilic anionic and cationic sites on potentiometric selectivity", *Talanta*, **1994**, *41*, 881-890.

[9] D. Ammann, M. Huser, B. Kräutler, B. Rusterholz, P. Schulthess, B. Lindemann, E. Halder, W. Simon, "Anion selectivity of metalloporphyrins in membranes", *Helv. Chim. Acta*, **1986**, *69*, 849-854.

[10] N. A. Chaniotakis, A. M. Chasser, M. E. Meyerhoff, J. T. Groves, "Influence of porphyrin structure on anion selectivities of manganese(III) porphyrin based membrane electrodes", *Anal. Chem.*, **1988**, *60*, 185-188.

[11] J. Buchler, C. Dreher, F. Künzel, S. Licoccia, R. Paolesse, J. Šima, in *Metal Complexes with Tetrapyrrole Ligands III, Vol. 84*, Springer Berlin / Heidelberg, **1995**, pp. 71-133.

[12] A. H. Iris, G. Zeev, "Coordination chemistry of corroles with focus on main group elements", *Coord. Chem. Rev.*, **2011**, *255*.

[13] L. Lvova, C. Di Natale, A. D'Amico, R. Paolesse, "Corrole-based ion-selective electrodes", *J. Porphyrins Phthalocyanines*, **2009**, *13*, 1168-1178.

[14] P. Schulthess, D. Ammann, B. Krautler, C. Caderas, R. Stepanek, W. Simon, "Nitrite-selective liquid membrane-electrode", *Anal. Chem.*, **1985**, *57*, 1397-1401.

[15] E. Malinowska, M. E. Meyerhoff, "Role of axial ligation on potentiometric response of Co(III) tetraphenylporphyrin-doped polymeric membranes to nitrite ions", *Anal. Chim. Acta*, **1995**, *300*, 33-43.

[16] L. Jun-Zhong, W. Xiao-Chun, Y. Ruo, L. Hui-Gai, Y. Ru-Qin, "Cobalt phthalocyanine derivatives as neutral carriers for nitrite-sensitive poly(vinyl chloride) membrane electrodes", *Analyst*, **1994**, *119*.

[17] M. Atif, G. Ilona, G. Israel, G. Zeev, "Synthesis and structural characterization of a novel covalently-bound corrole dimer", *Chem. Eur. J.*, **2001**, *7*.

[18] M. Pietrzak, M. E. Meyerhoff, "Polymeric membrane electrodes with high nitrite selectivity based on rhodium(III) porphyrins and salophens as ionophores", *Anal. Chem.*, **2009**, *81*, 3637-3644.

[19] E. Bakker, P. Bühlmann, E. Pretsch, "Carrier-Based Ion-Selective Electrodes and Bulk Optodes. 1. General Characteristics", *Chem. Rev.*, **1997**, *97*, 3083-3132.

[20] M. M. Shultz, O. K. Stefanova, S. B. Mokrov, K. N. Mikhelson, "Potentiometric estimation of the stability constants of ion−ionophore complexes in ion-selective membranes by the sandwich membrane method: theory, advantages, and limitations", *Anal. Chem.*, **2001**, *74*, 510-517.

[21] Y. Mi, E. Bakker, "Determination of complex formation constants of lipophilic neutral ionophores in solvent polymeric membranes with segmented sandwich membranes", *Anal. Chem.*, **1999**, *71*, 5279-5287.

[22] R. Paolesse, *The Porphyrin Handbook, Vol. 2*, Academic Press, New York, **2000**.

[23] R. Paolesse, S. Licoccia, G. Bandoli, A. Dolmella, T. Boschi, "First direct synthesis of a corrole ring from a monopyrrolic precursor: crystal and molecular structure of (triphenylphosphine)(5,10,15-triphenyl-2,3,7,8,12,13,17,18-octamethylcorrolato) cobalt(III)-dichloromethane", *Inorg. Chem.*, **1994**, *33*, 1171-1176.

[24] V. A. Adamian, F. D'Souza, S. Licoccia, M. L. Di Vona, E. Tassoni, R. Paolesse, T. Boschi, K. M. Kadish, "Synthesis, characterization, and electrochemical behavior of (5,10,15-Tri-X-phenyl-2,3,7,8,12,13,17,18-octamethylcorrolato)cobalt(III) triphenylphosphine complexes, where X = *p*-OCH_3, *p*-CH_3, *p*-Cl, *m*-Cl, *o*-Cl, *m*-F, *o*-F, or H", *Inorg. Chem.*, **1995**, *34*, 532-540.

[25] R. Paolesse, S. Mini, F. Sagone, T. Boschi, L. Jaquinod, D. J. Nurco, K. M. Smith, "5,10,15-Triphenylcorrole: a product from a modified Rothemund reaction", *Chem. Commun.*, **1999**, *0*, 1307-1308.

[26] Y. Murakami, S. Yamada, Y. Matsuda, K. Sakata, "Transition-metal complexes of pyrrole pigments. XV. coordination of pyridine bases to the axial sites of cobalt corroles", *Bull. Chem. Soc. Jpn.*, **1978**, *51*, 123-129.

[27] B. Ramdhanie, L. Zakharov, A. Rheingold, D. Goldberg, "Synthesis, structures, and properties of a series of four-, five-, and six-coordinate cobalt(III) triazacorrole complexes: the first examples of transition metal corrolazines", *Inorg. Chem.*, **2002**, *41*, 4105-4107.

[28] V. V. Egorov, E. M. Rakhman'ko, A. A. Rat'ko, "Metalloporphyrin-based anion-selective electrodes with unusual selectivity", *J. Anal. Chem.*, **2002**, *57*, 46-53.

[29] W. E. Morf, *The principles of ion-selective electrodes and of membrane transport*, Elsevier, **1981**.

[30] Y. Qin, E. Bakker, "Quantitive binding constants of H^+-selective chromoionophores and anion ionophores in solvent polymeric sensing membranes", *Talanta*, **2002**, *58*, 909-918.

Chapter 3

Study of Rhodium(III) Corrole as a Neutral Ionophore for Nitrite Detection via Polymeric Membrane Electrodes

3.1. Introduction

As stated in Chapter 1, nitrite plays an important role in many fields. Our group is interested in nitrite detection, especially owing to the reduction of nitrite to nitric oxide (NO) *in vivo*, Nitric oxide is a potent biological messenger, through both enzymatic and nonenzymatic pathways [1-3]. Nitrite levels in physiological fluids provide indirect information regarding NO levels, and low NO levels can signify higher risk of thrombotic events [4]. Additionally, nitrite has been used as a food preservative in some foods, especially cured meats as a corrosion inhibitor [5], which is an important public health concern since nitrite can react with secondary amines to form carcinogenic nitrosamines [6]. Consequently, there is an essential need for sensors that could detect nitrite with good sensitivity and selectivity in biological /environmental/food samples with the presence of other ions.

As documented already in prior chapters in this thesis, polymeric membrane type

ion-selective electrodes (ISEs) can act as simple, inexpensive and portable sensor devices for nitrite determination. Among a wide range of ionophores studied for fabricating nitrite ISEs, data obtained with Rh(III) porphyrin-doped membrane electrodes suggest that Rh(III) porphyrins can function as either/both a charged carrier and neutral carrier with respect to serving as an ionophore for nitrite. In the neutral carrier mode, two nitrites must bind as axial ligands to the Rh(III) center to create a negatively charged complex. For the charged carrier mechanism, only one nitrite binds as axial ligand, yielding a neutral species. The mixed mechanism complicates the sensing chemistry and worsens the sensitivity and/or selectivity to nitrite.

As described in Chapter 2, unlike diprotonic porphyrins and monoprotonic corrins, corroles are -3 charged ligands when complexed to metal(III) ions, for example, rhodium(III). After being metallated with Rh(III), the given Rh(III) corrole complex can only be neutral, which also ensures that there's only one sensing chemistry of the ionophore in the polymeric membrane for nitrite detection (i.e., binding of anion as axial ligand to the Rh(III) center results in a negatively charged complex). Recently reported Co(III) corrole species show strong binding affinity to nitrite (see Chapter 2), so it is plausible that a Rh(III) corrole species could also be used as an ionophore for nitrite detection, since Rh(III) and Co(III) exhibit similar ligation chemistry [7].

In this chapter, rhodium(III) 5,10,15-tris(4-tert-butylphenyl) corrole (Rh-tBC) is synthesized and incorporated into polymeric membranes along with lipophilic anion-exchanger sites and different types of plasticizers to fabricate nitrite sensors. It will be shown that membrane electrodes prepared with Rh-tBC as the ionophore exhibit near Nernstian response slope toward nitrite when appropriate amounts of lipophilic

anion-exchanger sites are added to the membrane phase. Such sensors also display a selectivity pattern that differs significantly from the classical Hofmeister sequence, with enhanced nitrite selectivity over most anions, including perchlorate. However, the sensors do experience substantial interference from thiocyanate ion, indicating that the binding affinity between nitrite and Rh-tBC is not as strong as that between nitrite and Co-tBC. An experiment to obtain the complex formation constant for nitrite interaction with the Rh-tBC species provides results that suggest that the binding affinity is more than one and a half orders of magnitude lower than that between nitrite and Co-tBC.

3.2. Experimental

3.2.1. Materials and Reagents

5,10,15-Tris(4-tert-butylphenyl) corrole was purchased from Frontier Scientific (Logan, UT, U.S.A.). Rhodium carbonyl chloride(I), potassium carbonate, benzene, hexane and dichloromethane were products of Sigma Aldrich (Milwaukee, WI, U.S.A.). Triphenylphosphine (PPh_3) was obtained from TCI America (Portland, OR, U.S.A.).

For polymeric membrane preparation, poly(vinyl chloride) (PVC), *o*-nitrophenyloctyl ether (*o*-NPOE), dioctyl sebacate (DOS), tridodecylmethylammonium chloride (TDMACl), and anhydrous tetrahydrofuran (THF) were purchased from Fluka and used without further purification. All anion salts prepared in aqueous solutions for testing selectivity were obtained from Fluka.

3.2.2. Ionophore Preparation

The rhodium(III) 5,10,15-tris(4-tert-butylphenyl) corrole with triphenylphosphine as an axial ligand (Rh-tBP) was prepared according to the metallization reaction reported previously [8]. Briefly, 39.4 mg of the free base corrole (0.06 mmol) was initially dissolved in anhydrous benzene and stirred for 5 min. Then, 70 mg (0.18 mmol) $[Rh(CO)_2Cl]_2$, 82 mg (0.31 mmol) PPh_3 and 0.87 g (6.3 mmol) K_2CO_3 were added to the solution. After the solution was heated to reflux for 4 h, it was cooled to room temperature, followed by filtration and solvent evaporation. The residue was purified by chromatography with silica gel and CH_2Cl_2/hexane (1:4) as the eluent. The obtained product was confirmed by NMR, UV-Vis spectroscopy and ESI-MS spectrometry.

3.2.3. ISE Membrane Preparation and Potentiometric Measurements

One wt% ionophore, 33 wt% PVC, 66 wt% plasticizer (*o*-NPOE or DOS) and different amounts of TDMACl (molar ratio relative to the ionophore) were dissolved in 2 mL THF, and the mixture was cast in a glass ring (i.d. 24 mm) placed on a glass slide as described elsewhere [9]. A membrane was formed after solvent evaporation. To assemble the working electrode, a disk of diameter 8 mm was cut from the parent membrane and mounted into an electrode body (Oesch Sensor Technology, Sargans, Switzerland). The inner filling solution was a phosphate buffer solution (pH 4.5, 50 mM) with 10^{-2} M NaCl and 10^{-3} $NaNO_2$. Before any testing, the assembled ISEs were conditioned in solutions with same composition as the inner filling solution for 24 h. All potentiometric measurements were taken at ambient temperature and recorded using an EMF16 high impedance interface with EMF Suite 1.03 software (Lawson Labs, Malvern, PA).

Potentiometric selectivity coefficients were determined by the separate solutions method [10].

3.2.4. Binding Constant Measurements

The binding constant of nitrite and nitrate with the new ionophore was measured by the segmented sandwich potentiometric method reported previously [11-12]. Briefly, for measurement of the nitrite binding constant, two individual membranes were prepared; one contained 1.0 wt% ionophore, 33 wt% PVC, 66 wt% *o*-NPOE and 50 mol% TDMACl, and the other membrane was formulated to contain essentially the same composition but without any ionophore. A series of 8-mm-diameter disks were cut from the two parent membranes and conditioned in the solution of 0.1 M $NaNO_2$ and 10^{-6} M NaCl overnight. For the following measurements, both the sample and inner filling solutions were the same as the conditioning solution. Each disk was incorporated in an electrode body for an individual test before making the segmented sandwich membrane. If the cell with the membrane with ionophore and the one without ionophore had a potential value that deviated < 5 mV, those two membranes were selected. To avoid developing an aqueous phase between the membranes, the two individual membranes were dried thoroughly with Kimwipes before preparing the segmented sandwich membrane ISE device. The sandwich membrane was prepared by pressing the two individual membranes disks tightly together. The sandwich membrane was immediately mounted into an electrode body after drying. During the EMF measurement, the segment containing ionophore was at the sample/membrane interface, while the segment without ionophore was at the membrane/inner filling solution interface. To calculate the

membrane potential for a two-membrane system, the cell potential of the individual membrane without ionophore was subtracted from that of the cell potential measured for the sandwich membrane configuration to correct for the constant potentials coming from the inner and outer reference electrodes. The reported binding constant value was averaged for three repeated tests.

3.3. Results and Discussion

Similar to the cobalt(III) corrole studied in Chapter 2, the rhodium(III) corrole also needs one or two axial ligands (to form five- or six- coordinated complexes, respectively) to stabilize the metal ion-ligand complex. In this study, triphenylphosphine is again used as the fifth ligand directly binding to the metal center. The insertion reaction was monitored by TLC examination until quantitative disappearance of starting material was observed. The final ligated Rh(III) corrole product was dark red, which is significantly different in color from free base corrole (dark green).

3.3.1. Potentiometric Response to Nitrite

As shown in Fig. 3.2, electrodes prepared with either *o*-NPOE or DOS plasticized PVC membranes doped with Rh-tBC exhibit near Nernstian responses (with slopes of -58.6 and -57.8 mV decade^{-1}, respectively) to nitrite over a wide range of concentrations, with detection limits shown in Table 3.1. Similar to the results obtained previously with Rh(III) porphyrins [9], the EMF response data suggests that nitrite can be a good axial

ligand for the Rh(III) corrole species, and that the binding affinity is strong enough to provide sufficient EMF response within a short period of time.

It is known that response of an ion-selective membrane electrode is governed by the binding strength between the target ion as well as membrane ionic strength, which is influenced by both the plasticizer dielectric constants and the amount of lipophilic ionic sites. Table 3.1 summarizes the response characteristics of membrane electrodes with different formulations. Indeed, when using *o*-NPOE (ε = 23.9) as the plasticizer, the Rh-tBC based electrodes have better response slopes and lower detection limit toward nitrite than membrane electrodes plasticized with DOS (ε = 3.9) when all other components of the membranes are the same. Moreover, when more TDMACl is added for either *o*-NPOE or DOS plasticized membranes, the electrodes exhibit better response slopes (more approaching a Nernstian response) and lower detection limits. When 50 mol% TDMACl is doped within the membranes, the detection limit becomes around 1 order of magnitude lower than electrodes containing 10 mol% TDMACl. Compared to Co-tBC based electrodes (see Chapter 2), Rh-tBC-based sensors require more TDMACl to achieve Nernstian response when the same plasticizer is used.

3.3.2. Selectivity and Binding Constant

Compared to classic anion-exchanger-based electrodes, Rh-tBC based electrodes exhibit different selectivity patterns from the Hofmeister sequence (ClO_4^- > SCN^- > NO_3^- > Br^- > Cl^-). When 10 mol% of TDMACl is doped within the membranes, electrodes exhibit enhanced nitrite response with relatively high selectivity for nitrite over most other anions (e.g., shift of ~ 4 logarithmic units in the case of perchlorate; shift of ~3

logarithmic units in the case of chloride; shift of ~ 2 logarithmic units in the case of thiocyanate and nitrate; shift of ~1 logarithmic unit in the case of bromide), suggesting that nitrite can preferentially interact with the Rh-tBC species to form an anion/ionophore complex within the polymeric membrane. Similar to that reported for electrodes formulated previously with Rh(III) porphyrin and other Co(III) complexes species [9, 13-14], thiocyanate is the most interfering anionic species. As shown in Fig. 3.3, although electrodes doped with Rh-tBC show selectivity to nitrite over most anions, they do not adequately discriminate thiocyanate which can interfere during nitrite detection in real samples. Compared to Co-tBC based electrodes which show greatly enhanced selectivity to nitrite over thiocyanate, the selectivity results obtained from Rh-tBC-based sensors suggest weaker interaction between the metal ion center of rhodium(III) with nitrite, compared to cobalt(III) and nitrite.

Amounts of lipophilic ion-exchanger in the polymeric membrane have a substantial impact on sensor performance. As shown in Fig. 3.3, in the case of o-NPOE plasticized membrane electrodes, by adding 10 mol% TDMACl, selectivity to nitrite is enhanced over most anions including perchlorate. As the TDMACl level increases, there is more interference from other anions, especially lipophilic anions, leading to worse selectivity. For example, with 25 mol% TDMACl present in the membrane, sensors show selectivity to nitrite over nitrate, bromide, and chloride, and equivalent response to perchlorate, but significant interference from thiocyanate. At higher TDMACl levels (50%) the membrane electrodes exhibit nitrite selectivity over bromide and chloride only, and yield very large interference from thiocyanate, perchlorate and nitrate. The resulting selectivity pattern is somewhat different from a classic Hofmeister sequence, since

thiocyanate is a much greater interferent species than perchlorate.

To study the influence of plasticizers on sensor performance, two plasticizers with different dielectric constants (*o*-NPOE, ε = 23.9; DOS, ε = 3.9) were used. With smaller amount of TDMACl (10 mol%; see Fig. 3.3 column 6), membrane electrodes show enhanced selectivity to nitrite over nitrate, bromide and chloride compared to classical lipophilic ion-exchanger-based membrane electrodes, indicating there is interaction between the Rh-tBC species and nitrite. Unlike *o*-NPOE plasticized membrane electrodes that contain the same amount of TDMACl, DOS plasticized membrane electrodes show a selectivity pattern with perchlorate as the most favored anion. As the amount of TDMACl increases, sensors exhibit larger response to thiocyanate with a similar selectivity pattern as that observed with the *o*-NPOE plasticized membrane electrodes. When there is 25 mol% and 50 mol% TDMACl present in the membrane, electrodes only show nitrite selectivity over bromide and chloride. Overall, membrane electrodes doped with Rh-tBC as the ionophore have worse response and selectivity to nitrite comparing to Co-tBC based membrane electrodes. In the presence of the ionophore, the potentiometric selectivity is governed by both the single anion partition coefficient and the relative anion-ionophore complexation constant. The moderate enhanced nitrite selectivity over other anions suggests that there is some binding affinity between Rh-tBC and nitrite but not large enough to discriminate from all other anions, especially the lipophilic ones.

As mentioned in Chapter 2, the complex formation constant can be determined by the following equation (without considering ion pairing) [12]:

$$\beta_{xI_n} = (I_T - \frac{nR_T}{z_x})^{-n} \exp(\frac{E_M z_x F}{RT}) \qquad \text{(Eq. 3.1)}$$

In which, x is the tested ion, and I is the ionophore. The symbol I_T is the total concentration of ionophore in the membrane, and R_T is the total concentration of ion additives in the membrane phase. The value of n is the complex stoichiometry which is 1 in this case, and z is the charge of the ion which is -1. Based on membrane electrodes formulated with 10 mmol/kg Co-tBC, 5 mmol/kg TDMACl in *o*-NPOE plasticized PVC membrane, the calculated logarithmic value of the binding constant, from the above equation, between nitrite and Rh-tBC, is 4.04±0.08 with overall potential change of 122±5 mV (n=3, see experimental section). This binding affinity allows membrane electrodes doped with Rh-tBC to discriminate perchlorate ion by ~ 4 orders of magnitude and thiocyanate ion by ~ 2 orders of magnitude compared to an ionophore-free membrane. However, the binding constant between nitrite and Rh-tBC is more than 1.5 orders of magnitude lower than that of nitrite and Co-tBC, which can explain the better response and selectivity obtained from membrane electrodes formulated with Co-tBC as the ionophore (see Chapter 2). Indeed, both the metal ion center and the specific ligand structure can influence selectivity.

3.4. Summary

In this chapter, a nitrite-selective sensor has been developed using rhodium(III) corrole as the active membrane ionophore. Membrane electrodes incorporating the rhodium(III) corrole species show near Nernstian response and low detection limit in the μM range toward nitrite when optimal amounts of lipophilic ion-additives are added to the

membranes plasticized with either *o*-NPOE and DOS. Sensors exhibit enhanced selectivity to nitrite over most anions, displaying selectivity patterns that differ significantly from the Hofmeister sequence, including perchlorate with a selectivity coefficient shift of ~4 orders of magnitude, indicating a high binding affinity between nitrite and the ionophore. However, membrane electrodes experience large interference from thiocyanate, indicating a weaker binding affinity between nitrite and Rh-tBC compared to that between nitrite and Co-tBC. Complex formation constant measurement by segmented sandwich membrane method yield a binding affinity of 4.04 ± 0.08 (logarithmic value), which is one and a half orders of magnitude less than that of the cobalt(III) corrole species.

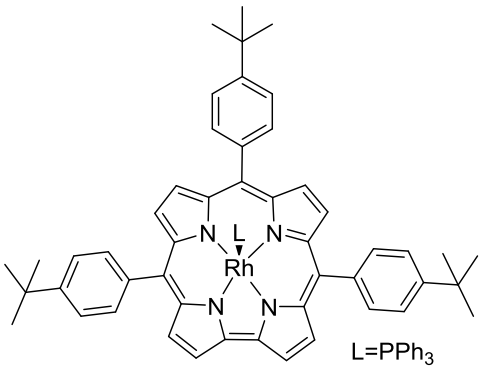

Fig. 3.1. Structure of Rh(III) 5,10,15-tris(4-tert-butylphenyl) corrole with triphenylphosphine as the axial ligand.

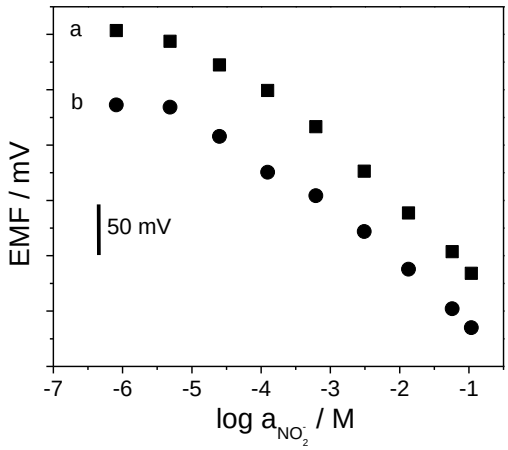

Fig. 3.2. Potentiometric nitrite responses in phosphate buffer solution (pH 4.5) for membrane electrodes with (a) 1 wt% Rh-tBC and 50 mol% TDMACl in *o*-NPOE plasticized PVC; (b) 1 wt% Rh-tBC and 50 mol% TDMACl in DOS plasticized PVC.

Table 3.1. Potentiometric response characteristics toward nitrite for membrane electrodes formulated with different polymeric membrane compositions. All membranes are plasticized PVC membranes containing 1 wt% of the ionophore.

Membrane		Slope[a] (mV/dec)	Detection Limit (M)
Plasticizers	Amount of TDMACl (mol%)		
o-NPOE	10	-54.2 ± 0.04	5.2×10^{-5}
	25	-57.1 ± 0.07	7.9×10^{-6}
	50	-58.6 ± 0.06	5.9×10^{-6}
DOS	10	-53.7 ± 0.08	1.2×10^{-4}
	25	-56.3 ± 0.05	8.9×10^{-5}
	50	-57.8 ± 0.06	2.3×10^{-5}

([a]average $\pm$ s.d. of $n = 3$ electrodes of each type.)

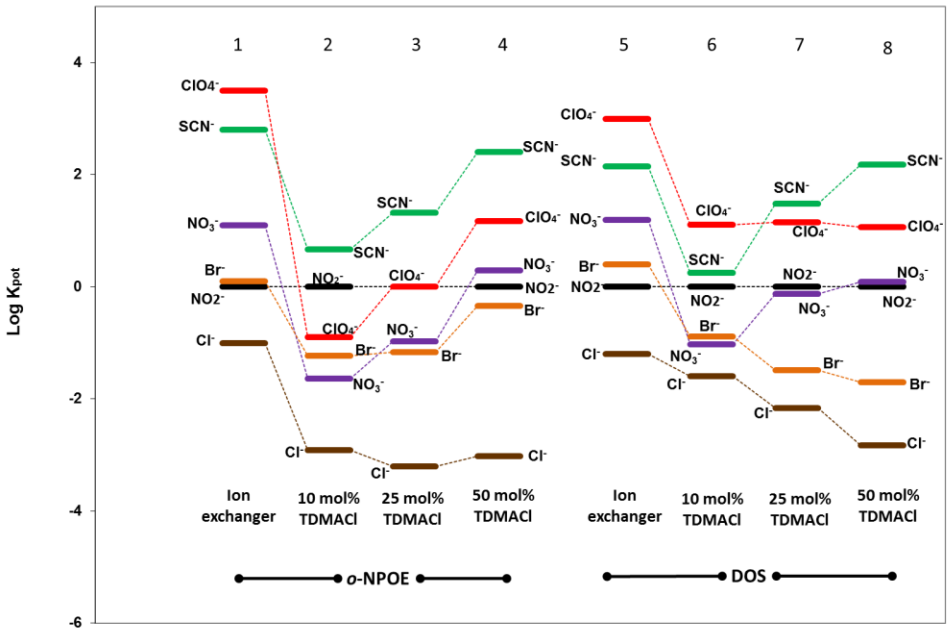

Fig. 3.3. Logarithm of potentiometric selectivity coefficients (relative to nitrite) of Rh-tBC-based polymer membrane electrodes in comparison with dissociated ion-exchanger-based membrane electrodes; Polymer membranes were formulated with (1, 5) 0.5 wt% TDMACl; (2 - 4) 1.0 wt% Rh-tBC and different mole percent of TDMACl relative to the ionophore; (6 - 8) 1.0 wt% Rh-tBC and different mole percent of TDMACl relative to the ionophore. To compare the effect of membrane plasticizers, membrane 1-4 were made with *o*-NPOE, and membranes 5-8 were prepared with DOS.

3.5. References

[1] N. Benjamin, F. Odriscoll, H. Dougall, C. Duncan, L. Smith, M. Golden, H. McKenzie, "Stomach NO synthesis", *Nature*, **1994**, *368*, 502-502.

[2] J. O. N. Lundberg, E. Weitzberg, J. M. Lundberg, K. Alving, "Intragastric nitric oxide production in humans - measurements in expelled air", *Gut*, **1994**, *35*, 1543-1546.

[3] J. L. Zweier, P. H. Wang, A. Samouilov, P. Kuppusamy, "Enzyme-independent formation of nitric oxide in biological tissues", *Nat. Med.*, **1995**, *1*, 804-809.

[4] J. Shao, T. Miyata, K. Yamada, N. Hanafusa, T. Wada, K. L. Gordon, R. Inagi, K. Kurokawa, T. Fujita, R. J. Johnson, M. Nangaku, "Protective role of nitric oxide in a model of thrombotic microangiopathy in rats", *J. Am. Soc. Nephrol.*, **2001**, *12*, 2088-2097.

[5] D. Reddy, J. R. Lancaster, D. P. Cornforth, "Nitrite inhibition of clostridium-botulinum-electron-spin resonance detection of iron nitric oxide complexes", *Science*, **1983**, *221*, 769-770.

[6] W. Fiddler, J. W. Pensabene, E. G. Piotrowski, J. G. Phillips, J. Keating, W. J. Mergens, H. L. Newmark, "Inhibition of formation of volatile nitrosamines in fried bacon by the use of cure-solubilized alpha-tocopherol", *J. Agric. Food. Chem.*, **1978**, *26*, 653-656.

[7] J. Palmer, A. Mahammed, K. Lancaster, Z. Gross, H. Gray, "Structures and reactivity patterns of group 9 metallocorroles", *Inorg. Chem.*, **2009**, *48*, 9308-9315.

[8] L. Simkhovich, A. Mahammed, I. Goldberg, Z. Gross, "Synthesis and characterization of germanium, tin, phosphorus, iron, and rhodium complexes of tris(pentafluorophenyl)corrole, and the utilization of the iron and rhodium corroles as cyclopropanation catalysts", *Chem. Eur. J.*, **2001**, *7*, 1041-1055.

[9] M. Pietrzak, M. E. Meyerhoff, "Polymeric membrane electrodes with high nitrite selectivity based on rhodium(III) porphyrins and salophens as ionophores", *Anal. Chem.*, **2009**, *81*, 3637-3644.

[10] E. Bakker, P. Bühlmann, E. Pretsch, "Carrier-based ion-selective electrodes and bulk optodes. 1. general characteristics", *Chem. Rev.*, **1997**, *97*, 3083-3132.

[11] M. M. Shultz, O. K. Stefanova, S. B. Mokrov, K. N. Mikhelson, "Potentiometric estimation of the stability constants of ion−ionophore complexes in ion-selective membranes by the sandwich membrane method: theory, advantages, and limitations", *Anal. Chem.*, **2001**, *74*, 510-517.

[12] Y. Mi, E. Bakker, "Determination of complex formation constants of lipophilic neutral ionophores in solvent polymeric membranes with segmented sandwich membranes", *Anal. Chem.*, **1999**, *71*, 5279-5287.

[13] R. Stepanek, B. Krautler, P. Schulthess, B. Lindemann, D. Ammann, W. Simon, "Aquocyanocobalt(III)-hepta(2-phenylethyl)-cobyrinate as a cationic carrier for nitrite-selective liquid-membrane electrodes", *Anal. Chim. Acta*, **1986**, *182*, 83-90.

[14] E. Malinowska, M. E. Meyerhoff, "Role of axial ligation on potentiometric response of Co(III) tetraphenylporphyrin-doped polymeric membranes to nitrite ions", *Anal. Chim. Acta*, **1995**, *300*, 33-43.

Chapter 4

Polymeric Optical Sensors for Selective and Sensitive Nitrite Detection Using Co(III) Corrole and Rh(III) Porphyrin as Ionophores

4.1. Introduction

Nitrite (NO_2^-) is an important target analyte because of its presence in food and the environment, as well as within industrial, biological/physiological samples. Physiologically, nitrite can be reduced to nitric oxide (NO) through several pathways [1-3], making nitrite therapeutically valuable, including for its cytoprotective [4] and blood-pressure lowering effects [5-6]. Nitrite itself can act as a biological signalling molecule in terms of regulation of protein expression through the formation of *S*-nitrosothiols [7]. Therefore, an individual's levels of endogenous nitrite in blood plasma may convey valuable diagnostic information. Additionally, nitrite has been used as a food preservative for many years, especially in cured meats and bacon, mainly to inhibit deterioration [8-9]. Moreover, ground waters, including well water and river water, contain nitrite that is likely to be present in drinking water derived from these

sources [10-11]. Reactions of nitrite with secondary amines and amides from natural breakdown products of proteins form compounds known as nitrosamines which are regarded as carcinogenic [12-13]. Consequently, monitoring the concentration of nitrite in these sources is of great importance.

Many methods have been developed for nitrite detection [14], including spectroscopic [15-18], electrochemical [19-21] and chromatographic [22-25] methods. Among these, ionophore (ion-carrier) based chemical sensors, including ion-selective polymeric membrane electrodes (ISEs) and bulk optodes, are, simple, inexpensive and fully portable nitrite sensing devices. Plasticized polymeric membranes/films containing an appropriate lipophilic ionophore and an ion-exchanger (plus a chromoionophore for optodes) are widely used to create such ion selective sensors. For anion detection, in order to achieve selectivity for the target anion and avoid response based on ion lipophilicity, ionophores (most commonly hydrophobic metal ion-ligand complexes) with specific binding affinity to the primary target anion through axial ligation reactions are often incorporated into the polymeric membrane/film. Relatively few highly selective anion ionophores have been reported in comparison to cation ion carriers. However, in the case of nitrite, a number of potentially useful ionophores have been suggested to prepare potentiometric nitrite-selective membrane electrodes. These include a vitamin B_{12} derivative [26-27], cobalt(III) tetraphenylporphyrins [28], palladium organophosphine [29], as well as rhodium(III) porphyrins and salophens [30]. Our group has also recently studied corrole-based Co(III) complexes as nitrite ionophores to prepare polymeric membrane electrodes [31], and that such Co(III) corrole species provide greatly enhanced nitrite response and selectivity.

Even fewer ionophore-based polymeric film type optical sensors (so-called "optodes") for nitrite have been studied. Palladium organophosphines as charged carriers have been incorporated into polymeric films to fabricate optical sensors for nitrite detection in the absorbance mode [32]. Different film formulations were studied with different types of chromoionophores in the presence and absence of lipophilic ion additives depending on the charge of the chromoinophore. The Kopelman group fabricated fluorescence sensors by applying nitrite-selective polymeric films containing a Vitamin B_{12} derivative ionophore (charged carrier) with optical fibers [33]. An optical flow-through cell setup was integrated with the polymeric membrane optodes for nitrite detection in fluorescence mode using a Vitamin B_{12} derivative ionophore [34]. All previously reported work involved charged carrier type ionophores, and it should be noted that significant interference from thiocyanate was observed.

Herein, we report on the use of a cobalt(III) corrole species, cobalt(III) 5,10,15-tris(4-tert-butylphenyl) corrole (Co-tBC) possessing triphenylphosphine as an axial ligand to stabilize this corrole species, as a neutral carrier to fabricate nitrite-selective bulk polymeric film type optodes. Films formulated with both neutral proton chromoionophores (chromoionophores that are neutral when deprotonated) and charged proton chromoionophores (chromoionophores that are charged when deprotonated) with appropriate amounts of lipophilic ion additives are evaluated in terms of nitrite response and selectivity. It is shown that sensors made with either neutral chromoionophores or charged chromoionophores have significantly improved nitrite response and selectivity over other anions, including thiocyanate and perchlorate. For comparison purposes, rhodium(III) 5,10,15,20-tetra(*p-tert*-butylphenyl)porphyrin

(Rh-tBTPP) is also examined as a charged carrier within polymeric films for optical nitrite sensing. Sensors made with Co-tBC doped polymeric films are used to determine NO emission rates from polymer films containing *S*-nitroso-*N*-acetyl-penicillamine. Results are in excellent agreement with those obtained from the classic colorimetric method.

4.2. Experimental

4.2.1. Materials and Reagents

Cobalt(III) 5,10,15-tris(4-tert-butylphenyl) corrole triphenylphosphine (Co-tBC) (see Fig. 1A) and rhodium(III) 5,10,15,20-tetra(*p-tert*-butylphenyl)porphyrin (Rh-tBTPP) (see Fig. 1B) were synthesized via previously reported procedures [30-31]. The 5,10,15-tris(4-tert-butylphenyl) corrole and 5,10,15,20-tetra(*p-tert*-butylphenyl)porphyrin were purchased from Frontier Scientific (Logan, UT, U.S.A.). Cobalt(II) acetate tetrahydrate ($Co(OAc)_2 \bullet 4H_2O$), sodium acetate anhydrous (NaOAc) and ethanol (EtOH) were products of Sigma Aldrich (Milwaukee, WI, U.S.A.). Triphenylphosphine (PPh_3) was obtained from TCI America (Portland, OR, U.S.A.). For Griess assay measurement, sulphonamide, *N*-(1-Naphthyl)ethylenediamine and hydrochloric acid were also obtained from Sigma Aldrich.

For optical sensor film preparation, poly(vinyl chloride) (PVC), *o*-nitrophenyloctyl ether (*o*-NPOE), tridodecylmethylammonium chloride (TDMACl), chromoionophore I (9-(diethylamino)-5-(octadecanoylimino)-5H-benzo[a]phenoxazine (ETH 5294)),

chromoionophore II (9-dimethylamino-5-[4-(16-butyl-2,14-dioxo-3,15-dioxaeicosyl) phenylimino]benzo[a]phenoxazine (ETH 2439)), chromoionophore III (9-(diethylamino)-5-[(2-octyldecyl)imino]benzo[a]phenoxazine (ETH 5350)), chromoionophore IV (5-octadecanoyloxy-2-(4-nitrophenylazo)phenol (ETH 2412)), chromoionophore V (9-(diethylamino)-5-(2-naphthoylimino)-5H-benzo[a]phenoxazine), chromoionophore VI (4′,5′-dibromofluorescein octadecyl ester (ETH 7075)), chromoionophore VII (9-dimethylamino-5-[4-(15-butyl-1,13-dioxo-2,14-dioxanonadecyl) phenylimino]benzo[a]phenoxazine (ETH 5418)) and anhydrous tetrahydrofuran (THF) were purchased from Fluka and used without further purification. For NO releasing film preparation, *S*-nitroso-*N*-acetyl-penicillamine (SNAP) was synthesized using a previously reported method [35]. *N*-Acetyl-DL-penicillamine (NAP), and methanol were purchased from Sigma Aldrich. The CarboSil polymer was purchased from the Polymer Technology Group (Berkeley, CA).

All salts for standard solutions were purchased from Sigma Aldrich and were used as received. Measurements were performed in 50 mM NaH_2PO_4/Na_2HPO_4 buffer solutions with pH 4.5 or 5.0. All solutions were prepared with 18.2 MΩ water (Milli-Q, Millipore Corporation, Billerica, MA, USA). Activity coefficients were calculated according to the two-parameter Debye-Hückel formalism of Meier [36].

4.2.2. Film Preparation for Bulk Optodes

For optode thin film cocktail preparations, a total of 100 mg of components containing 10 or 20 mmol/kg of the ionophore, 10 mmol/kg of the neutral chromoionophore or 10 mmol/kg of the charged chromoionophore with 10 mmol/kg of TDMACl plus *o*-NPOE

and PVC with a mass ratio of 2:1 were dissolved in 1 mL THF. To obtain the optical sensing thin films, 50 μL aliquots of the membrane cocktail were coated with a pipette onto glass slides (51 mm × 9 mm), and the remaining THF was allowed to evaporate completely in fume hoods before testing.

4.2.3. Absorbance Measurements

All absorbance measurements were made using a PerkinElmer Lambda35 UV/Vis spectrophotometer. Before testing, film-coated glass slides were inserted into 1 cm cuvettes containing sample solutions to condition for 30 min. For each sample, a ratiometric method was used for calculation of α value (fraction of unprotonated chromoionophore) by recording the absorbance ratio of two peaks at two given wavelengths corresponding to the deprotonation peak and protonation peak of each chromoionophore. More specifically, for films prepared with chromoionophore I, ratios of absorbance values at 666 nm and 545 nm were measured for different sample solutions. The ratios of absorbance values at 668 nm and 526 nm, 648 nm and 512 nm, 428 nm and 568 nm, 665 nm and 566 nm, 472 nm and 536 nm and 677 nm and 550 nm were recorded for films formulated with chromoionophore II, III, IV, V, VI and VII, respectively. For calculation of α values, absorbance spectra of fully protonated and deprotonated chromoionophores were recorded by conditioning the optode membranes in 0.1 M HCl and 0.1 M NaOH solutions. All calculated curves were fitted to experimental points by adjusting K_{coex}.

The sensor reversibility experiments were carried out by using one optical sensing film and changing the sample solution only. Noise due to opening the instrument chamber

was removed from the absorbance tracings.

4.2.4. Preparation of SNAP-doped NO Release Film

The casting solution was prepared by dissolving 400 mg CarboSil in 3 mL THF. Ten wt% SNAP (44.5 mg) was then added into the polymer solution, and the mixture was stirred for 10 min. The film solution was cast into a Teflon ring (d=2.5cm) on a Teflon plate and dried overnight under ambient conditions, followed by 48 h of drying under vacuum to remove any additional solvent. The disk formed was evenly cut into 8 pieces and those pieces were divided into 2 portions, one portion containing 3 pieces and the other portion containing the remaining 5 pieces (to provide higher rate of NO production compared to 1^{st} portion in given volume of solution phase). Since in the presence of oxygen within aqueous test solutions, nitric oxide is converted to nitrite with a stoichiometry of 1:1 [37], the concentration of nitrite after a given time can be used to calculate the total NO released from the film. To convert NO released from the polymer film to nitrite, the portions with 3 film pieces and that with 5 film pieces were incubated in 50 mM phosphate buffer solution (4 mL, pH 4.5) for 12 h under 37 ^{o}C in two separate amber vials and the resulting solutions were labeled as sample # 1 and sample # 2, respectively.

4.2.5. Determination of NO

To determine the NO level in the samples by using the conventional colorimetric Griess method [38-39], the Griess assay reagent solutions were prepared as follows: 21.52 mg sulphonamide was dissolved in 10 mL water to yield a 12.5 mM solution;

concentrated HCl was diluted to 6 M; 32.4 mg *N*-(1-Naphthyl)ethylenediamine was dissolved in 10 mL water to give a solution with the concentration of 12.5 mM. Both the sulphonamide and *N*-(1-Naphthyl)ethylenediamine solutions were stored at 4 ^{o}C and the latter was kept away from light. For sample measurements, 100 μL of a sample solution was added into a cuvette and diluted with 700 μL phosphate buffer (50 mM, pH 4.5), followed by addition of the Griess reagent (100 μL sulphonamide, 100 μL HCl and 100 μL *N*-(1-Naphthyl)ethylenediamine). After color development for 15 min at room temperature, the absorbance at 540 nm was measured. Results for each sample solution were compared to absorbance values obtained using nitrite standard solutions treated in the same manner (to obtain the calibration curve). For measurements via the new Co-tBC based polymeric optical sensors, the same sample solution dilution procedure was performed and the diluted sample was detected by the *o*-NPOE plasticized PVC membrane optodes doped with 20 mmol/kg Co-tBC and 10 mmol/kg chromoionophore I in the absorbance mode. All tests were conducted in triplicate.

4.3. Results and Discussion

4.3.1. Anion Carrier Optode Response Mechanism

Nitrite-selective bulk optode responses are based on the coextraction of nitrite and protons into the polymer film containing both the nitrite-selective ionophore, which may be neutral or charged, and a proton-sensitive chromoionophore in the presence or absence of lipophilic cationic sites (R^+) depending on the neutrality of the membrane. When a

neutral ionophore is employed, either a neutral chromoionophore (see Fig. 4.2a) or a charged chromoionophore with a proper amount of lipophilic cationic sites (see Fig. 4.2b) can be incorporated into the polymeric film. When a charged ionophore is present, a charged chromoionophore is required to maintain membrane neutrality in the organic polymeric phase (see Fig. 4.2c). The coextraction processes can be summarized as simple net ionic equations:

$$H^+(aq) + X^-(aq) + I(org) + C(org) \rightleftharpoons IX^-(org) + CH^+(org) \quad \text{(Eq. 4.1)}$$

$$H^+(aq) + X^-(aq) + I(org) + C^-(org) \rightleftharpoons IX^-(org) + CH(org) \quad \text{(Eq. 4.2)}$$

$$H^+(aq) + X^-(aq) + I^+(aq) + C^-(aq) \rightleftharpoons IX(org) + CH(org) \quad \text{(Eq. 4.3)}$$

where X^- is the analyte anion, I is the neutral carrier, I^+ is the charged carrier ionophore, C is a neutral chromoionophore and C^- is a charged chromoionophore. Taking mass balance and charge balance into account, the above three net ionic equations can be rewritten in an analytically more useful form to relate proton (a_{H^+}) and ion activities (a_{X^-}) to optical responses and membrane parameters as follows [32, 40-41]:

$$a_{H^+} \cdot a_{X^-} = \frac{1}{K_{coex}} \cdot \frac{(1-\alpha)^2}{\alpha} \cdot \frac{[C_T]}{[I_T] - [C_T](1-\alpha)} \quad \text{(Eq. 4.4)}$$

$$a_{H^+} \cdot a_{X^-} = \frac{1}{K_{coex}} \cdot \frac{1-\alpha}{\alpha} \cdot \frac{[R_T] - \alpha[C_T]}{[I_T] - ([R_T] - \alpha[C_T])} \quad \text{(Eq. 4.5)}$$

$$a_{H^+} \cdot a_{X^-} = \frac{1}{K_{coex}} \cdot \frac{1-\alpha}{\alpha^2} \cdot \left(\frac{[I_T]}{[C_T]} - \alpha\right) \quad \text{(Eq. 4.6)}$$

where K_{coex} is the coextraction constant, C_T is the total amount of chromoionophore, I_T is the total amount of ionophore, and R_T is the total amount of lipophilic ionic sites. The value of 1-α is the protonation degree of the chromoionophore, which is defined as the ratio of the chromoionophore concentration in its protonated form to its total

concentration and can be connected to the apparent absorbance values (see Eq. 4.7), where A is the absorbance of the chromoionophore for a given equilibrium condition, and A_{prot} and A_{deprot} are the absorbance values at fully protonated and deprotonated forms respectively. In a buffered system, 1-α is only dependent on the analyte ion activity since the proton activity is constant.

$$1-\alpha = \frac{[CH]}{[C_T]} = \frac{A - A_{deprot}}{A_{prot} - A_{deprot}} \qquad \text{(Eq. 4.7)}$$

4.3.2. Cobalt(III) Corrole as a Neutral Ionophore for Optical Nitrite Sensing

4.3.2.1. Optodes Response

The response mechanism of the anion carrier largely determines the composition of the optical sensing films. It was reported and determined previously by potentiometry that Co-tBC is a neutral carrier within polymeric membrane electrodes [31]. Therefore, to maintain membrane neutrality, a neutral chromoionophore or a charged chromoionophore with the appropriate amount of lipophilic ionic sites should be employed together with the neutral ionophore in polymeric film optodes. In the presence of a neutral chromoionophore and neutral carrier, the binding of nitrite and Co-tBC is accompanied by a concomitant protonation of the chromoionophore to maintain the charge neutrality within the film. As shown in Fig. 4.3a, as the nitrite concentration increases and more nitrite enters the film to bind with the ionophore, more protons are coextracted to protonate chromoionophore I, resulting in the absorbance change (increase of protonation peak at 666 nm and decrease of deprotonation peak at 545 nm). In contrast, if a charged chromoionophore is incorporated into the polymeric membrane, a proper amount

of lipophilic ionic sites should also be introduced to act as the initial counterion to the chromoionophore. Similarly, an increase in nitrite level in the sample phase is accompanied by an increased degree of protonation of the chromoionophore, as indicated by a spectra change (increase of protonation peak at 472 nm and decrease of deprotonation peak at 536 nm). As the binding of nitrite and the ionophore occurs, the ion-ionophore complex is charged while the protonated chromoionophore becomes neutral. In the presence of lipophilic ionic additives, the electroneutrality of the sensing film is still ensured. The spectra changes observed in Fig. 4.3 indicate Co-tBC can successfully function as a nitrite-selective ionophore when incorporated in a polymeric membrane to fabricate sensitive bulk optodes for nitrite detection.

The response calibration curves toward nitrite are shown in Fig. 4.4. The solid lines are the theoretical curves according to equation 4.4 and the points (□, ■ and ●) are from experimental data, which fit well with the theoretical curves. Since the film composition and buffer pH can substantially affect membrane equilibrium and sensor response characteristics, optodes made with two different film compositions were initially studied as well as two different pH buffered test solutions. Fig. 4.4 illustrates that when the ionophore amount is doubled (□), almost all the chromoionophores are protonated in the presence of a high concentration of nitrite, while only ~ 90% of the chromoionophores are protonated when there is less ionophore in the membrane (●) with the response range shifted to a higher concentration range. Comparing the two buffer solutions, the pH 4.5 yields higher α values than pH 5.0, indicating a better sensor response with increased proton activity. However, if the buffer pH value is < pH 4.5, nitrite will start to be protonated in the sample phase, resulting in lower nitrite activity.

4.3.2.2. Selectivity

Experimental selectivity coefficients for different films can be estimated from the horizontal distance of two optical response calibration curves at a given degree of protonation, 1-α, which was 0.5 in this study. Since the response of ionophore-based ion-selective sensors (both optical and potentiometric) is highly dependent on the ionophore, selectivity patterns obtained from bulk optodes formulated with Co-tBC are similar to the selectivity patterns observed previously with potentiometric anion sensors employing the same ionophore, and completely different than the classical Hofmeister series. For example, optical sensor 1 (20 mmol/kg ionophore and 10 mmol/kg chromoionophore I) yields the same selectivity pattern as potentiometric polymer membrane electrodes formulated with 1 wt% ionophore and 10 mol% TDMACl (NO_2^-> ClO_4^- > SCN^- > NO_3^- > Br^- > Cl^-), but is more selective to nitrite (with more negative log selectivity coefficient values ($\log K^{opt}_{NO_2^-,X}$)) over SCN^-, ClO_4^- and NO_3^- [31]. With the proper amount of ionophore, type and amount of chromoionophore, lipophilic ion additives, and sample phase pH, the sensors also exhibit good nitrite selectivity over the most lipophilic ones (ClO_4^- and SCN^-). Generally, polymer film optodes (1-5, Fig. 4.5) doped with neutral chromoionophores have better selectivity towards nitrite than those with charged chromoionophores (6-7, Fig. 4.5), especially regarding interference from lipophilic anions. A possible reason for this is that the incorporation of lipophilic ionic sites increases the ionic strength of the film, which favors other anions that can compete with nitrite, leading to worse selectivity for nitrite over other anions. Since the response of anion-selective optodes is based on a carrier-mediated coextraction equilibrium, it

relates to both the complex formation constant of the ionophore and the proton-binding affinity of the chromoionophore in the film (p*K*a) [42]. Membrane optodes containing chromoionophores with higher p*K*a values (order of p*K*a values: chromoionophore I > V > II > VII > III [43-44]) generally have better selectivity, and this can be seen in Fig. 4.5.

4.3.2.3. Response Time and Reversibility

The response time of the optical sensor is measured as the time require for the films to reach 95% of the equilibrium response. The dynamic response time is shown in Fig. 4.6 and is found to be less than 1 min, with excellent signal reproducibility of the nitrite optode film when switching between sample solutions containing 10^{-5} M and 10^{-2} M sodium nitrite. The response time observed is comparable to the previously reported organopalladium-based membrane optodes tested in the absorbance mode [32] and is much shorter than optodes based on the same ionophore tested in the fluorescence mode [45] and optodes based on electropolymerized cobalt(II) porphyrin [46].

4.3.3. Rhodium(III) Porphyrin as a Charged Ionophore for Optical Nitrite Sensing

Rhodium(III) porphyrins have recently been discovered to exhibit excellent performance in terms of nitrite selectivity over other common anions [30]. Rhodium is from the same group as cobalt and exhibits similar axial ligation chemistry, although not exactly the same. Unlike corroles, when complexed to metal(III) ions, porphyrins are -2 charged and the resulting metal complex functions as a charged carrier when incorporated into polymeric films. Fabricating polymeric optodes by employing Rh(III) porphyrins as ionophores requires that a charged chromoionophore be present in the film to maintain

charge neutrality (see Fig. 4.2c). As shown in Fig. 4.7, sensors formulated with 10 mmol/kg Rh-tBTPP and 10 mmol/kg chromoionophore VI show very sensitive and selective response to nitrite over the range of 10^{-7} to 10^{-2} M. As shown in Fig. 4.7, the selectivity pattern deviates substantially from the Hofmeister selectivity pattern. Sensors prepared with the Rh(III) porphyrin exhibit selectivity to nitrite over other anions including more lipophilic perchlorate and thiocyanate ($\log K^{opt}_{NO_2^-,X}$: SCN^-, -1; ClO_4^-, -1.9; NO_3^-, -2.7; Br^-, -3.2; Cl^-, -3.9), which is consistent with the selectivity coefficients data observed via potentiometry using an ion-selective membrane electrode. The signal reproducibility is shown in Fig. 8, with a very reversible optical response when nitrite concentration is switched between 10^{-5} and 10^{-2} M. The response time of the optode, t_{95}, is found to be within 1 min with a longer recovery time of ~ 8min, indicating strong binding affinity between nitrite and Rh-tBTPP, indicating a larger on-rate constant and a much smaller off-rate constant. The Rh-tBTPP-based bulk optodes provide better selectivity to nitrite over ClO_4^- compared to Co-tBC-based optical sensors (see above, Fig. 4.5), while Co-tBC-based sensors are more selective to nitrite over NO_3^- than Rh-tBTPP-based sensors. Comparable selectivity over other anions (SCN^-, Br^-, Cl^-) is observed by sensors prepared with both ionophores.

4.3.4. Nitric Oxide Detection

To establish the usefulness of optical sensors made with polymeric membranes prepared with Co-tBC (20 mmol/kg) and chromoionophore I (10 mmol/kg), the determination of nitrite converted from nitric oxide released by S-nitroso-N-acetyl-penicillamine-doped CarboSil films were carried out and compared

with the conventional Griess colorimetric assay method. In oxygen-containing aqueous solution, NO can be oxidized to nitrite with a stoichiometry of 1:1 [37]. Thus, the concentration of nitrite in the soaking solution can provide information about the amounts of NO released from such polymeric films. Such NO release polymers are very useful biomedically to coat various devices to prevent clotting and infection [35, 47-49]. As shown in Table 4.1, the results obtained for NO released from SNAP-doped films with the polymeric membrane nitrite optode are in excellent agreement with the results obtained using the colorimetric Griess method for the two samples examined. The biggest advantage of the optical sensor over the Griess assay method is that one sensor can be used multiple times (owing to the reversibility), and there are no reagents that need to be made fresh each day for analytical measurements.

4.4. Summary

In summary, both the cobalt(III) 5,10,15-tris(4-tert-butylphenyl) corrole triphenylphosphine and rhodium(III) 5,10,15,20-tetra(*p-tert*-butylphenyl)porphyrin ionophores can function as nitrite-selective ionophores in polymeric film type optical sensors and provide similar anion selectivity patterns with previously reported polymeric membrane electrodes [30-31]. For the Co-tBC (neutral carrier)-based optical sensors, films formulated with neutral chromoionophores show better selectivity to nitrite than charged chromoionophores due to the presence of lipophilic ion additives. Sensors doped with chromoionophores I and V (see Fig. 4.5) provide greatly enhanced nitrite

selectivity over other anions including the most lipophilic anions, perchlorate and thiocyanate. Chromoionophores with different *p*Ka values also influence sensor performance. The higher the *p*Ka of the chomoionophore the better the response and selectivity observed for nitrite. It is also observed that the lower the pH value of the buffer, the more sensitive the sensor is. Sensor response ranges and detection limits can be tuned by changing film formulations and test buffer pH values. For Rh-tBTPP (charged carrier)-based optical sensors, a charged chromoionophore must be employed in the sensing membrane to maintain charge neutrality. Selectivity patterns and coefficients obtained from the Rh-tBTPP-based optical sensors are in excellent agreement with those obtained when using same ionophore to prepare potentiometric membrane electrodes [30]. Sensors based on both of the two ionophores have fast response and recovery times in response to changes in nitrite concentration. Results also demonstrate the potential for immediate application of sensors in quantitating the rates of nitric oxide release from polymeric films doped with various NO donors, with data for the new optical sensors correlating well with the classical Griess assay for determining nitrite levels derived from the liberated NO.

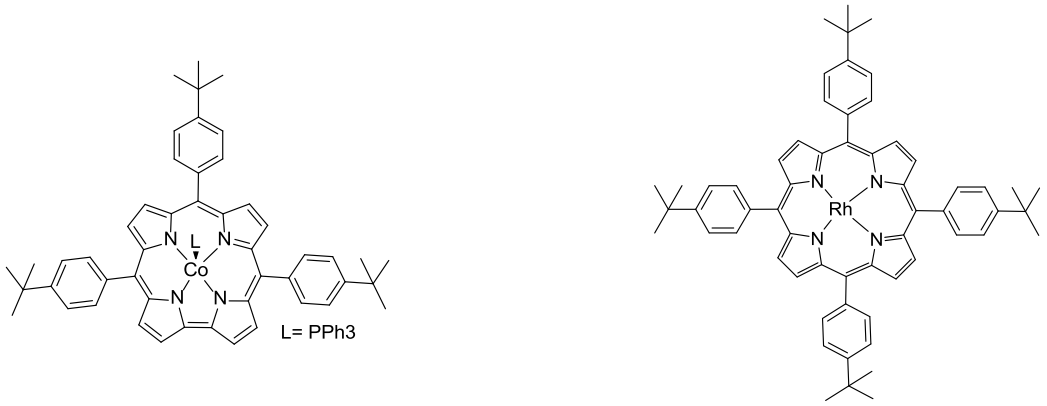

(a) (b)

Fig. 4.1. (a) Structure of Co(III) 5,10,15-tris(4-tert-butylphenyl) corrole with triphenylphosphine as the axial ligand (Co-tBC) and (b) Rh(III) 5,10,15,20-tetra(p-tert-butylphenyl)porphyrin chloride (Rh-tBTPP).

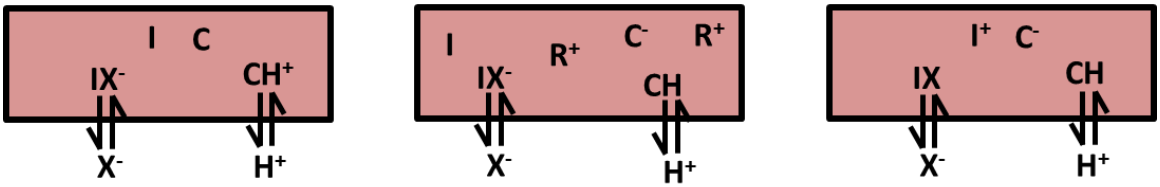

(a) (b) (c)

Fig. 4.2. Optical sensing schemes for nitrite ion with a neutral carrier coupled with (a) a neutral chromoionophore, (b) a charged chromoionophore and lipophilic ionic sites and (c) a charged carrier coupled with a charged chromoionophore. Note: C=chromoionophore; I = ionophore; X^- = nitrite or other anion; R^+ = lipophilic cationic site additive.

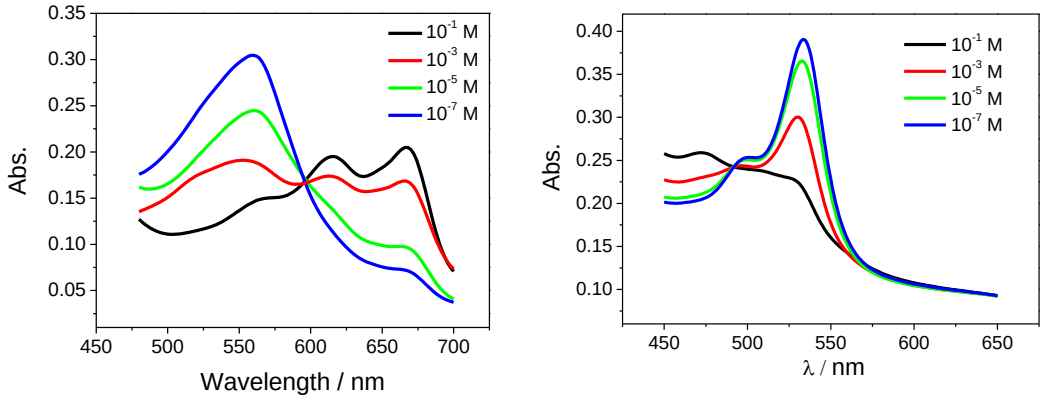

(a) (b)

Fig. 4.3. Absorption spectra of nitrite optical sensing films prepared with a PVC-NPOE cocktail containing (A) 20 mmol/kg ionophore, 10 mmol/kg chromoionophore I; and (B) 20 mmol/kg ionophore, 10 mmol/kg chromoionophore VI and 10 mmol/kg TDMACl, measured at varying nitrite levels, ranging from 0.1 μM to 0.1 M, in 50 mM phosphate buffer solutions (pH 4.5)..

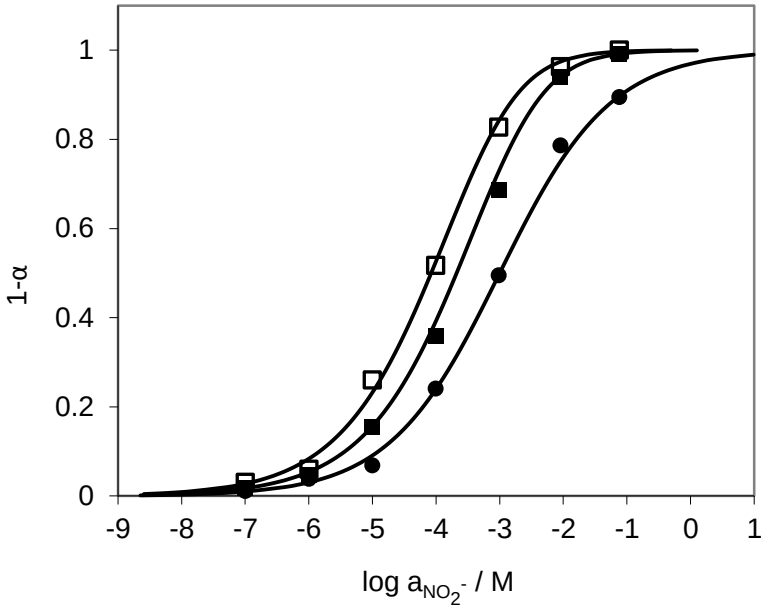

Fig. 4.4. Response of optical nitrite sensing polymeric films to solutions prepared in 50 mM phosphate buffer solutions with different nitrite concentrations as function of sample pH and different amount of ionophore in film. Films were *o*-NPOE plasticized PVC doped with (□) 20 mmol/kg ionophore and 10 mmol/kg chromoionophore I (buffer pH 4.5); (■) 20 mmol/kg ionophore and 10 mmol/kg chromoionophore I (buffer pH 5.0); and (●) 10 mmol/kg ionophore and 10 mmol/kg chromoionophore I (buffer, pH 4.5).

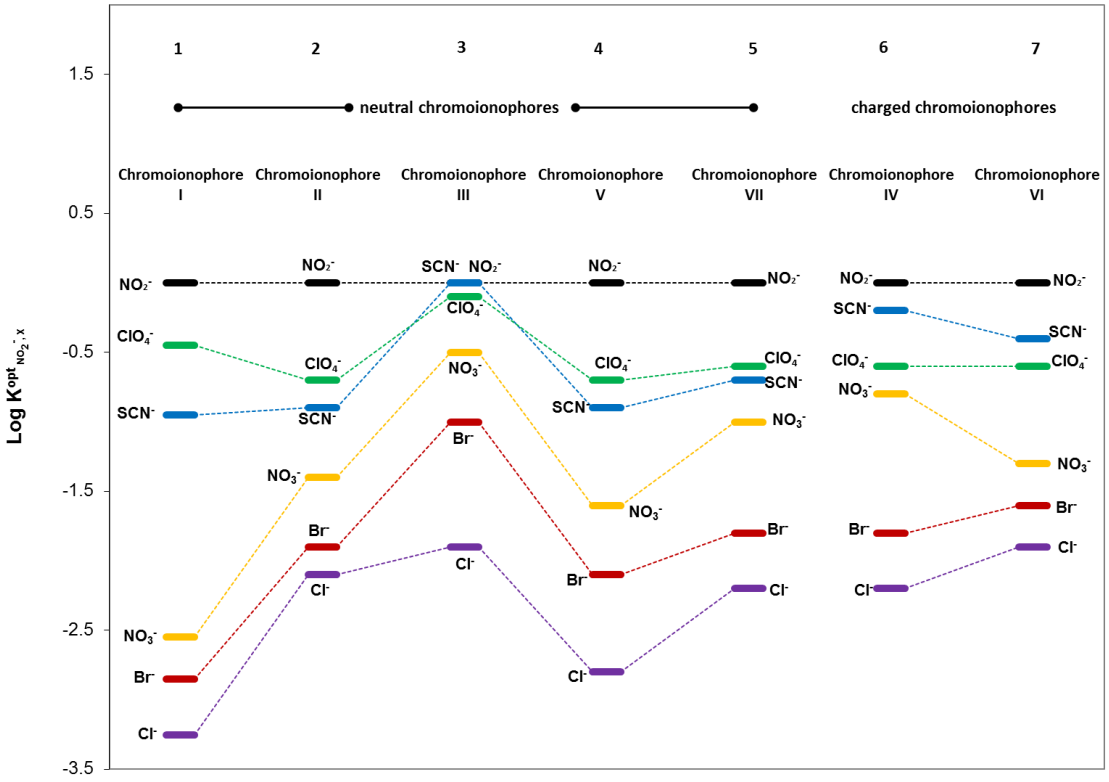

Fig. 4.5. Logarithm of optical selectivity coefficients (relative to nitrite) of Co-tBC (20 mmol/kg)-based polymer film optodes doped with different chromoionophores in the presence or absence of TDMACl. Polymeric films were doped with (1) 10 mmol/kg chromoionophore I; (2) 10 mmol/kg chromoionophore II; (3) 10 mmol/kg chromoionophore III; (4) 10 mmol/kg chromoionophore V; (5) 10 mmol/kg chromoionophore VII; (6) 10 mmol/kg chromoionophore IV and 10 mmol/kg TDMACl; (7) chromoionophore VI and 10 mmol/kg TDMACl. Measurements were carried out in 50 mM phosphate buffer, pH 4.5.

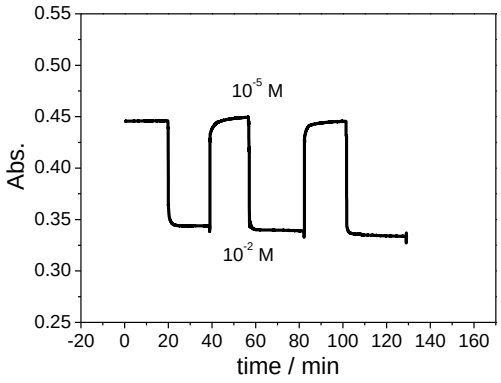

Fig. 4.6. Reversibility of optical nitrite response in phosphate buffer solution (pH 4.5) for polymer film optodes formulated with 20 mmol/kg Co-tBC and 10 mmol/kg chromoionophore I in *o*-NPOE plasticized PVC, when changing nitrite concentration back and forth between 10^{-2} M and 10^{-5} M. Absorbance values were measured at 545 nm.

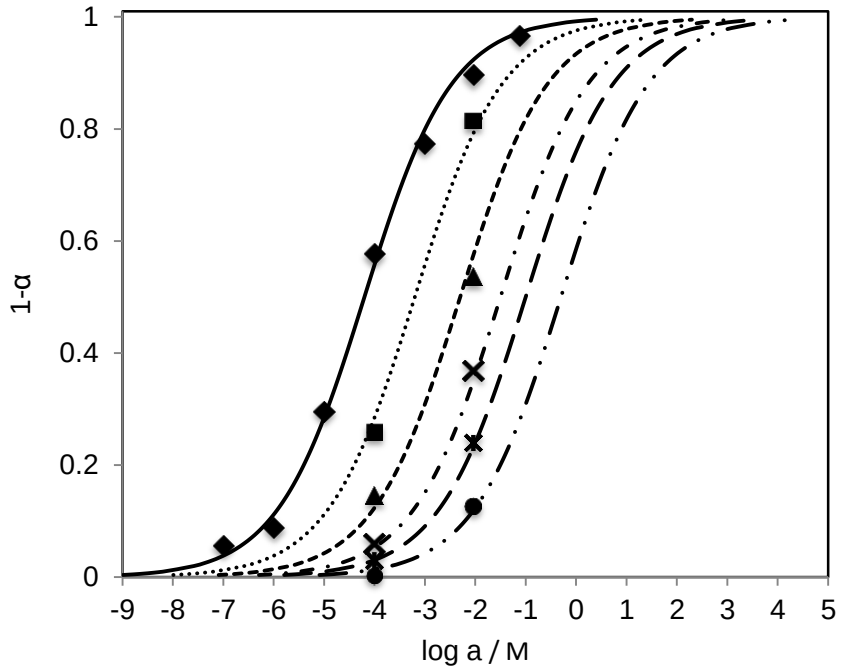

Fig. 4.7. Optical response of *o*-NPOE-PVC sensing film doped with 10 mmol/kg Rh-tBTPP and 10 mmol/kg chromoionophore VI toward various anions measured in 50 mM phosphate buffer, pH 4.5: (●) chloride, (*) bromide, (×) nitrate, (▲) perchlorate, (■) thiocyanate, (♦) nitrite.

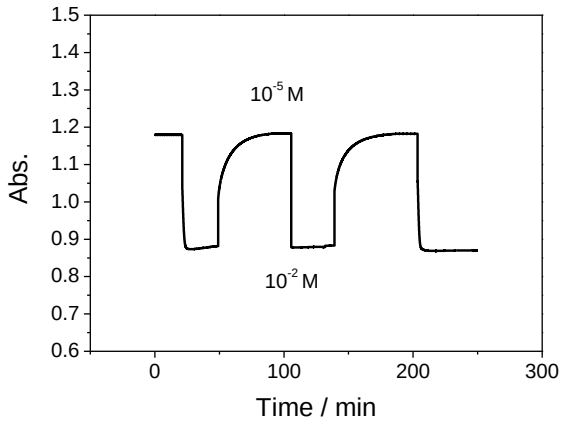

Fig. 4.8. Reversibility of potentiometric response to nitrite in phosphate buffer solution (pH 4.5) for optical sensing films formulated with 10 mmol/kg Rh-tBTPP and 10 mmol/kg chromoionophore VI in *o*-NPOE plasticized PVC, when changing nitrite concentration back and forth between 10^{-2} M and 10^{-5} M. Absorbance measured at 536 nm.

Table 4.1. Results of NO release rates from SNAP-doped CarboSil film over 12 h period by using both conventional Griess assay and polymeric film-based nitrite-selective bulk optodes based the on Co-tBC ionophore (n=3).

Sample	Optical Sensors		Griess Assay	
	$[NO_2^-]$ ($mol \cdot L^{-1}$)	NO emission rate ($mol \cdot min^{-1}$)	$[NO_2^-]$ ($mol \cdot L^{-1}$)	NO emission rate ($mol \cdot min^{-1}$)
#1	$1.91 \pm 0.09 \times 10^{-4}$	$1.06 \pm 0.05 \times 10^{-9}$	$1.96 \pm 0.06 \times 10^{-4}$	$1.09 \pm 0.02 \times 10^{-9}$
#2	$3.37 \pm 0.1 \times 10^{-4}$	$1.88 \pm 0.08 \times 10^{-9}$	$3.29 \pm 0.03 \times 10^{-4}$	$1.82 \pm 0.08 \times 10^{-9}$

4.5. References

[1] J. L. Zweier, P. H. Wang, A. Samouilov, P. Kuppusamy, "Enzyme-independent formation of nitric-oxide in biological tissues", *Nat. Med.*, **1995**, *1*, 804-809.

[2] J. O. N. Lundberg, E. Weitzberg, J. M. Lundberg, K. Alving, "Intragastric nitric oxide production in humans - measurements in expelled air", *Gut*, **1994**, *35*, 1543-1546.

[3] N. Benjamin, F. Odriscoll, H. Dougall, C. Duncan, L. Smith, M. Golden, H. McKenzie, "Stomach NO synthesis", *Nature*, **1994**, *368*, 502-502.

[4] M. R. Duranski, J. J. M. Greer, A. Dejam, S. Jaganmohan, N. Hogg, W. Langston, R. P. Patel, S. F. Yet, X. D. Wang, C. G. Kevil, M. T. Gladwin, D. J. Lefer, "Cytoprotective effects of nitrite during in vivo ischemia-reperfusion of the heart and liver", *J. Clin. Investig.*, **2005**, *115*, 1232-1240.

[5] C. J. Hunter, A. Dejam, A. B. Blood, H. Shields, D. Kim-Shapiro, R. F. Machado, S. Tarekegn, N. Mulla, A. O. Hopper, A. N. Schechter, G. G. Power, M. T. Gladwin, "Inhaled nebulized nitrite is a hypoxia-sensitive NO-dependent selective pulmonary vasodilator", *Nat. Med.*, **2004**, *10*, 1122-1127.

[6] K. Tsuchiya, Y. Takiguchi, M. Okamoto, Y. Izawa, Y. Kanematsu, M. Yoshizumi, T. Tamaki, "Malfunction of vascular control in lifestyle-related diseases: Formation of systemic hemoglobin-nitric oxide complex (HbNO) from dietary nitrite", *J. Pharmacol. Sci.*, **2004**, *96*, 395-400.

[7] N. Bryan, B. Fernandez, S. Bauer, M. Garcia-Saura, A. Milsom, T. Rassaf, R. Maloney, A. Bharti, J. Rodriguez, M. Feelisch, "Nitrite is a signaling molecule and regulator of gene expression in mammalian tissues", *Nat. Chem. Biol.*, **2005**, *1*, 290-297.

[8] W. J. R. Santos, P. R. Lima, A. A. Tanaka, S. M. C. N. Tanaka, L. T. Kubota, "Determination of nitrite in food samples by anodic voltammetry using a modified electrode", *Food Chem.*, **2009**, *113*, 1206-1211.

[9] K.-O. Honikel, "The use and control of nitrate and nitrite for the processing of meat products", *Meat Sci.*, **2008**, *78*, 68-76.

[10] M. H. Ward, J. R. Cerhan, J. S. Colt, P. Hartge, "Risk of non-hodgkin lymphoma and nitrate and nitrite from drinking water and diet", *Epidemiology*, **2006**, *17*, 375-382.

[11] Z. Binghui, Z. Zhixiong, Y. Jing, "Ion chromatographic determination of trace iodate, chlorite, chlorate, bromide, bromate and nitrite in drinking water using suppressed conductivity detection and visible detection", *J. Chromatogr. A*, **2006**, *1118*, 106-110.

[12] W. Fiddler, J. W. Pensabene, E. G. Piotrowski, J. G. Phillips, J. Keating, W. J. Mergens, H. L. Newmark, "Inhibition of formation of volatile nitrosamines in fried bacon by the use of cure-solubilized .alpha.-tocopherol", *J. Agric. Food Chem.*, **1978**, *26*, 653-656.

[13] A. Tricker, "N-nitroso compounds and man: sources of exposure, endogenous formation and occurrence in body fluids", *Eur. J. Cancer Prev.*, **1997**, *6*, 226-268.

[14] M. J. Moorcroft, J. Davis, R. G. Compton, "Detection and determination of nitrate and nitrite: a review", *Talanta*, **2001**, *54*, 785-803.

[15] S. Senra-Ferreiro, F. Pena-Pereira, I. Lavilla, C. Bendicho, "Griess micro-assay for the determination of nitrite by combining fibre optics-based cuvetteless UV-Vis micro-spectrophotometry with liquid-phase microextraction", *Anal. Chim. Acta*, **2010**, *668*, 195-200.

[16] M. J. Martínez-Tomé, R. Esquembre, R. Mallavia, C. R. Mateo, "Development of a dual-analyte fluorescent sensor for the determination of bioactive nitrite and selenite in water samples", *J. Pharm. Biomed. Anal.*, **2010**, *51*, 484-489.

[17] M. I. H. Helaleh, T. Korenaga, "Fluorometric determination of nitrite with acetaminophen", *Microchem. J.*, **2000**, *64*, 241-246.

[18] A. Lapat, L. Székelyhidi, I. Hornyák, "Spectrofluorimetric determination of 1,3,5-trinitro-1,3,5-triazacyclohexane (Hexogen, RDX) as a nitramine type explosive", *Biomed. Chromatogr.*, **1997**, *11*, 102-104.

[19] S. M. Shariar, T. Hinoue, "Simultaneous voltammetric determination of nitrate and nitrite ions using a copper electrode pretreated by dissolution/redeposition", *Anal. Sci.*, **2010**, *26*, 1173-1179.

[20] M. Muchindu, T. Waryo, O. Arotiba, E. Kazimierska, A. Morrin, A. J. Killard, M. R. Smyth, N. Jahed, B. Kgarebe, P. G. L. Baker, E. I. Iwuoha, "Electrochemical nitrite nanosensor developed with amine- and sulphate-functionalised polystyrene latex beads self-assembled on polyaniline", *Electrochim. Acta*, **2010**, *55*, 4274-4280.

[21] A. P. Doherty, M. A. Stanley, D. Leech, J. G. Vos, "Oxidative detection of nitrite at an electrocatalytic $[Ru(bipy)_2poly\text{-}(4\text{-}vinylpyridine)_{10}Cl]Cl$ electrochemical sensor applied for the flow injection determination of nitrate using a Cu/Cd reductor column", *Anal. Chim. Acta*, **1996**, *319*, 111-120.

[22] H. Kodamatani, S. Yamazaki, K. Saito, T. Tomiyasu, Y. Komatsu, "Selective determination method for measurement of nitrite and nitrate in water samples using high-performance liquid chromatography with post-column photochemical reaction and chemiluminescence detection", *J. Chromatogr. A*, **2009**, *1216*, 3163-3167.

[23] A. K. Malik, W. Faubel, "Capillary electrophoretic determination of tetramethylthiuram disulphide (thiram)", *Anal. Lett.*, **2000**, *33*, 2055 - 2064.

[24] G. M. Greenway, S. J. Haswell, P. H. Petsul, "Characterisation of a micro-total analytical system for the determination of nitrite with spectrophotometric detection", *Anal. Chim. Acta*, **1999**, *387*, 1-10.

[25] Z. Liu, X. Xi, S. Dong, E. Wang, "Liquid chromatography-amperometric detection of nitrite using a polypyrrole modified glassy carbon electrode doped with tungstodiphosphate anion", *Anal. Chim. Acta*, **1997**, *345*, 147-153.

[26] P. Schulthess, D. Ammann, B. Krautler, C. Caderas, R. Stepanek, W. Simon, "Nitrite-selective liquid membrane-electrode", *Anal. Chem.*, **1985**, *57*, 1397-1401.

[27] R. Stepanek, B. Krautler, P. Schulthess, B. Lindemann, D. Ammann, W. Simon, "Aquocyanocobalt(III)-hepta(2-phenylethyl)-cobyrinate as a cationic carrier for nitrite-selective liquid-membrane electrodes", *Anal. Chim. Acta*, **1986**, *182*, 83-90.

[28] E. Malinowska, M. E. Meyerhoff, "Role of axial ligation on potentiometric response of Co(III) tetraphenylporphyrin-doped polymeric membranes to nitrite ions", *Anal. Chim. Acta*, **1995**, *300*, 33-43.

[29] I. H. A. Badr, M. E. Meyerhoff, S. S. M. Hassan, "Potentiometric anion selectivity of polymer membranes doped with palladium organophosphine complex", *Anal. Chem.*, **1995**, *67*, 2613-2618.

[30] M. Pietrzak, M. E. Meyerhoff, "Polymeric membrane electrodes with high nitrite selectivity based on rhodium(III) porphyrins and salophens as ionophores", *Anal. Chem.*, **2009**, *81*, 3637-3644.

[31] S. Yang, M. E. Meyerhoff, "Study of cobalt(III) corrole as the neutral ionophore for nitrite and nitrate detection via polymeric membrane electrodes", *Electroanalysis*, **2013**, *25*, 2579-2585.

[32] I. H. A. Badr, "Nitrite-selective optical sensors based on organopalladium ionophores", *Anal. Lett.*, **2001**, *34*, 2019-2034.

[33] S. L. R. Barker, M. R. Shortreed, R. Kopelman, "Anion selective optodes: development of a fluorescent fiber optic sensor for the determination of nitrite activity", *Proc. SPIE*, **1996**, *2836*, 304-310.

[34] C. Demuth, U. E. Spichiger, "Response function and analytical parameters of nitrite-selective optode membranes in absorbance and fluorescence mode", *Anal. Chim. Acta*, **1997**, *355*, 259-268.

[35] E. J. Brisbois, H. Handa, T. C. Major, R. H. Bartlett, M. E. Meyerhoff, "Long-term nitric oxide release and elevated temperature stability with S-nitroso-N-acetylpenicillamine (SNAP)-doped Elast-eon E2As polymer", *Biomaterials*, **2013**, *34*, 6957-6966.

[36] P. C. Meier, "Two-parameter debye-hückel approximation for the evaluation of mean activity coefficients of 109 electrolytes", *Anal. Chim. Acta*, **1982**, *136*, 363-368.

[37] L. J. Ignarro, J. M. Fukuto, J. M. Griscavage, N. E. Rogers, R. E. Byrns, "Oxidation of nitric oxide in aqueous solution to nitrite but not nitrate: comparison with enzymatically formed nitric oxide from L-arginine", *Proc. Natl. Acad. Sci. USA*, **1993**, *90*, 8103-8107.

[38] P. Griess, "Bemerkungen zu der Abhandlung der HH. Weselsky und Benedikt „Ueber einige Azoverbindungen"", *Ber. Dtsch. Chem. Ges.*, **1879**, *12*, 426-428.

[39] M. B. Shinn, "Colorimetric method for determination of nitrate", *Ind. Eng. Chem., Anal. Ed.*, **1941**, *13*, 33-35.

[40] K. Seiler, W. Simon, "Theoretical aspects of bulk optode membranes", *Anal. Chim. Acta*, **1992**, *266*, 73-87.

[41] E. Bakker, W. Simon, "Selectivity of ion-sensitive bulk optodes", *Anal. Chem.*, **1992**, *64*, 1805-1812.

[42] E. Bakker, P. Bühlmann, E. Pretsch, "Carrier-based ion-selective electrodes and bulk optodes. 1. general characteristics", *Chem. Rev.*, **1997**, *97*, 3083-3132.

[43] Y. Qin, E. Bakker, "Quantitive binding constants of H^+-selective chromoionophores and anion ionophores in solvent polymeric sensing membranes", *Talanta*, **2002**, *58*, 909-918.

[44] X. Liu, Y. Qin, "Ion-exchange reaction of silver(I) and copper(II) in optical sensors based on thiaglutaric diamide", *Anal. Sci.*, **2008**, *24*, 1151-1156.

[45] G. J. Mohr, O. S. Wolfbeis, "Optical nitrite sensor based on a potential-sensitive dye and a nitrite-selective carrier", *Analyst*, **1996**, *121*, 1489-1494.

[46] S. T. Yang, L. G. Bachas, "Fiber optic chemical sensor for nitrite based on an electropolymerized cobaltporphyrin film", *Talanta*, **1994**, *41*, 963-968.

[47] W. Cai, J. Wu, C. Xi, A. J. Ashe Iii, M. E. Meyerhoff, "Carboxyl-ebselen-based layer-by-layer films as potential antithrombotic and antimicrobial coatings", *Biomaterials*, **2011**, *32*, 7774-7784.

[48] W. Cai, J. Wu, C. Xi, M. E. Meyerhoff, "Diazeniumdiolate-doped poly(lactic-co-glycolic acid)-based nitric oxide releasing films as antibiofilm coatings", *Biomaterials*, **2012**, *33*, 7933-7944.

[49] Y. Wu, M. E. Meyerhoff, "Nitric oxide-releasing/generating polymers for the development of implantable chemical sensors with enhanced biocompatibility", *Talanta*, **2008**, *75*, 642-650.

Chapter 5

Electrocatalytic Oxidation of Nitrite on Solid Electrodes Modified with Electropolymerized Rhodium(III) Porphyrin

5.1. Introduction

As stated in previous chapters, the determination nitrite concentration is important in many fields. Nitrite is commonly used as an additive in some foods and as a corrosion inhibitor [1-2]. Nitrite can be viewed as a storage pool for (nitric oxide) NO, since nitrite can be reduced in blood and tissues to form NO, a diverse and potent biological messenger, through several enzymatic and non-enzymatic pathways [3-5]. Many methods reported in the literature for nitrite measurement involve complex ion chromatography [6-9] and spectroscopy [10-13]. Electrochemistry, however, can provide a rapid and simple way for characterization of nitrite levels.

Chapters 2 - 4 of this thesis focused on the development of potentiometric and optical methods to detect nitrite by use of an active ion-carrier/ionophore in a polymeric membrane or film as the sensing material. In such sensing devices, in order to achieve sufficient response and selectivity for nitrite (avoiding interference from the more

lipophilic anions), ionophores with specific binding affinity to nitrite through axial ligation reactions are required to be incorporated into the polymeric membrane. An alternative way of monitoring nitrite levels is via amperometric methods. However, this approach is frequently limited by slow kinetics of charge transfer for nitrite oxidation or reduction at conventional electrode surfaces [14-15]. Various designs of chemically modified electrodes (CMEs) have been suggested to address this problem through surface modifications on bare electrodes [16-18]. Some surface modifications have made use of metal ion-ligand complexes to lower the overpotential of nitrite oxidation or reduction [19-20].

Among the techniques for developing CMEs (not only for nitrite detection), metalloporphyrin-coated electrodes have shown beneficial features because they have the ability to substantially lower the electrochemical overpotential of various species [19, 21-23]. Electrode modification by porphyrins can be conveniently pursued by electropolymerization of suitable porphyrins/metalloporphyrins [24]. Electropolymerization of porphyrins offers the advantage of controlling the process of film deposition and conductivity by choosing an appropriate electroactive monomer and/or deposition conditions [21]. The electroactive monomer can participate in polymer coupling reactions via electroreduction or oxidation of the certain functional groups, for example, amino-, pyrrole- and hydroxyl-substituted tetraphenylporphyrins [25]. In particular, amino-substituted porphyrins and derivatives have been most commonly electropolymerized and studied to yield electrocatalytic layers for fabrication of CMEs [26-28]. The electropolymerization process can be simply carried out by using cyclic voltammetry or under constant-potential conditions. In previously reported

studies, conductive poly-tetrakis(3-aminophenyl) porphyrin-Fe(III) chloride films were prepared by electropolymerization process and the electrocatalytic behavior of these films for nitrite oxidation were investigated [29]. Three out of the five different electrode surfaces investigated in this previous work exhibited catalytic oxidization of nitrite.

The aim of this chapter is to examine the electrocatalytic behavior of rhodium(III) porphyrins towards nitrite oxidation, since cobalt(III) complexes have been studied previously [30] and showed such a catalytic effect, and it is known from research reported in Chapter 3, that nitrite can bind Rh(III) centers with reasonable affinity. To pursue this area of research, a water-soluble Rh(III) porphyrin was studied first in the solution phase as an electron transfer mediator and is shown to lower the overpotential for nitrite oxidation. Then, tetrakis(3-aminophenyl) porphyrin-Rh(III) was electropolymerized on a fluorine doped tin oxide electrode to provide an electron conducting layer as well as immobilize rhodium(III) porphyrin species on the electrode surface. It will be shown that this Rh(III)-porphyrin modified electrode has the ability to oxidize nitrite at a lower potential and exhibits clear linear relationship between current and nitrite concentration at a fixed potential applied to the electrode.

5.2. Experimental

5.2.1. Materials and Reagents

Rhodium(III) 5,10,15,20-tetrakis-(N-methyl-4-pyridyl)-21,23H-porphyrin tetratosylate (Rh-TMPP) and tetrakis(4-aminophenyl)porphyrin (TAPP) were purchased from Frontier Scientific (Logan, UT, U.S.A.). Rhodium(III) chloride and tetrabutylammonium

perchlorate (TBAP) were products of Sigma Aldrich (Milwaukee, WI, U.S.A.). FTO (fluorine-doped tin oxide (FTO)) electrodes were obtained from Pilkington Glass (Morrisville NC, U.S.A.). All organic solvents and salts for standard solutions were also from Sigma Aldrich and were used as received. Measurements were performed in 50 mM NaH_2PO_4/Na_2HPO_4 buffer solutions, pH 7.4. All solutions were prepared with 18.2 MΩ water (Milli-Q, Millipore Corporation, Billerica, MA, USA).

5.2.2. Measurements with Water-Soluble Rh(III) Porphyrin in Aqueous Solution Phase

The measurements were conducted using a CHI 800b (CH Instruments, Inc., Austin, TX, U.S.A.). A traditional three-electrode system was employed that included a glassy carbon disk electrode (diameter 3.0 mm) as the working electrode, a platinum wire (diameter 0.125 mm, length 50 mm) as the auxiliary electrode and a silver/silver chloride (Ag/AgCl) as the reference. The glassy carbon disk electrode was polished with 1.0, 0.3 and 0.05 μm alumina powders, consecutively to obtain a mirror-like surface and then sonicated in water for 5 min.

5.2.3. Electropolymerization and Film Characterization

FTO electrodes were cleaned by sonication in acetone, ethanol and water for 10 min, respectively. After drying, the electrodes were used immediately for electropolymerization. Poly-tetrakis(4-aminophenyl) porphyrin (poly-TAPP) conductive films were electropolymerized on a FTO glass electrode surface (0.63 cm × 0.5 cm) with a non-aqueous reference electrode, $Ag/AgNO_3$, and a platinum wire (diameter 0.2 mm, length 50 mm) as the auxiliary electrode, from a 0.15 mM TAPP and

10 mM TBAP as supporting electrolyte in dichloromethane (DCM) solution (all solutions were purged with DCM-saturated nitrogen for 20 min prior to electrodeposition). Film coatings were achieved by repeated cyclic voltammetry between -0.5 V to +1.2 V for 15 scans and adding a 30 s vertex delay at +1.2 V after the final scan. The resulting poly-TAPP coated electrodes were rinsed with fresh DCM and then ethanol and dried under nitrogen. Films were used immediately for characterization and electrochemical measurements.

In order to insert the metal center into the porphyrin rings to provide a poly-Rh(III)-TAPP, a metallization process was followed similar to that used for metal ion insertion of rhodium(III) into free porphyrins [31]. Briefly, the whole electrode with the surface poly-TAPP film was refluxed with rhodium(III) chloride (100 mg, 0.48 mmol (anhydrous basis)) in 30 mL benzonitrile for 24 h. After this reaction period, the electrode was washed with fresh benzonitrile, DCM and acetone. The surface modified electrode was immediately used for UV-Vis, SEM and electrochemical measurements.

The UV-Vis spectra of the FFO electrodes were performed on a PerkinElmer Lambda35 UV/Vis spectrophotometer (PerkinElmer, Waltham, MA, U.S.A.). Scanning electron microscopy (SEM) images were obtained using an Amray FE 1900 Scanning Electron Microscope (Amray Inc., Bedford, MA, U.S.A.). Electrochemical impedance spectroscopy was carried out on a Gamery Reference 600 (Warminster, PA, U.S.A.).

5.3. Results and Discussion

5.3.1. Electrocatalytic Oxidation of Nitrite by Rh-TMPP

A few metalloporphyrins, including ruthenium(III) and cobalt(III) porphyrin [32-33], have been studied and utilized as catalysts for nitrite oxidation. To evaluate the feasibility of rhodium(III) porphyrin functioning as a catalyst for nitrite electrooxidation, a water-soluble porphyrin, Rh-TMPP (see Fig. 5.1a for structure), was examined first in bulk solution phase. Fig. 5.1b illustrates the cyclic voltammograms of Rh-TMPP with a redox couple observed at ca. 0.52 V (vs. Ag/AgCl)) which is attributed to the Rh^{III}/Rh^{II} [34] redox couple. Fig. 5.2a shows the cyclic voltammograms obtained on a glassy carbon electrode for the oxidation of nitrite at a concentration of 1 mM in the presence of Rh-TMPP in the solution. An anodic oxidation peak is observed at ca. +0.64 V, and its intensity is dramatically increased compared to the current obtained by nitrite oxidation on the bare electrode (Fig. 5.2c), clearly indicating the electrocatalytic activity of Rh-TMPP towards nitrite oxidation as indicated by a negative shift of the peak potential and an increase of the current density. As nitrite concentration increases, the current intensity increases (Fig. 5.2b).

5.3.2. FTO Electrode Modified with Poly-Rh-TAPP Thin Film

The electropolymerization process is conducted by repeated cyclic voltammetry over the potential range of -0.5 – +1.2 V. Fig. 5.3a presents the recorded current – voltage behavior during the electropolymerization of TAPP monomer at the FTO surface. Cyclic voltammograms of TAPP in deaerated CH_2Cl_2 on the FTO electrode shows one redox couple with an $E_{1/2}$ = 0.26 V. The continuous growth of the electroactive polymer film is indicated by the increasing current for both the anodic and cathodic peaks upon

continuous scanning. It was reported previously that the electropolymerization of TAPP proceeds via a radial cation polymerization mechanism which is similar to poly(aniline) [35-37] and this means that the oxidation of the amino groups is a key step [28, 38-39]. The formed radical cation centered on the amino group diffuses to the solution where it attacks a neutral molecule at a carbon of the phenyl substituent or a radical cation, forming a neutral dimer. This process repeats itself over and over to create the electropolymerized surface layer on the electrode.

After electropolymerization, a thin and adhesive film is formed on the FTO electrode surface. The entire film coated electrode was then refluxed with rhodium(III) chloride in benzonitrile for conducting the metallization reaction to prepare the poly-Rh-TAPP modified electrode. After refluxing for 24 h, the resulting film exhibits a significant color change from deep purple to dark yellow/light brown. Fig. 5.3b shows the UV-Vis absorption of both free poly-TAPP (curve 1) and poly-Rh-TAPP (curve 2). Compared to the TAPP monomer absorption spectrum, the spectra for polymer films are broadened, accompanied by a red shift of the soret band, which has been noted in other reported work [40]. After metallization, besides the visible color change of the films, the absorption spectra obviously changes with a blue shift of the soret band and reduced amount of Q bands. Attempts were made to metalize free TAPP first and then electropolymerize Rh-TAPP monomer on to the electrode surface, but without success.

It was reported that electropolymerized TAPP in its oxidation state gives an electron conductive film, which is structurally similar to the *para*-coupled octamer, emeraldine [41]. The conductivity of the free poly-TAPP films and poly-Rh-TAPP films were therefore examined by electrochemical impedance spectroscopy. Impedance spectra

(see Fig. 5.3c) show that both films have the resistance of a few hundred ohms which are close to results reported in other papers [42]. It can be seen that the poly-Rh-TAPP film (see Fig. 5.3c solid diamond) has higher resistance than the free poly-TAPP film (see Fig. 5.3c solid square), but it can still be considered as an electron conducting polymer film.

The surface morphology of the poly-Rh-TAPP film was examined with scanning electron microscopy (SEM). It can be seen from Fig. 5.4 that the resulting homogeneous film fully covers the FTO electrode surface without any pinholes. The inset presents the interconnected and nanofiber-like porous structure, which can facilitate mass access making electroactive species transport effective and avoid diffusion barrier.

5.3.3. Electrocatalytic Oxidation of Nitrite on Poly-Rh-TAPP Modified FTO Electrodes

As shown in Fig. 5.5a4, the oxidation of nitrite on bare FTO electrode does not occur until the potential reaches to +1.0 V, indicating the slow electron transfer between nitrite and the electrode surface. When nitrite is not present in the electrolyte solution (only background buffer solution), two anodic peaks are observed (see Fig. 5.5a1) on poly-Rh-TAPP modified FTO electrodes. The peak at +0.44 V, which also shows up on curve 3, corresponds to the oxidation of amino groups from the porphyrin, and the other peak at around +0.5 V is attributed to the metal ion center. It also can be seen from curve 1 that, in the absence of nitrite, the background current on FTO electrode modified with poly-Rh-TAPP is high when potential reaches +0.6 V, which is likely due to water oxidation. With only 1 mM nitrite present along with the background buffer solution, the anodic current dramatically increases, indicating the electrocatalytic oxidation of nitrite. If FTO electrodes are only modified with poly-TAPP, there is no clear anodic

current observed in the presence of 1 mM nitrite except the oxidation peak of amino groups of the porphyrin rings, indicating the important role of the metal ion center.

At the working potential of +0.6 V, $NaNO_2$ was regularly added into the stirred PBS (pH 7.4) to obtain the typical steady-state amperometric current-time plot (see Fig. 5.5b). The oxidation current increases rapidly upon addition of nitrite with a response time within 5 s, indicating the fast mass transfer from the solution to the electrode surface. The inset of Fig. 5.5b shows the corresponding calibration curve between anodic current and $NaNO_2$ concentration. The linear response range is from 0.01 to 0.10 mM with a correlation coefficient of 0.9988 and a detection limit of 4.7 μm at a signal to noise ratio of 3.

The selectivity and anti-interference ability of poly-Rh-TAPP modified electrode was preliminarily evaluated by oxidizing other electrochemically active species at the same applied potential +0.6 V (*vs.* Ag/AgCl) to assess potential application in real sample measurement. In the presence of 0.1 mM $NaNO_2$, no obvious interference was observed when adding 50-fold of sulfite and 20-fold of ascorbic acid. However 100-fold amount of sulfite and 50-fold of ascorbic acid exhibit noticeable interference on the poly-Rh-TAPP modified FTO electrode.

5.4. Summary

The electrocatalytic effect for nitrite oxidation by a water-soluble rhodium(III) porphyrin was first examined. Results show clear electrocatalytic anodic current of

nitrite oxidation at a much lower potential. Then, a chemically modified FTO electrode was prepared by electropolymerizing tetrakis(p-aminophenyl) porphyrin via a radical cation polymerization mechanism, followed by metallization reaction with rhodium(III) chloride to yield the poly-Rh-TAPP film coated electrode. The oxidation of nitrite occurred at a lower potential on the modified electrode compared to only poly-TAPP modified electrode, suggesting the importance of the rhodium center. The modified electrode has fast response to nitrite with a linear range of 0.01 mM to 0.1 mM and lower detection limit of 4.7 μM. This poly-Rh-TAPP modified FTO electrode can be applied to create nitrite sensing devices based on amperometry. Preliminary selectivity study shows that the modified electrode exhibits anti-interference ability over some common electrochemically active species like sulfite and ascorbic acid.

(a)

(b)

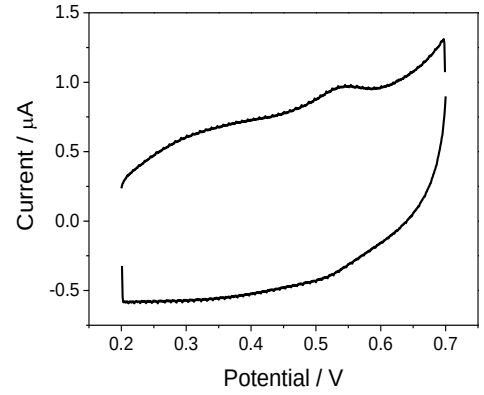

Fig. 5.1. (a) Structure of water-soluble rhodium(III) 5,10,15,20-tetrakis-(N-methyl-4-pyridyl) porphyrin tetratosylate (Rh-TMPP); (b) Cyclic voltammogram of 0.5 mM Rh-TMPP in 0.1 M NaCl with scan rate of 50 mV/s. Reference electrode: Ag/AgCl.

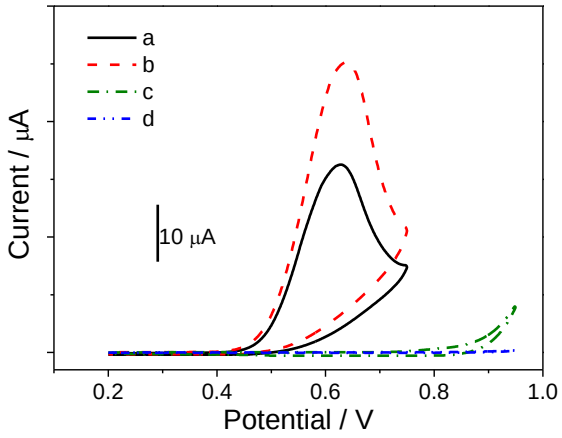

Fig. 5.2. Cyclic voltammograms of (a) 1 mM and (b) 10 mM $NaNO_2$ in 0.1 M NaCl on GC electrode in the presence of 0.5 mM Rh-TMPP; cyclic voltammograms of (c) 1 mM $NaNO_2$ and (d) no $NaNO_2$ in 0.1 M NaCl without Rh-TMPP. Scan rate: 50 mV/s. Reference electrode: Ag/AgCl

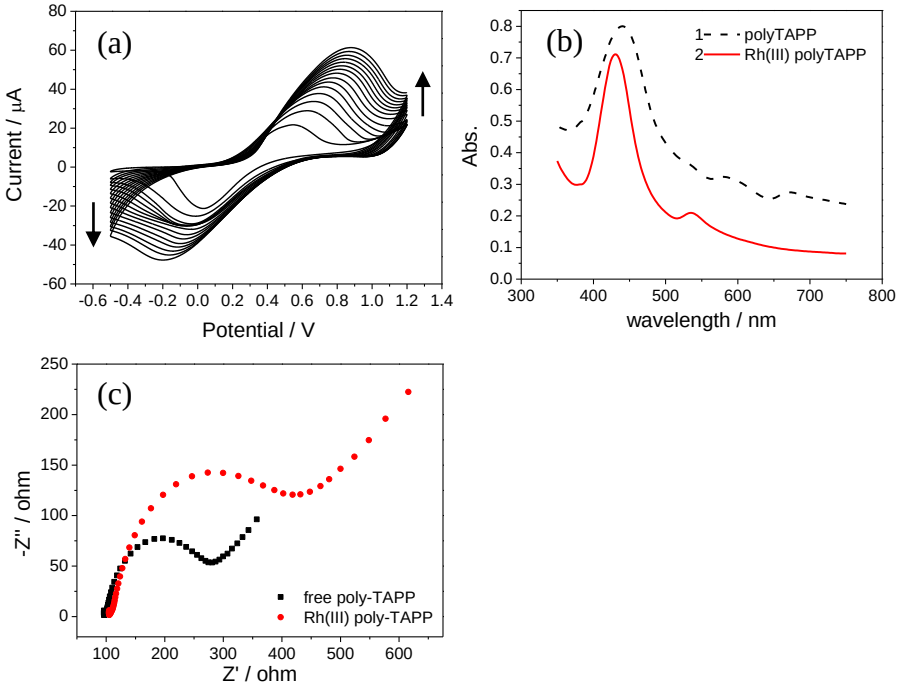

Fig. 5.3. (a) Cyclic voltammograms of 0.15 mM TAPP in CH_2Cl_2 deposited onto FTO electrode with scan rate of 20 mV/s, using 10 mM TBAP as the supporting electrolyte and $Ag/AgNO_3$ as the reference electrode. Cycles of scan: 15. (b) UV-Vis spectra of free poly-TAPP and poly-Rh-TAPP. (c) Nyquist plot of free poly-TAPP film (solid square) and poly-Rh-TAPP (solid diamond) on FTO electrodes. Electrolyte: 5 mM $K_4[Fe(CN)_6]$, 5 mM $K_3[Fe(CN)_6]$ and 1 M KCl. Reference electrode: Ag/AgCl.

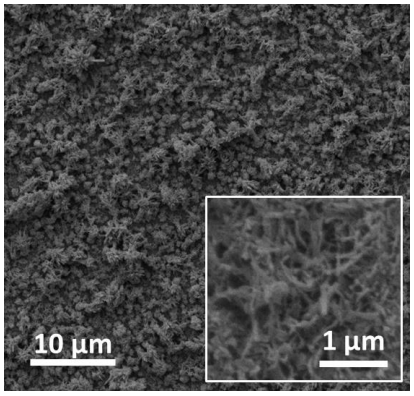

Fig. 5.4. SEM images of FTO electrode modified with poly-Rh-TAPP via electropolymerization of 0.15 mM TAPP in CH_2Cl_2 via cyclic voltammatry with scan rate of 20 mV/s using 10 mM TBAP as supporting electrolyte and $Ag/AgNO_3$ reference after 15 cycles of scan followed by metallization reaction with rhodium(III) chloride in benzonitrile for 24 h.

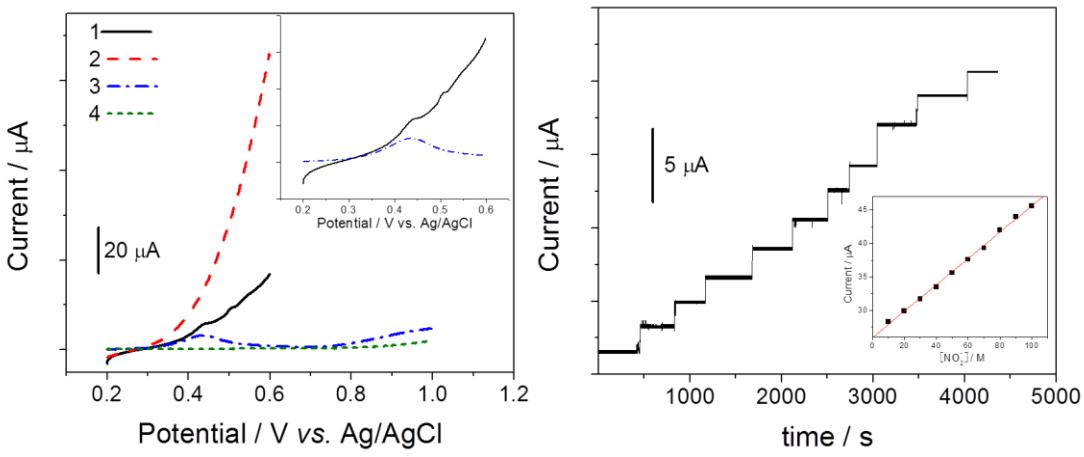

Fig. 5.5. (a) Linear sweep voltammogram of 1 mM $NaNO_2$ in 50 mM phosphate buffer (pH 7.4) with 0.1 M NaCl on FTO electrode modified with (2) poly-Rh-TAPP film, (3) poly-TAPP film and (4) bare FTO electrode. For comparison, LSV of (1) poly-Rh-TAPP modified electrode in 50 mM phosphate buffer (pH 7.4) containing 0.1 M NaCl without any $NaNO_2$ was also recorded; scan rate: 50 mV/s. The inset shows details of curve 1 and 3. (b) Plot of current vs. nitrite concentration between 10 μM to 100 μM in phosphate buffer (pH 7.4) with 0.1 M NaCl on FTO electrode modified with poly-Rh-TAPP film. Potential applied: +0.6 V vs. Ag/AgCl. The inset presents the linear relationship between nitrite concentration and response current.

5.5. References

[1] K.O. Honikel, "The use and control of nitrate and nitrite for the processing of meat products", *Meat Sci.*, **2008**, *78*, 68-76.

[2] W. J. R. Santos, P. R. Lima, A. A. Tanaka, S. M. C. N. Tanaka, L. T. Kubota, "Determination of nitrite in food samples by anodic voltammetry using a modified electrode", *Food Chem.*, **2009**, *113*, 1206-1211.

[3] N. Benjamin, F. Odriscoll, H. Dougall, C. Duncan, L. Smith, M. Golden, H. McKenzie, "Stomach NO synthesis", *Nature*, **1994**, *368*, 502-502.

[4] J. O. N. Lundberg, E. Weitzberg, J. M. Lundberg, K. Alving, "Intragastric nitric oxide production in humans-measurements in expelled air", *Gut*, **1994**, *35*, 1543-1546.

[5] J. L. Zweier, P. H. Wang, A. Samouilov, P. Kuppusamy, "Enzyme-independent formation of nitric-oxide in biological tissues", *Nat. Med.*, **1995**, *1*, 804-809.

[6] H. Kodamatani, S. Yamazaki, K. Saito, T. Tomiyasu, Y. Komatsu, "Selective determination method for measurement of nitrite and nitrate in water samples using high-performance liquid chromatography with post-column photochemical reaction and chemiluminescence detection", *J. Chromatogr. A*, **2009**, *1216*, 3163-3167.

[7] A. K. Malik, W. Faubel, "Capillary electrophoretic determination of tetramethylthiuram disulphide (thiram)", *Anal. Lett.*, **2000**, *33*, 2055 - 2064.

[8] G. M. Greenway, S. J. Haswell, P. H. Petsul, "Characterisation of a micro-total analytical system for the determination of nitrite with spectrophotometric detection", *Anal. Chim. Acta*, **1999**, *387*, 1-10.

[9] Z. Liu, X. Xi, S. Dong, E. Wang, "Liquid chromatography-amperometric detection of nitrite using a polypyrrole modified glassy carbon electrode doped with tungstodiphosphate anion", *Anal. Chim. Acta*, **1997**, *345*, 147-153.

[10] S. Senra-Ferreiro, F. Pena-Pereira, I. Lavilla, C. Bendicho, "Griess micro-assay for the determination of nitrite by combining fibre optics-based cuvetteless UV-Vis micro-spectrophotometry with liquid-phase microextraction", *Anal. Chim. Acta*, **2010**, *668*, 195-200.

[11] M. J. Martínez-Tomé, R. Esquembre, R. Mallavia, C. R. Mateo, "Development of a dual-analyte fluorescent sensor for the determination of bioactive nitrite and selenite in water samples", *J. Pharm. Biomed. Anal.*, **2010**, *51*, 484-489.

[12] M. I. H. Helaleh, T. Korenaga, "Fluorometric determination of nitrite with acetaminophen", *Microchem. J.*, **2000**, *64*, 241-246.

[13] A. Lapat, L. Székelyhidi, I. Hornyák, "Spectrofluorimetric determination of 1,3,5-trinitro-1,3,5-triazacyclohexane (Hexogen, RDX) as a nitramine type explosive", *Biomed. Chromatogr.*, **1997**, *11*, 102-104.

[14] Z. F. Zhao, X. H. Cai, "Determination of trace nitrite by catalytic polarography in ferrous iron thiocyanate medium", *J. Electroanal. Chem.*, **1988**, *252*, 361-370.

[15] J. A. Cox, P. J. Kulesza, "Oxidation and determination of nitrite at modified electrodes", *J. Electroanal. Chem. Interfacial Electrochem.*, **1984**, *175*, 105-118.

[16] A. P. Doherty, R. J. Forster, M. R. Smyth, J. G. Vos, "Development of a sensor for the detection of nitrite using a glassy carbon electrode modified with the electrocatalyst $[Os(bipy)_2(PVP)_{10}Cl]Cl$", *Anal. Chim. Acta*, **1991**, *255*, 45-52.

[17] A. P. Doherty, M. A. Stanley, D. Leech, J. G. Vos, "Oxidative detection of nitrite at an electrocatalytic $[Ru(bipy)_2$poly-(4-vinylpyridine)$_{10}Cl]Cl$ electrochemical sensor applied for the flow injection determination of nitrate using a Cu/Cd reductor column", *Anal. Chim. Acta*, **1996**, *319*, 111-120.

[18] J. Davis, R. G. Compton, "Sonoelectrochemically enhanced nitrite detection", *Anal. Chim. Acta*, **2000**, *404*, 241-247.
[19] N. S. Trofimova, A. Y. Safronov, O. Ikeda, "Electrochemical and spectral studies on the catalytic oxidation of nitric oxide and nitrite by high-valent manganese porphyrins at an ITO electrode", *Electrochim. Acta*, **2005**, *50*, 4637-4644.
[20] C. Caro, "Electrocatalytic oxidation of nitrite on a vitreous carbon electrode modified with cobalt phthalocyanine", *Electrochim. Acta*, **2002**, *47*.
[21] F. Bedioui, J. Devynck, C. Bied-Charreton, "Immobilization of metalloporphyrins in electropolymerized films: design and applications", *Acc. Chem. Res.*, **1995**, *28*, 30-36.
[22] H. Winnischofer, S. de Souza Lima, K. Araki, H. E. Toma, "Electrocatalytic activity of a new nanostructured polymeric tetraruthenated porphyrin film for nitrite detection", *Anal. Chim. Acta*, **2003**, *480*, 97-107.
[23] M. Biesaga, K. Pyrzyńska, M. Trojanowicz, "Porphyrins in analytical chemistry. A review", *Talanta*, **2000**, *51*, 209-224.
[24] K. A. Macor, T. G. Spiro, "Porphyrin electrode films prepared by electrooxidation of metalloprotoporphyrins", *J. Am. Chem. Soc.*, **1983**, *105*, 5601-5607.
[25] A. Bettelheim, B. A. White, S. A. Raybuck, R. W. Murray, "Electrochemical polymerization of amino-, pyrrole-, and hydroxy-substituted tetraphenylporphyrins", *Inorg. Chem.*, **1987**, *26*, 1009-1017.
[26] H. Li, T. F. Guarr, "Electrocatalytic oxidation of oxalic acid at electrodes coated with polymeric metallophthalocyanines", *J. Electroanal. Chem. Interfacial Electrochem.*, **1991**, *317*, 189-202.
[27] B. A. White, R. W. Murray, "Electroactive porphyrin films from electropolymerized metallotetra(o-aminophenyl)porphyrins", *J. Electroanal. Chem. Interfacial Electrochem.*, **1985**, *189*, 345-352.
[28] S.-M. Chen, Y.-L. Chen, "The electropolymerization and electrocatalytic properties of polymerized MnTAPP film modified electrodes in aqueous solutions", *J. Electroanal. Chem.*, **2004**, *573*, 277-287.
[29] A. Francisco, M. C. Goya, R. Matías, M. J. Canales, M. C. Arévalo, M. J. Aguirre, "Electrocatalytic oxidation of nitrite to nitrate mediated by Fe(III) poly-3-aminophenyl porphyrin grown on five different electrode surfaces", *J. Mol. Catal. A: Chem.*, **2007**, *268*.
[30] A. C. Ion, I. Ion, A. Ficai, "Chemically modified electrode for NO_2^- determination in environmental applications", *Meeting Abstracts*, **2007**, *MA2007-02*, 1462.
[31] M. Pietrzak, M. E. Meyerhoff, "Polymeric membrane electrodes with high nitrite selectivity based on rhodium(III) porphyrins and salophens as ionophores", *Anal. Chem.*, **2009**, *81*, 3637-3644.
[32] J. R. C. da Rocha, L. Angnes, M. Bertotti, K. Araki, H. E. Toma, "Amperometric detection of nitrite and nitrate at tetraruthenated porphyrin-modified electrodes in a continuous-flow assembly", *Anal. Chim. Acta*, **2002**, *452*, 23-28.
[33] K. Araki, L. Angnes, C. M. N. Azevedo, H. E. Toma, "Electrochemistry of a tetraruthenated cobalt porphyrin and its use in modified electrodes as sensors of reducing analytes", *J. Electroanal. Chem.*, **1995**, *397*, 205-210.
[34] S. Fukuzumi, *The Porphyrin Handbook, Vol. 8*, Academic Press, New York, **2000**..
[35] T. Kobayashi, H. Yoneyama, H. Tamura, "Polyaniline film-coated electrodes as electrochromic display devices", *J. Electroanal. Chem. Interfacial Electrochem.*, **1984**, *161*, 419-423.
[36] T. Kobayashi, H. Yoneyama, H. Tamura, "Oxidative degradation pathway of polyaniline film electrodes", *J. Electroanal. Chem. Interfacial Electrochem.*, **1984**, *177*, 293-297.
[37] W.-S. Huang, B. D. Humphrey, A. G. MacDiarmid, "Polyaniline, a novel conducting polymer. Morphology and chemistry of its oxidation and reduction in aqueous

electrolytes", *J. Chem. Soc. Faraday Trans. 1*, **1986**, *82*, 2385-2400.
[38] M. Lucero, G. Ramírez, A. Riquelme, I. Azocar, M. Isaacs, F. Armijo, J. E. Förster, E. Trollund, M. J. Aguirre, D. Lexa, "Electrocatalytic oxidation of sulfite at polymeric iron tetra (4-aminophenyl) porphyrin—modified electrode", *J. Mol. Catal. A: Chem.*, **2004**, *221*, 71-76.
[39] F. Armijo, M. C. Goya, Y. Gimeno, M. C. Arévalo, M. J. Aguirre, A. H. Creus, "Study of the electropolymerization of tetrakis (3-aminophenyl) porphyrin Fe(III) chloride on Au electrodes by cyclic voltammetry and STM", *Electrochem. Commun.*, **2006**, *8*, 779-784.
[40] G. W. Michael, C. W. Carl, "Synthesis and characterization of electropolymerized nanostructured aminophenylporphyrin films", *J. Phys. Chem. C*, **2010**, *114*.
[41] A. Bettelheim, B. A. White, S. A. Raybuck, W. M. Royce, "Electrochemical polymerization of amino-, pyrrole-, and hydroxy-substituted tetraphenylporphyrins", *Inorg. Chem.*, **1987**, *26*.
[42] B. Enrico Maria, G. Marco, M. Giovanni, S. Renato, "Electropolymerization of tetrakis(o-aminophenyl)porphyrin and relevant transition metal complexes from aqueous solution. The resulting modified electrodes as potentiometric sensors", *Electroanalysis*, **1999**, *11*.

Chapter 6

Conclusions and Future Directions

6.1. Summary of this Dissertation Research

This dissertation research was focused mainly on the development, fundamental study, and application of polymeric membrane/film based ion-selective electrodes and optodes with novel ionophores for sensitive and selective detection nitrite. Efforts were made to synthesize new nitrite-selective ionophores, optimize the sensing systems both for potentiometric and optical measurements, as well as implementing new applications of the sensors.

Several nitrite-selective ionophores have been reported previously, all of which are metal ion ligand complexes, including a cobalt(III) complex with a vitamin B_{12} derivative as the ligand (NI-1) [1-3] and various Rh(III) porphyrins [4]. The commercially available nitrite-selective ionophore NI-1 indeed has strong binding affinity to nitrite and can discriminate against most common anions, but sensors based on this ionophore do experience substantive interference from thiocyanate ($\log K^{pot}_{NO_2^-,X}$ (SSM): SCN^-, +0.2;

o-NPOE, KTFPB) [3]. As discussed previously in this dissertation, the Rh(III) porphyrins can function as either/both charged carriers and neutral carriers type ionophores within the membrane phase and this complicates the sensing chemistry. Since cobalt(III) and rhodium(III) have already been proven to have strong interaction with nitrite, other Co(III)/Rh(III)-ligand complexes with corrole as the surrounding ligand were examined as nitrite-selective ionophores in this dissertation research.

Corrole is a member of porphynoid compound family. Like porphyrins, corroles possess a tetrapyrrolic macrocycle structure with an aromatic 18π electron system. Unlike porphyrins, there is a direct linkage between two adjacent pyrrole rings so that the skeletons of corroles are contracted by one carbon [5]. Corroles are known to form complexes with various transition and main group metal ions [6], but very few of them have been reported as anion ionophores for ISEs or optical ion sensors. Owing to the unique structure, corroles are -3 charged ligands when complexed to metal(III) ions, like Co(III) and Rh(III). After metallation, the given Co(III)/Rh(III) corrole complex can only be neutral, which also ensures that there's only one sensing chemistry of the ionophore in the polymeric membrane for nitrite detection. To date, there have been no other reports of neutral ionophores based on metal ion ligand complexes with Co(III) and Rh(III).

Chapter 2 examined for the first time polymeric membrane electrodes based on cobalt(III) 5,10,15-tris(4-tert-butylphenyl) corrole (Co-tBC) as a neutral carrier for nitrite detection. The resulting electrodes yielded reversible and Nernstian response toward

nitrite with the low detection limit of ca. 5 μM. With optimized membrane composition, the observed selectivity pattern differs significantly from the classical Hofmeister series with greatly enhanced nitrite selectivity over other anions, including lipophilic anions such as thiocyanate and perchlorate. This indicates a strong ligation interaction between the Co(III) corrole and nitrite. Experiments to measure binding constant between nitrite and the ionophore via segmented sandwich membrane method were conducted and yielded a logarithm value of the binding constant to be 5.57 ± 0.13. Surprisingly, moderately enhanced nitrate response was observed when sensors were plasticized with tributylphosphate (equivalent selectivity coefficient with perchlorate), indicating some weak interaction between nitrate and the ionophore. As shown in Table 6.1, although Co-tBC based potentiometric sensors experience more interference from perchlorate, these sensors have better selectivity to nitrite over thiocyanate than sensors based on NI-1 and Rh-tBTPP.

Chapter 3 studied the rhodium(III) 5,10,15-tris(4-tert-butylphenyl) corrole (Rh-tBC) species as a new ionophore for preparing potentiometric nitrite-selective sensors. Since rhodium is in the same group as cobalt and exhibits similar chelating chemistry, the Rh-tBC complex was incorporated into polymeric membranes for nitrite sensor development. Membrane electrode sensors prepared with this ionophore do show near Nernstian response and low detection limit (i.e., in the μM range) to nitrite when the proper amount of lipophilic ion-additives are present in the polymeric membrane. In addition, enhanced selectivity to nitrite over most anions is observed; however,

thiocyanate remains a very significant interference. Complex formation constant measurement by the segmented sandwich membrane method yielded the binding affinity of 4.04±0.08 (logarithmic value), which is one and a half orders of magnitude less than that of the cobalt(III) corrole species, and this helped explain the lack of higher selectivity over thiocyanate.

With the knowledge that the cobalt(III) corrole species have strong and selective axial ligation reaction with nitrite to form a host-guest complex, attempts were made in applying this metallocorrole species to fabricate polymeric film type optical sensors. As described in Chapter 1, compared to polymeric membrane ISEs, optodes have the advantages of tunable dynamic response ranges and detection limits. Moreover, by coating the bottom of each well of a 96-well plate with a polymeric film and using a microplate reader, high throughput ion-selective measurements can be achieved [7]. In contrast to the many publications regarding attempts to prepare nitrite-selective potentiometric sensors, there are very few efforts reported aimed at developing nitrite-selective optodes.

Chapter 4 focused on fabrication of nitrite-selective bulk optodes by incorporating either Co-tBC with a triphenylphosphine axial ligand or rhodium(III) 5,10,15,20-tetra(*p-tert*-butylphenyl)porphyrin (Rh-tBTPP) into plasticized poly(vinyl chloride) films. Rh-tBTPP has been studied as a nitrite-selective ionophore in potentiometric sensors, but not optically [4]. The resulting films yielded sensitive, fast and fully reversible response toward nitrite with significantly enhanced nitrite selectivity

over other anions including lipophilic anions such as thiocyanate and perchlorate. The selectivity patterns differ greatly from the Hofmeister series and are consistent with selectivity obtained with potentiometric ion sensors based on the same ionophores in plasticized polymeric membranes [4, 8]. Sensor response ranges and detection limits can be tuned by changing film formulations (types of chromoionophores, amounts of ionopohores and chromoionophores, etc.) and test buffer pH values. The potential for immediate application of these sensors is demonstrated by quantifying the rates of NO release from polymeric films doped with various NO donors, and the results correlate well with those obtained using the classical Griess spectrophotometric assay method for nitrite.

Several palladium organophosphines which serve as charged carriers have previously been incorporated into polymeric films to fabricate optical sensors for nitrite detection in the absorbance mode [9]. The best of these was dichlorobis[methylene-bis(diphenylphosphine)]-dipalladium (diPd-dPP). Table 6.2 summarizes the comparison of the diPd-dPP-based sensors and sensors prepared with films doped with Co-tBC and Rh-tBTPP, in terms of selectivity and detection limit. As shown in the table, sensors based on Co-tBC and Rh-tBTPP have much lower detection limit and better selectivity to nitrite over thiocyanate than the prior sensor prepared with diPd-dpp.

In Chapter 5, a different approach regarding nitrite detection was pursued. A chemically modified FTO electrode was prepared by electropolymerizing

tetrakis(p-aminophenyl) porphyrin on the surface, followed by a metallization reaction of this surface bound species with rhodium(III) chloride. Polymerized metalloporphyrins have been studied as conducting layers on conventional electrode surfaces and are known to exhibit electrocatalytic effects towards different species [10]. The new Rh(III) porphyrin modified electrode was found to electrocatalytically oxidize nitrite at a much lower applied potential compared to bare electrodes. Amperometric nitrite responses are fast on the modified electrode with a linear range of 0.01 mM to 0.1 mM with a detection limit of 4.7 μM. The poly-Rh-TAPP modified FTO electrode can be applied to make nitrite sensing devices based on amperometric measurements. Preliminary selectivity study shows that the modified electrode exhibits anti-interference ability over some common electrochemically active species like sulfite and ascorbic acid.

6.2. Future Directions

6.2.1. New Ionophores Based on Neutral Co(III)-Ligand Complexes without Axial Ligands

The studied complex, Co-tBC with a triphenylphosphine axial ligand, is indeed an excellent ionophore which shows strong yet reversible interaction with nitrite. However, as described in Chapter 2, other previously reported nitrite-selective ionophores (charged-carriers) [1-2] have much larger binding constants with nitrite, which were calculated as (log values) 10.58 ± 0.04 or 10.59 ± 0.08 (with membranes prepared with

PVC-DOS and PVC-NPOE, respectively) [11]. The weaker binding between Co-tBC and nitrite is possibly due to the presence of triphenylphosphine which binds to the cobalt center strongly as a trans axial ligand to where nitrite binds. With such a structure, the cobalt(III) center is in an approximately square pyramidal coordination environment and displaced a little off the corrole plane toward the phosphorous atom [12], making nitrite binding to the metal ion center on the opposite side less favorable. Indeed, it is well known that the presence of a 5^{th} axial ligand will generally weaken interactions of other ligands at the 6^{th} site.

To address this issue, an alternative cobalt(III) complex can be employed, which is a triazacorrole species, the so-called cobalt(III) corrolazine (Co-Cz) [13-15]. Fig. 6.1 shows the structures of corrole and corrolazine. Corrolazines are *meso*-nitrogen-substituted analogues of corroles. This molecule retains the tetrapyrrolic, aromatic structure of a corrole and is a trianionic donor ligand when fully deprotonated. Many of the conventional cobalt(III) corroles have been isolated and fully characterized only in the presence of strong axial ligands (e.g., PPh_3, pyridine), affording the five- or six-coordinate complexes [12, 16-19]. It is reported that in the absence of axial ligands, cobalt corroles are not stable. Indeed, they oxidize and dimerize, linking two corrole rings by forming a direct C_β-C_β bond [14]. The Goldberg group has recently synthesized and isolated a neutral four-coordinated cobalt(III) complex (see Fig. 6.2 for synthesis route) of the corrolazine structure [14]. Co-Cz was prepared by heating free base corrolazine with an excess of cobalt(II) acetylacetonate in pyridine. The

researchers believe that the stability of Co-Cz is due to a combination of the oxidatively resistant meso nitrogen atoms and phenyl substituents that block all eight of the α positions in the Cz ring.

Since corrolazine is -3 charged when complexed with metal ions, a Co(III)-Cz can be expected to function as a neutral carrier within polymeric membranes. Without any additional axial ligands, this cobalt(III) complex can have stronger binding affinity to nitrite than the cobalt(III) corrole species reported in this dissertation.

6.2.2. Alternative Design of Ionopohore-Based Optical Sensors

Polymeric film-based optical sensors have shown to be flexible and versatile in design to achieve sensitive and selective detection of target ions. In order to examine the feasibility of employing the newly studied nitrite-ionophore, Co-tBC, a few optodes with different chromoionophores were tested via absorbance mode in this dissertation research (Chapter 4). To achieve even better sensitivity, another approach that can be pursued is a luminescence technique, basing the optical sensing principle on fluorescence instead of absorbance. This is due in part to its inherently greater sensitivity, its almost complete inertness to turbidity, and its flexibility with respect to geometric arrangements [20]. The most direct and convenient way to pursue this direction is to use chromoionophores as fluorescent indicators. Several chromoionophores of Nile Blue derivatives, such as ETH5294 and ETH2439, have been successfully employed in fabricating fluorescent optodes for both cations and anions detection [21-23]. The film formulations studied in

Chapter 4 can be simply examined in fluorescence mode using these dyes instead of the one employed herein.

A common indirect detecting method is to incorporate an additional fluorophore besides the original chromoionophore and the ionophore. The absorption spectrum of the protonated and unprotonated chromoionophore should overlap at least one emission band of the added fluorophore. Guo and coworkers [20] reported the use of tetraphenylporphyrin (TPP) as the fluorescent dye along with a sodium ionophore and chromoionophore I within polymeric films to fabricate fluorescent sodium optodes. The emission peak of TPP at 650 nm overlaps the absorption spectrum of protonated chromoionophore I.

Among the examined optode formulations in Chapter 4, sensors doped with chromoionophore I provided the best optical response to nitrite. Therefore, it is quite possible to employ TPP within the same sensing film with Co-tBC and chromoionophore I to fabricate a nitrite-selective fluorescent optode. Another possible candidate type of fluorophore is a nanomaterial. For example, $NaYF_4$:Er,Yb upconverting nanorods have been incorporated into polymeric films with chromoionophore VII and different ionophores to fabricate optical sensors for detection of different ions [24]. The absorption spectra of protonated and unprotonated ETH 5418 overlap the two emission bands of the upconverting material, providing a means to achieve modulation of the nanorod emission signal as a function of the concentration of target ion present.

In recent years, quantum dot (QD)-based ion-selective miniaturized optical sensors

have also been reported [25-28]. These types of optical transducers generally have a high luminescence quantum yield, good photochemical stability, broad excitation bands and narrow emission bands, size-dependent emission wavelength and large effective Stokes shifts [29]. Xu *et.al.* reported microsphere-based sodium sensors using a type of core-shell QD (CdSe/CdS) encoded as internal fluorescent dye [30]. The cocktail contained the sodium ionophore, lipophilic ion additives, a chromoionophore and QDs in DOS plasticized PVC. By changing some ingredients of the above cocktail (e.g., replace sodium ionophore with nitrite ionophore), it is likely possible to create miniaturized microsphere-based fluorescent nitrite-selective sensors. Even smaller sensors have been reported. A nanoscale ion-selective polymer-based sensor that incorporates quantum dots into the polymer matrix has been demonstrated [31]. The sensor has three components, the QDs, an ion-selective polymer matrix and a biocompatible coating. The QDs used in the paper have the emission peak overlapped with the absorption spectrum of protonated chromoionophore I. The mechanism of the sensor is based on a combination of traditional ion-selective optodes and an inner filter effect, which now, based on this thesis work, also has the potential to be extended to nitrite detection.

6.2.3. Application of Nitrite-Selective Electrodes and Optodes

One of the most important applications of nitrite sensors is in the detection of NO, because NO is a very important biological messenger, as mentioned in previous chapters.

In Chapter 4, it was demonstrated that Co-tBC-based optodes can successfully measure the rates of NO release from polymeric films doped with certain NO donors. Since optodes and ISEs share many similarities, the approach of using Co-tBC-based ISEs to detect NO emission rate is worth pursuing.

Another potential application is the determination of nitrite levels in meat products, which is essential for food regulatory agencies. Nitrite is added to cured meat mainly to inhibit the growth of pathogens, but nitrite can also react with secondary amines to produce nitrosamines, carcinogenic substances [32]. USDA regulates that the use of nitrites and nitrates, and the combination of these cannot result in more than 200 ppm total level within meats. Rhodium(III)-based polymeric membrane electrodes have been shown previously to provide accurate determinations of nitrite levels in cured meats with excellent agreement with Griess assay method [4]. The Co-tBC-based polymeric electrodes and optodes developed in this thesis work should also be explored as new tools to monitor nitrite concentrations in cured meats.

Table 6.1. Logarithm of potentiometric selectivity (relative to nitrite) and detection limit obtained for various sensors based on plasticized polymer membranes doped with different nitrite-selective ionophores and lipophilic ion additives.

Ionophore			NI-1[2]	Rh-tBTPP[4]	Co-tBC[8]
Membrane Composition	Plasticizer		*o*-NPOE	*o*-NPOE	*o*-NPOE
	Ionic Sites	Type	KTFPB	TDMACl	TDMACl
		Amount (mol%)	37	10	10
Selectivity	Cl^-		-3.7	-3.8	-4.5
	Br^-		-3.3	-3.2	-3.0
	NO_3^-		-3.5	-2.8	-1.5
	SCN^-		0.2	-0.4	-0.6
	ClO_4^-		-2.2	-1.7	-0.5
Detection Limit (M)			*	5×10^{-6}	6.9×10^{-6}

* Not reported in the cited literature.

Table 6.2. Logarithm of optical selectivity (relative to nitrite) and detection limit obtained for optode type sensors based on plasticized polymer films doped with different nitrite-selective ionophores and chromoionophores.

Ionophore		diPd-dPP [9]	Rh-tBTPP	Co-tBC
Membrane Composition	Chromoionophores	VI	VI	I
	Ionophore:Chromoionophore (molar ratio)	1:1	1:1	2:1
Selectivity	Cl^-	-2.5	-3.9	-3.3
	Br^-	-2.0	-3.2	-2.9
	NO_3^-	-3.4	-2.7	-2.6
	SCN^-	-0.2	-1	-0.9
	ClO_4^-	-1.2	-1.9	-0.5
Detection Limit (M)		3.2×10^{-6}	1.8×10^{-7}	3.5×10^{-7}

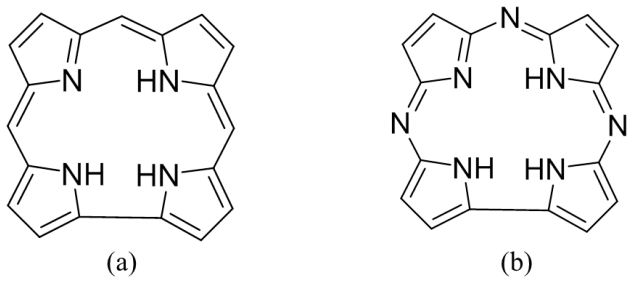

Fig. 6.1. Structures of (a) corrole and (b) corrolazine.

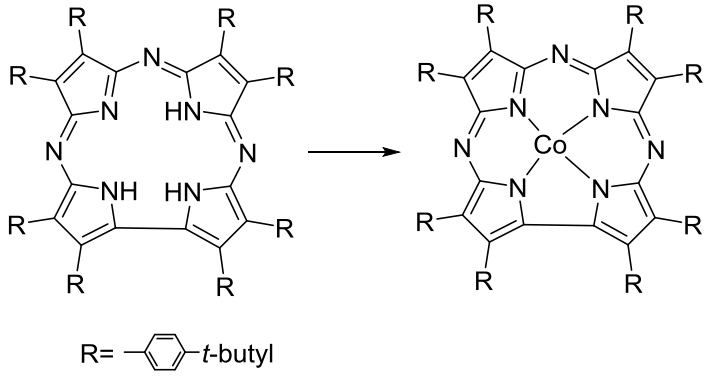

Fig. 6.2. Synthesis of cobalt(III) corrolazine from free corrolazine.

6.3. References

[1] P. Schulthess, D. Ammann, B. Krautler, C. Caderas, R. Stepanek, W. Simon, "Nitrite-selective liquid membrane-electrode", *Anal. Chem.*, **1985**, *57*, 1397-1401.

[2] R. Stepanek, B. Krautler, P. Schulthess, B. Lindemann, D. Ammann, W. Simon, "Aquocyanocobalt(III)-hepta(2-phenylethyl)-cobyrinate as a cationic carrier for nitrite-selective liquid-membrane electrodes", *Anal. Chim. Acta*, **1986**, *182*, 83-90.

[3] U. Schaller, E. Bakker, U. E. Spichiger, E. Pretsch, "Ionoic additives for ion-selective electrodes based on electrically charged carriers", *Anal. Chem.*, **1994**, *66*, 391-398.

[4] M. Pietrzak, M. E. Meyerhoff, "Polymeric membrane electrodes with high nitrite selectivity based on rhodium(III) porphyrins and salophens as ionophores", *Anal. Chem.*, **2009**, *81*, 3637-3644.

[5] J. Buchler, C. Dreher, F. Künzel, S. Licoccia, R. Paolesse, J. Šima, in *Metal Complexes with Tetrapyrrole Ligands III, Vol. 84*, Springer Berlin / Heidelberg, **1995**, pp. 71-133.

[6] A. H. Iris, G. Zeev, "Coordination chemistry of corroles with focus on main group elements", *Coord. Chem. Rev.*, **2011**, *255*.

[7] S. Dai, Q. Ye, E. Wang, M. E. Meyerhoff, "Optical detection of polycations via polymer film-modified microtiter pates: response mechanism and bioanalytical applications", *Anal. Chem.*, **2000**, *72*, 3142-3149.

[8] S. Yang, M. E. Meyerhoff, "Study of cobalt(III) corrole as the neutral ionophore for nitrite and nitrate detection via polymeric membrane electrodes", *Electroanalysis*, **2013**, *25*, 2579-2585.

[9] I. H. A. Badr, "Nitrite-selective optical sensors based on organopalladium ionophores", *Anal. Lett.* **2001**, *34*, 2019-2034.

[10] S.-M. Chen, Y.-L. Chen, R. Thangamuthu, "Electropolymerization of iron tetra(o-aminophenyl)porphyrin from aqueous solution and the electrocatalytic behavior of modified electrode", *J. Solid State Electrochem.*, **2007**, *11*, 1441-1448.

[11] Y. Qin, E. Bakker, "Quantitive binding constants of H^+-selective chromoionophores and anion ionophores in solvent polymeric sensing membranes", *Talanta*, **2002**, *58*, 909-918.

[12] R. Paolesse, S. Licoccia, G. Bandoli, A. Dolmella, T. Boschi, "First direct synthesis of a corrole ring from a monopyrrolic precursor: crystal and molecular structure of (triphenylphosphine)(5,10,15-triphenyl-2,3,7,8,12,13,17,18-octamethylcorrolato) cobalt(III)-dichloromethane", *Inorg. Chem.*, **1994**, *33*, 1171-1176.

[13] B. Ramdhanie, C. L. Stern, D. P. Goldberg, "Synthesis of the first corrolazine: a new member of the porphyrinoid family", *J. Am. Chem. Soc.*, **2001**, *123*, 9447-9448.

[14] B. Ramdhanie, L. Zakharov, A. Rheingold, D. Goldberg, "Synthesis, structures, and properties of a series of four-, five-, and six-coordinate cobalt(III) triazacorrole complexes: the first examples of transition metal corrolazines", *Inorg. Chem.*, **2002**, *41*, 4105-4107.

[15] D. Goldberg, "Corrolazines: new frontiers in high-valent metalloporphyrinoid stability and reactivity", *Acc. Chem. Res.*, **2007**, *40*, 626-634.

[16] R. Paolesse, *The Porphyrin Handbook, Vol. 2*, Academic Press, New York, **2000**.

[17] V. A. Adamian, F. D'Souza, S. Licoccia, M. L. Di Vona, E. Tassoni, R. Paolesse, T. Boschi, K. M. Kadish, "Synthesis, characterization, and electrochemical behavior of (5,10,15-Tri-X-phenyl-2,3,7,8,12,13,17,18-octamethylcorrolato)cobalt(III) triphenylphosphine complexes, where X = *p*-OCH_3, *p*-CH_3, *p*-Cl, *m*-Cl, *o*-Cl, *m*-F, *o*-F, or H", *Inorg. Chem.*, **1995**, *34*, 532-540.

[18] R. Paolesse, S. Mini, F. Sagone, T. Boschi, L. Jaquinod, D. J. Nurco, K. M. Smith, "5,10,15-Triphenylcorrole: a product from a modified Rothemund reaction", *Chem. Commun.*, **1999**, *0*, 1307-1308.

[19] Y. Murakami, S. Yamada, Y. Matsuda, K. Sakata, "Transition-metal complexes of pyrrole pigments. XV. coordination of pyridine bases to the axial sites of cobalt corroles", *Bull. Chem. Soc. Jpn.*, **1978**, *51*, 123-129.

[20] X. Yang, K. Wang, C. Guo, "A fluorescent optode for sodium ion based on the inner filter effect", *Anal. Chim. Acta*, **2000**, *407*, 45-52.

[21] M. Shortreed, E. Bakker, R. Kopelman, "Miniature sodium-selective ion-exchange optode with fluorescent pH chromoionophores and tunable dynamic range", *Anal. Chem.*, **1996**, *68*, 2656-2662.

[22] M. R. Shortreed, S. Dourado, R. Kopelman, "Development of a fluorescent optical potassium-selective ion sensor with ratiometric response for intracellular applications", *Sens. Actuators, B*, **1997**, *38*, 8-12.

[23] M. R. Shortreed, S. L. R. Barker, R. Kopelman, "Anion-selective liquid-polymer optodes with fluorescent pH chromoionophores, tunable dynamic range and diffusion enhanced lifetimes", *Sens. Actuators, B*, **1996**, *35*, 217-221.

[24] L. Xie, Y. Qin, H.-Y. Chen, "Polymeric optodes based on upconverting nanorods for fluorescent measurements of pH and metal ions in blood samples", *Anal. Chem.*, **2012**, *84*, 1969-1974.

[25] Y. Chen, Z. Rosenzweig, "Luminescent CdS quantum dots as selective ion probes", *Anal. Chem.*, **2002**, *74*, 5132-5138.

[26] H. Wu, J. Liang, H. Han, "A novel method for the determination of Pb^{2+} based on the quenching of the fluorescence of CdTe quantum dots", *Microchim. Acta*, **2008**, *161*, 81-86.

[27] W. J. Jin, J. M. Costa-Fernández, R. Pereiro, A. Sanz-Medel, "Surface-modified CdSe quantum dots as luminescent probes for cyanide determination", *Anal. Chim. Acta*, **2004**, *522*, 1-8.

[28] J. G. Liang, X. P. Ai, Z. K. He, D. W. Pang, "Functionalized CdSe quantum dots as selective silver ion chemodosimeter", *Analyst*, **2004**, *129*, 619-622.

[29] Q. Wang, Y. Kuo, Y. Wang, G. Shin, C. Ruengruglikit, Q. Huang, "Luminescent properties of water-soluble denatured bovine serum albumin-coated CdTe quantum dots", *J. Phys. Chem. B*, **2006**, *110*, 16860-16866.

[30] C. Xu, E. Bakker, "Multicolor quantum dot encoding for polymeric particle-based optical ion sensors", *Anal. Chem.,* **2007**, *79*, 3716-3723.

[31] J. M. Dubach, D. I. Harjes, H. A. Clark, "Ion-selective nano-optodes incorporating quantum dots", *J. Am. Chem. Soc.,* **2007**, *129*, 8418-8419.

[32] W. Fiddler, J. W. Pensabene, E. G. Piotrowski, J. G. Phillips, J. Keating, W. J. Mergens, H. L. Newmark, "Inhibition of formation of volatile nitrosamines in fried bacon by the use of cure-solubilized .alpha.-tocopherol", *J. Agric. Food. Chem.,* **1978**, *26*, 653-656.

Appendix I

Synthesis of Sterically Hindered Metalloporphyrins as Nitrite-Selective Ionophores

A.1. Introduction

There is great interest in developing new anion-selective potentiometric sensors based on ionophores with specific interactions with given anions within polymeric membranes. As discussed in Chapter 1, the introduction of ionophores inside the membrane can lead to analytically useful sensors exhibiting selectivity patterns which differ greatly from the so-called Hofmeister pattern (i.e., selectivity not based solely on the lipophilicity of anions). Among the compounds studied which have strong but reversible interactions with target anions, metalloporphyrins offer many exciting possibilities. Indeed, a large number of porphyrins with different metal ion centers have been incorporated into polymer membranes as ionophores and the resulting sensors have exhibited distinctly different anion selectivities, including Mn(III) [1-3], In(III) [4], Co(III) [1, 5-7], and Rh(III) porphyrins [8] employed in the design of sensors for detection of thiocyanate, chloride and nitrite (for both Co(III)- and Rh(III) porphyrins), respectively.

Anion carriers can be classified as two types, neutral carriers (electrically neutral when

not complexed, and negatively charged when complexed to the target anion) and charged carriers ionophore which are positively charged in native form and neutral when complexed to target anion. Lindner et al. found that ionophores acting as neutral carriers in the polymeric membranes require simultaneous incorporation of lipophilic cationic sites (e.g., tridodecylmethylammonium chloride, TDMACl) to yield appropriate anion response and selectivity [9]. On the other hand, for anion ionophores that function as charged carriers within the membrane phase, lipophilic anionic additives (e.g., potassium tetrakis[3,5-bis(trifluoromethyl)phenyl]borate, KTFPB) are necessary. However, due to the anionic impurities within poly(vinyl chloride) [10], plasticized PVC membrane electrodes containing charge carrier type anion ionophores can sometimes exhibit useful potentiometric anion response slopes and promising selectivities without adding exogenous lipophilic anionic sites.

Devising simple sensors to detect nitrite has drawn more attention, since it is present in food [11-12] and the environment [13-14], as well as in industrial, biological/physiological samples [15-16]. More importantly, nitrite is viewed as a storage pool of nitric oxide (NO), an important biological messenger [17-19]. Therefore, levels of nitrite in physiological fluids can reflect NO production rates.

As reviewed in Chapter 1, there are a few useful nitrite ionophores that have been reported to date. These include a vitamin B_{12} derivative [20-21], cobalt(III) tetraphenylporphyrins [22], palladium organophosphine [23], as well as rhodium(III) porphyrins and salophens [8]. Rh (III)-porphyrins have recently been discovered to exhibit the best performance, in terms of selectivity for nitrite over other anions. However, such Rh(III) complexes can function as either a neutral carrier (binding two

nitrites to form negatively charged complex in the presence of TDMACl additive) or a charged carrier (binding only one nitrite to form neutral complex with KTFPB added within the membrane), which significantly complicates the sensing chemistry. Even if one mechanism is favored by choosing a given type of lipophilic ionic site additive, there is always the possibility of a secondary mechanism taking place which worsens the selectivity or response slopes. For example, if an anion-exchanger (i.e., TDMACl) is added to force a neutral carrier mechanism for the Rh(III) porphyrin interaction with anions, the presence of these anion-exchangers can also degrade selectivity over lipophilic anions such as thiocyanate and perchlorate. However if a cation-exchanger (i.e., KTFPB) is added to force a charged carrier response mechanism, as was observed previously [8], the selectivity over lipophilic anions is better while lower response slopes (sub-Nernstian) are obtained. This is probably because a small degree of the neutral carrier mechanism can still occur simultaneously, and this creates sites that can help co-extract cations from the sample phase (leading to sub-Nernstian behavior). Therefore, to further improve the response characteristics of the new nitrite ion-selective electrodes, it is essential to utilize Rh(III) complexes that can operate via only a single nitrite interaction mechanism. This can be achieved in two ways. Chapter 3 focused on employing rhodium(III) complexes that function only as a neutral carrier by replacing the porphyrin with a corrole as the ligand. Another possible approach is to sterically block one axial ligation site on the Rh(III) complexes, thereby preventing nitrite or most other anions from binding (or greatly weakening the binding constant at this site).

Several sterically hindered porphyrins have been synthesized and reported in the literature [24-28]. In this Appendix, efforts to synthesize two different capped Rh(III)

porphyrins structures (see Fig. A.1) through multi-step synthesis (see Fig. A.2 and Fig. A.3) are summarized. It will be shown that intermediates have been successfully prepared, but the synthesis of the final desired capped porphyrin structures remains elusive.

A.2. Experimental

A.2.1. Materials and Reagents

1,2,4,5-benzenetetracarboxylic acid, oxalyl chloride ($C_2O_2Cl_2$), salicylaldehyde, dibromooctane, propionic acid, pyrrole, benzaldehyde, trifluoroacetic acid (TFA), triethylamine and all solvents were purchased from Sigma Aldrich (Milwaukee, WI, U.S.A.) and used as received. 2-(2'-hydoxyethoxy)benzaldehyde and chloranil were obtained from TCI America (Portland, OR, U.S.A.). Pyrrole was redistilled prior to use.

A.2.2. Synthesis

1,2,4,5-Benzenetetrakis(carbonyl chloride) (**2**) [24]. A mixture of 1,2,4,5-benzenetetracarboxylic acid (272 mg, 1.07 mmol), oxalyl chloride (3 mL), THF (30 mL) and DMF (1 drop) was held at reflux under N_2 for 20 min. The carboxylic acid was dissolved completely. The volatile components were removed under vacuum to leave a yellow powder which is the crude acid chloride and used in the next step without further purification.

1,2,4,5-tetrakis [2-(2-formylphenoxy)ethyl]benzenetetracarboxylate (**3**) [29]. A

solution of 1,2,4,5-benzenetetrakis(carbonyl chloride) (82 mg, 0.25 mmol) in anhydrous THF (5 mL) was added over 30 min to a stirred solution of 2-(2'-hydoxyethoxy)benzaldehyde (166 mg, 1 mmol) and triethylamine (139 μL) also in dry THF (25 mL), maintained at -20 ± 5 ^{o}C. After all the acid chloride was added, the reaction mixture was stirred for another 1 h and allowed to warm up to room temperature overnight. The precipitate formed was filtered out and washed with fresh anhydrous THF (10 mL × 3). The combined filtrate and washings were evaporated to give a brown gum, which was then dissolved in chloroform (10 mL) and washed successively with brine (5 mL × 3) and water (5 mL × 3). The organic phase was dried over Na_2SO_4, filtered, and evaporated under vacuum. The resultant oil was dissolved in acetonitrile and kept stirring. Water (5 mL) was added dropwise to this stirred solution over 10 min. More water (7 mL) was added to the stirred solution at room temperature through a dropping funnel over 1 h. The precipitate that formed was collected, washed with water (5 mL × 3) and then dried.

Preparation of "capped" porphyrin with four straps (**4**) [29]. A three necked flask equipped with a condenser, a magnetic stir bar, a dropping funnel and an air injection inlet was charged with 50 mL distilled propionic acid and brought to near reflux. Redistilled pyrrole (51.6 mg, 0.77 mmol) was added to the solution. A stream of air was blown through the vigorously stirred solution. A solution of the tetraaldehyde (**3**) (78.2 mg, 0.092 mmol) in warm redistilled propionic acid (5 mL) was added over 5 min. Some extra pyrrole (51.6 mg, 0.77 mmol) was added after approximately half of the tetraaldehyde was dissolved. After refluxing for 1.5 h, the reaction mixture was allowed to cool, filtered and washed with chloroform (5 mL × 2). The filtrate was dried under

vacuum and the resulted solid was redissolved in the chloroform washings, which was then treated with saturated $NaHCO_3$ solution (10 mL × 2) and water until the aqueous phase became neutral. The organic phase was dried over Na_2SO_4 and the solvent was evaporated.

1,10-Bis(2-formylphenoxy)decane **(6)** [28]. Salicyladehyde (16 mL, 0.15 mol) was dissolved in an alcoholic solution (150 mL) of KOH (8.4 g, 1 M), and then 1,10-dibromooctane (15g, 0.05 mol) was added. The solution was brought to reflux and maintained under continuous reflux overnight. The mixture was cooled to room temperature and then filtered. The filtrate was cooled at 0 ^oC to yield a precipitate. The precipitate was collected and recrystallized from ethanol, which yielded a crystalline product.

5-phenyl substituted dipyrromethane (**7**) [30]. Redistilled pyrrole (14.5 mL, 0.21 mol) and benzaldehyde (0.85 mL, 8.33 mmol) were added into a three necked round bottom flask containing a magnetic stir bar. The solution was purged with N_2 for 5 min, and then trifluoroacetic acide (TFA) (65 μL, 0.38 mmol) was added. The mixture was stirred for 5 min at room temperature and then the reaction was quenched by adding NaOH solution (1 M, 20 mL). The solution was extracted with ethyl acetate (400 mL × 3), dried over Na_2SO_4 and the solvent was evaporated under vacuum, which yield a brownish oil. The product was purified by recrystallization from ethanol.

Basket-handle porphyrin (**8**) [31]. Dipyrromethane (**7**) (35.4 mg, 0.16 mmol) was dissolved in methylene chloride (10 mL) and the solution was stirred under N_2 flow at room temperature for 5 min. 1,10-Bis(2-formylphenoxy)decane (**6**) (21.8 mg, 0.057 mmol) was added into the above solution. After stirred for 5 min, TFA (27 μL, 0.16

mmol) was introduced and the reaction was stirred for 30 min. Afterward, chloronil (24.8 mg, 0.1 mmol) was added to oxidize formed chlorin, and the reaction mixture was stirred at room temperature for a further 1 h. NaOH solution (1 M, 25 mL) was then added to the mixture to neutralize TFA. The solution was extracted with ethyl acetate (400 mL × 3), dried over Na_2SO_4 and the solvent was evaporated under vacuum. The dark residue was loaded on a silica gel and eluted with cyclohexane/methylene chloride (1:1).

A.3. Results and Discussion

Attempts were made to synthesize two types of sterically hindered porphyrins in accordance with the synthetic schemes shown in Fig. A.2 and Fig. A.3. The first type of structure has a four-strap cap which completely covers one side of the porphyrin ring while leaving the other side open. The synthesis of this species starts with compound **1** to give the acid chloride, compound **2**. Acylation of four equivalents of the benzaldehyde with pyromellitoyl chloride (**2**) in THF/triethylamine gave the required tetraaldehyde (**3**) (see Fig. A.4 for NMR spectrum of **3**). However, preparation of the porphyrin from compound **3** by a standard condensation reaction with pyrrole was very challenging and not successful. TLC results suggest there are more than 3 byproducts in the mixture, which might be due to the fact that one tetraaldehyde (**3**) is not necessarily reacting with four pyrroles (e.g., one compound **3** reacts with 2 pyrroles). Surprisingly, the corresponding m/z peak of the capped porphyrin does not show up in the mass

spectrum of the final reaction mixture.

The effort to prepare a basket-handle shaped porphyrin (**8**) (Fig. A.3), starting from a substitution reaction with dibromooctane and salicyladehyde to yield the "handle" part. To ensure that the handle only links on the trans-phenyl groups, dipyrromethane was employed in the synthesis of the hindered porphyrin, instead of pure pyrrole. The preparation of the dipyrromethane species followed the Lindsey method [30]. Reaction between dipyrromethane and compound **6** gives the basket-handle porphyrin which is the so-called "2+2" synthesis [31]. Mass spectrometry results and the observed UV-Vis spectrum indicates the formation of this porphyrin species (see Fig. A.5 and Fig. A.6) with trace amount of 5,10,15,20-tetraphenylporphyrin and 5,10,15,20-tetrakis(o-hydroxyphenyl)porphyrin. All the absorption bands, including the soret band and Q bands, are in good agreement with the literature [31]. However, the NMR spectrum (see Fig. A.7) indicates the formation of two types of porphyrins with the same yield based on integration data of the bands the positioned at around -2.7 ppm, 3.7 ppm and 3.9 ppm. The NMR data suggests there are two different α carbons on the alkane chain of the handle part, which may have resulted from the different possible alignments of the alkane chain handle (e.g. a pair of *cis* and *trans* atropisomers, see below Fig. A.8). These two porphyrins cannot be isolated from each other by column chromatography. If the above assumption is true, one structure would be preferred under a certain temperature and the final product might be able to be purified at a lower or higher temperature [32]. Another issue related to this synthesis method is the instability of dipyrromethane reagent, which turns darker after a few days due to the oxidation of this compound [30]. Therefore, fresh dipyrromethane is required for each

synthesis to ensure the purity.

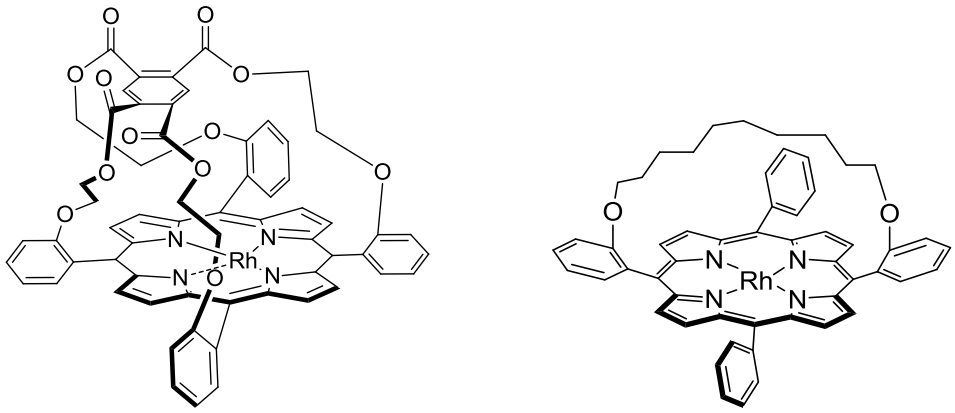

(a) (b)

Fig. A.1. Structures of two different capped rhodium(III) porphyrins with one side of the Rh(III) center sterically blocked. (a) capped porphyrin with four straps ; (b) basket-handle porphyrin with one strap.

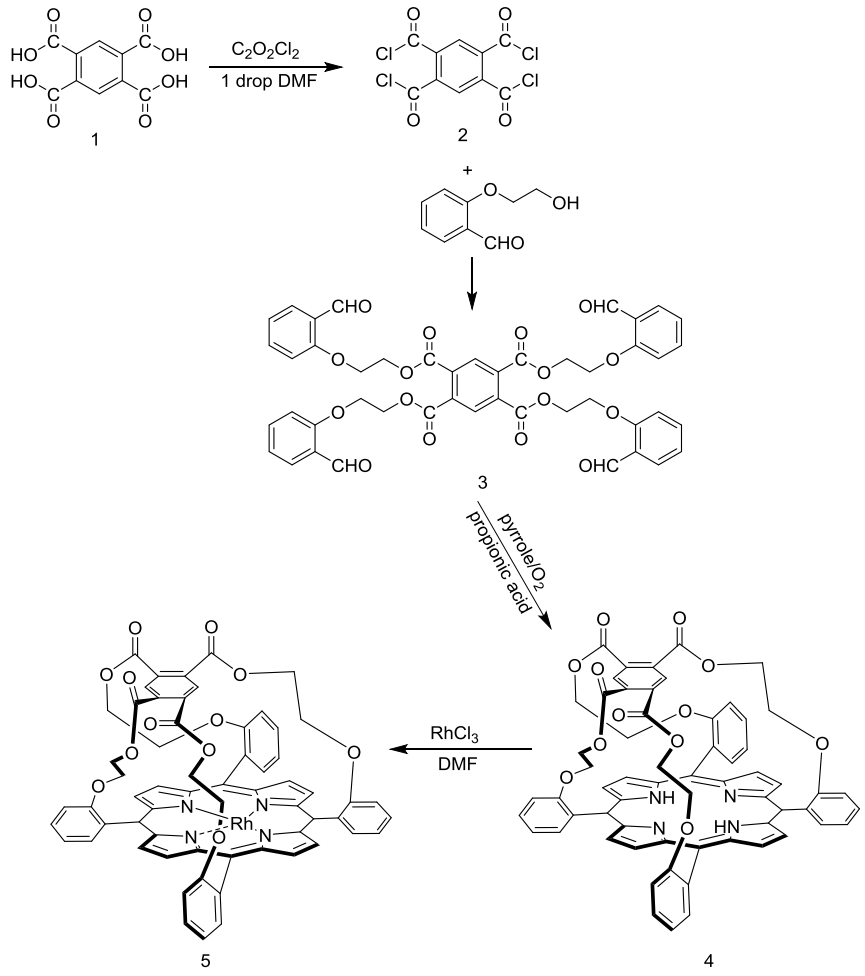

Fig. A.2. Synthetic route to prepare capped rhodium(III) porphyrin with a four-strap cap.

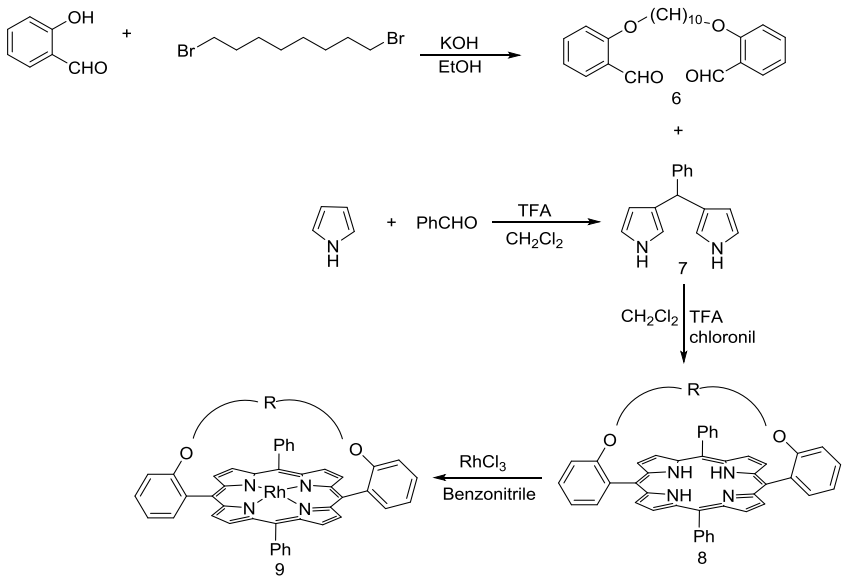

Fig. A.3. Synthesis of capped rhodium(III) porphyrin with a basket-handle like structure.

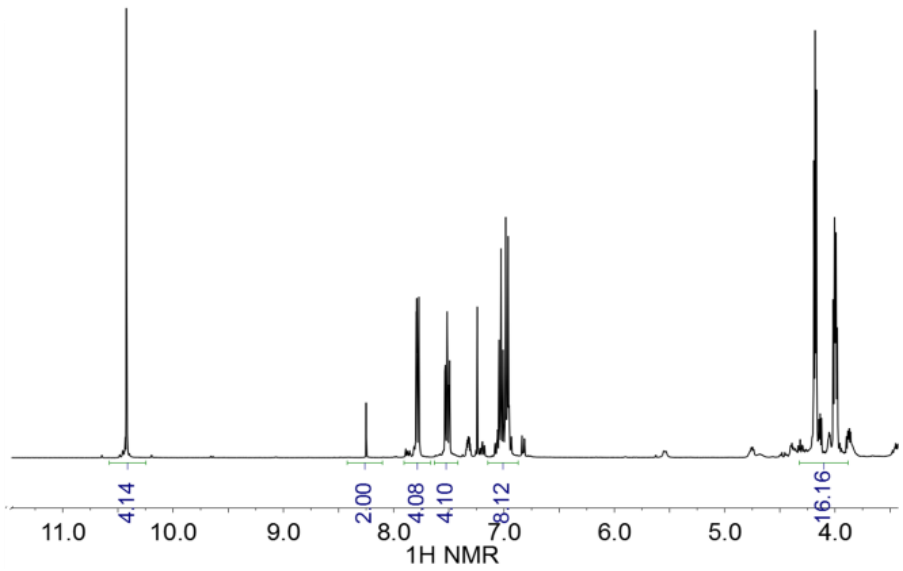

Fig. A.4. 400 MHz ^{1}H NMR spectra of tetraaldehyde **3**.

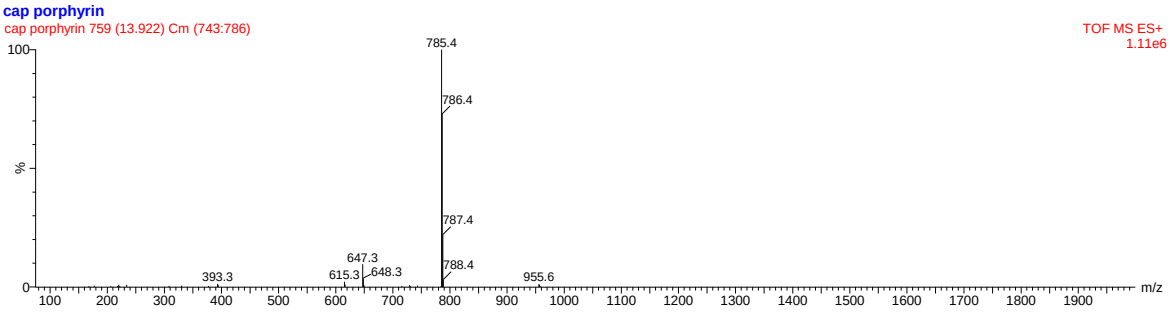

Fig. A.5. Mass spectrometry spectrum of compound **8**.

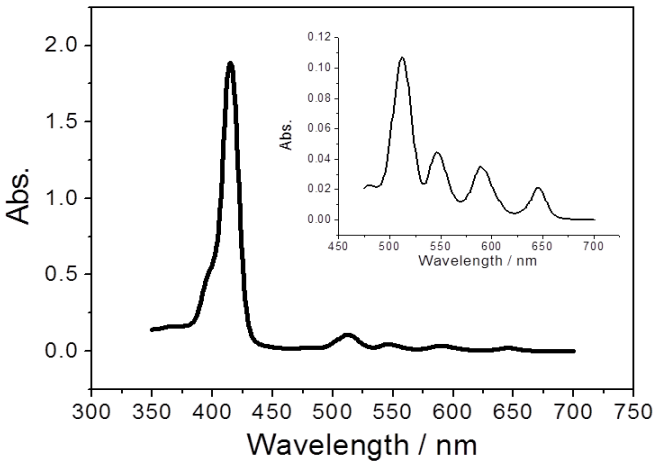

Fig. A.6. UV-Vis spectrum of compound **8**. Inset shows the detailed Q bands.

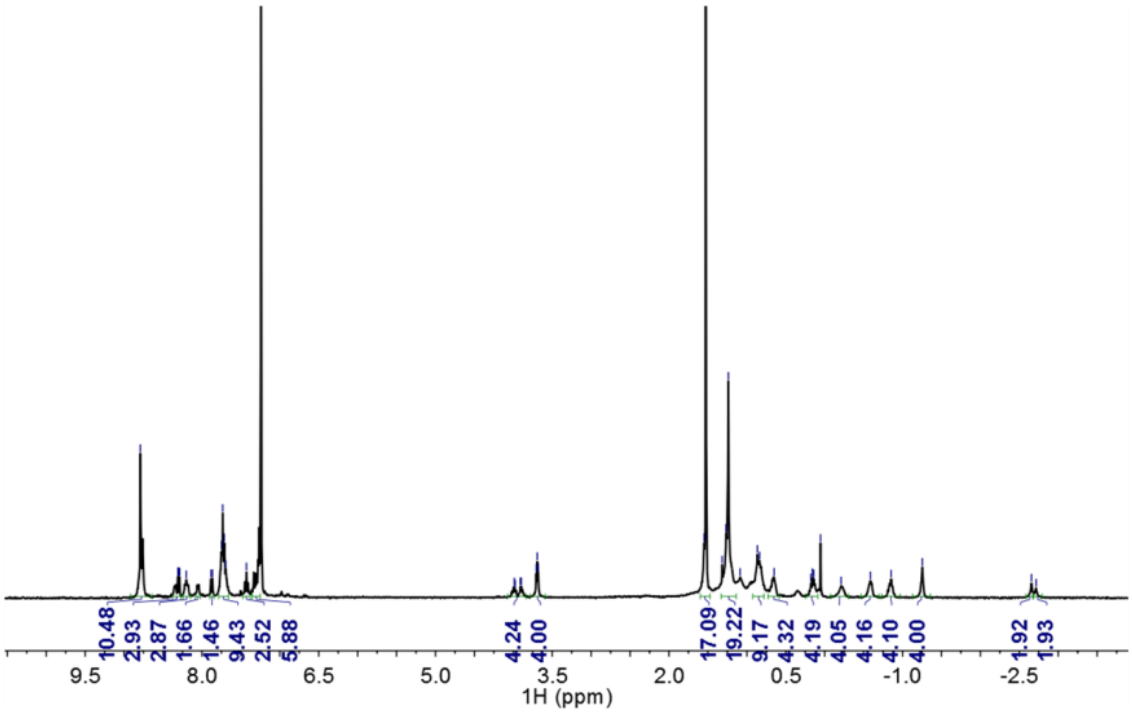

Fig. A.7. 400 MHz ^{1}H NMR spectrum of compound **8**.

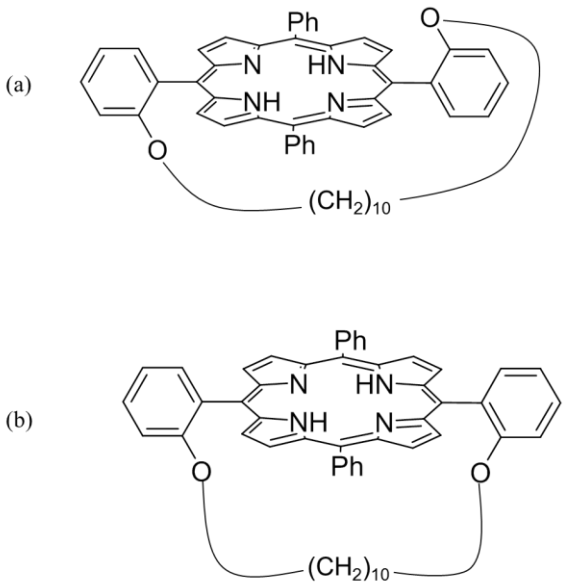

Fig. A.8. Two possible basket-handle porphyrins of a pair of *trans*- (a) and *cis*- (b) atropisomers.

A.4. References

[1] D. Ammann, M. Huser, B. Kräutler, B. Rusterholz, P. Schulthess, B. Lindemann, E. Halder, W. Simon, "Anion selectivity of metalloporphyrins in membranes", *Helv. Chim. Acta*, **1986**, *69*, 849-854.

[2] N. A. Chaniotakis, A. M. Chasser, M. E. Meyerhoff, J. T. Groves, "Influence of porphyrin structure on anion selectivities of manganese(III) porphyrin based membrane electrodes", *Anal. Chem.*, **1988**, *60*, 185-188.

[3] A. Jyo, H. Egawa, "Effect of membrane matrices on performances of a thiocyanate ion-selective electrode based on the (5,10,15,20-tetraphenylporphyrinato)manganese(III) anion carrier", *Anal. Sci.*, **1992**, *8*, 823-828.

[4] S. B. Park, W. Matuszewski, M. E. Meyerhoff, Y. H. Liu, K. M. Kadish, "Potentiometric anion selectivities of polymer membranes doped with indium(III)-porphyrins", *Electroanalysis*, **1991**, *3*, 909-916.

[5] A. Hodinar, A. Jyo, "Thiocyanate solvent polymeric membrane ion-selective electrode based on cobalt(III) α,β,γ,δ-tetraphenylporphyrin anion carrier ", *Chem. Lett.*, **1988**, *17*, 993-996.

[6] M. Huser, W. E. Morf, K. Fluri, K. Seiler, P. Schulthess, W. Simon, "Transport properties of anion-selective membranes based on cobyrinates and metalloporphyrin complexes as ionophores", *Helv. Chim. Acta*, **1990**, *73*, 1481-1496.

[7] X. Li, D. J. Harrison, "Measurement of concentration profiles inside a nitrite ion-selective electrode membrane", *Anal. Chem.*, **1991**, *63*, 2168-2174.

[8] M. Pietrzak, M. E. Meyerhoff, "Polymeric membrane electrodes with high nitrite selectivity based on rhodium(III) porphyrins and salophens as ionophores", *Anal. Chem.*, **2009**, *81*, 3637-3644.

[9] E. Lindner, E. Graf, Z. Niegreisz, K. Toth, E. Pungor, R. P. Buck, "Responses of site-controlled, plasticized membrane electrodes", *Anal. Chem.*, **1988**, *60*, 295-301.

[10] A. Van den Berg, P. D. Van der Wal, M. Skowronska-Ptasinska, E. J. R. Sudholter, D. N. Reinhoudt, P. Bergveld, "Nature of anionic sites in plasticized poly(vinyl chloride) membranes", *Anal. Chem.*, **1987**, *59*, 2827-2829.

[11] W. J. R. Santos, P. R. Lima, A. A. Tanaka, S. M. C. N. Tanaka, L. T. Kubota, "Determination of nitrite in food samples by anodic voltammetry using a modified electrode", *Food Chem.*, **2009**, *113*, 1206-1211.

[12] K.-O. Honikel, "The use and control of nitrate and nitrite for the processing of meat products", *Meat Sci.*, **2008**, *78*, 68-76.

[13] M. H. Ward, J. R. Cerhan, J. S. Colt, P. Hartge, "Risk of non-hodgkin lymphoma and nitrate and nitrite from drinking water and diet", *Epidemiology*, **2006**, *17*, 375-382.

[14] Z. Binghui, Z. Zhixiong, Y. Jing, "Ion chromatographic determination of trace iodate, chlorite, chlorate, bromide, bromate and nitrite in drinking water using suppressed conductivity detection and visible detection", *J. Chromatogr. A*, **2006**, *1118*, 106-110.

[15] K. Tsuchiya, Y. Takiguchi, M. Okamoto, Y. Izawa, Y. Kanematsu, M. Yoshizumi, T. Tamaki, "Malfunction of vascular control in lifestyle-related diseases: Formation of systemic hemoglobin-nitric oxide complex (HbNO) from dietary nitrite", *J. Pharmacol. Sci.*, **2004**, *96*, 395-400.

[16] C. J. Hunter, A. Dejam, A. B. Blood, H. Shields, D. Kim-Shapiro, R. F. Machado, S. Tarekegn, N. Mulla, A. O. Hopper, A. N. Schechter, G. G. Power, M. T. Gladwin, "Inhaled nebulized nitrite is a hypoxia-sensitive NO-dependent selective pulmonary vasodilator", *Nat. Med.*, **2004**, *10*, 1122-1127.

[17] J. L. Zweier, P. H. Wang, A. Samouilov, P. Kuppusamy, "Enzyme-independent formation of nitric-oxide in biological tissues", *Nat. Med.*, **1995**, *1*, 804-809.
[18] J. O. N. Lundberg, E. Weitzberg, J. M. Lundberg, K. Alving, "Intragastric nitric oxide production in humans - measurements in expelled air", *Gut*, **1994**, *35*, 1543-1546.
[19] N. Benjamin, F. Odriscoll, H. Dougall, C. Duncan, L. Smith, M. Golden, H. McKenzie, "Stomach NO synthesis", *Nature*, **1994**, *368*, 502-502.
[20] R. Stepanek, B. Krautler, P. Schulthess, B. Lindemann, D. Ammann, W. Simon, "Aquocyanocobalt(III)-hepta(2-phenylethyl)-cobyrinate as a cationic carrier for nitrite-selective liquid-membrane electrodes", *Anal. Chim. Acta*, **1986**, *182*, 83-90.
[21] P. Schulthess, D. Ammann, B. Krautler, C. Caderas, R. Stepanek, W. Simon, "Nitrite-selective liquid membrane-electrode", *Anal. Chem.*, **1985**, *57*, 1397-1401.
[22] E. Malinowska, M. E. Meyerhoff, "Role of axial ligation on potentiometric response of Co(III) tetraphenylporphyrin-doped polymeric membranes to nitrite ions", *Anal. Chim. Acta*, **1995**, *300*, 33-43.
[23] I. H. A. Badr, M. E. Meyerhoff, S. S. M. Hassan, "Potentiometric anion selectivity of polymer membranes doped with palladium organophosphine complex", *Anal. Chem.*, **1995**, *67*, 2613-2618.
[24] C. Slebodnick, M. L. Duval, J. A. Ibers, "Structural characterization of OC_3OPor capped porphyrins: $H_2(OC_3OPor)$, $Fe(OC_3OPor)(Cl)$, $Fe(OC_3OPor)(CO)(1\text{-MeIm})$, and $Fe(OC_3OPor)(CO)(1,2\text{-}Me_2Im)$", *Inorg. Chem.*, **1996**, *35*, 3607-3613.
[25] M. R. Johnson, W. K. Seok, W. P. Ma, C. Slebodnick, K. M. Wilcoxen, J. A. Ibers, "Four-atom-linked capped porphyrins: Synthesis and characterization", *J. Org. Chem.*, **1996**, *61*, 3298-3303.
[26] K. Kim, J. A. Ibers, "Structure of a carbon-monoxide adduct of a capped porphyrin-$Fe(C_2\text{-cap})(CO)$(1-methylimidazole)", *J. Am. Chem. Soc.*, **1991**, *113*, 6077-6081.
[27] M. Momenteau, "Synthesis and coordination properties of superstructured iron-porphyrins", *Pure Appl. Chem.*, **1986**, *58*, 1493-1502.
[28] M. Momenteau, J. Mispelter, B. Loock, E. Bisagni, "Both-faces hindered porphyrins. Part 1. Synthesis and characterization of basket-handle porphyrins and their iron complexes", *J. Chem. Soc., Perkin Trans. 1*, **1983**, 189-196.
[29] J. Almog, J. E. Baldwin, M. J. Crossley, J. F. Debernardis, R. L. Dyer, J. R. Huff, M. K. Peters, "Synthesis of "capped porphyrins"", *Tetrahedron*, **1981**, *37*, 3589-3601.
[30] J. F. N. S. Abílio, G. C. L. R. Nuno, S. Melo da, H. L. Sandra, M. R. Silva, A. M. Beja, J. A. Paixão, M. d. A. R. G. António, "One-step synthesis of dipyrromethanes in water", *Tetrahedron Lett.*, **2003**, *44*.
[31] B. J. Littler, Y. Ciringh, J. S. Lindsey, "Investigation of conditions giving minimal scrambling in the synthesis of trans-porphyrins from dipyrromethanes and aldehydes", *J. Org. Chem.*, **1999**, *64*, 2864-2872.
[32] E. R. James, K. M. S. Jeremy, "Disulfide-strapped porphyrins for monolayer formation on gold", *Org. Lett.*, **2000**, *2*.